UNIVERSITY OF ICELAND

Ph.D. Thesis

in Environmental Engineering

Gravity-driven Membrane Filtration of Municipal Wastewater: Process Optimization and Life Cycle Assessment

Selina Hube

October 2023

FACULTY OF CIVIL AND ENVIRONMENTAL ENGINEERING

Gravity-driven Membrane Filtration of Municipal Wastewater: Process Optimization and Life Cycle Assessment

Selina Hube

Dissertation submitted in partial fulfillment of a
Philosophiae Doctor degree in Environmental Engineering

Ph.D. Committee
Dr. Bing Wu
Dr. Michael Burkhardt
Dr. Sigurður Brynjólfsson

Opponents
Dr. John Chew
Dr. Alberto Tiraferri

Faculty of Civil and Environmental Engineering
School of Engineering and Natural Sciences
University of Iceland
Reykjavik, October 2023

Gravity-driven Membrane Filtration of Municipal Wastewater: Process Optimization and Life Cycle Assessment
Dissertation submitted in partial fulfillment of a *Ph.D.* degree in Environmental Engineering

Faculty of Civil and Environmental Engineering
School of Engineering and Natural Sciences
University of Iceland
Hjardarhagi 2-6
107, Reykjavik
Iceland

Telephone: 525 4000

Bibliographic information:
Selina Hube, 2023, *Gravity-driven Membrane Filtration of Municipal Wastewater: Process Optimization and Life Cycle Assessment*, PhD dissertation, Faculty of Civil and Environmental Engineering, University of Iceland, 128 pp.

Author ORCID: 0000-0001-6473-1644
ISBN: 978-9935-9742-0-4

Abstract

Towards fulfilling increasingly stricter wastewater discharge standards, there is a need for developing reliable decentralized wastewater treatment processes. The goal of this research was to optimize gravity-driven membrane (GDM) filtration and assess its technical, environmental, and economical feasibility for decentralized wastewater treatment under cold climate. The GDM systems treated primary municipal wastewater at different temperatures (22°C and 8°C), with different membrane configurations (side-stream organic membrane and submerged ceramic membrane), and different periodic cleaning strategies. The results highlighted that (1) the treated water quality in the GDM systems met EU discharge standards, regardless of temperature and membrane configurations; (2) In the GDM systems, the dominant fouling mechanism shifted with filtration time and cake fouling was predominant after flux stabilization (1.6-4.3 L/m^2h); (3) Compared to periodic backwash, two-phase flow cleaning, and chemical-enhanced physical cleaning, periodic ultrasonication improved water productivity more efficiently through creating a porous cake nature by cake expansion and detachment of particulate foulants and soluble organics from the membrane; (4) The presence of microplastics in the feed water led to a reduced water productivity and more accumulation of heavy metals in the GDM system. The cake layer morphology was strongly associated with microplastic sizes and amounts. A comparative LCA revealed that the GDM system could achieve ~90% lower global warming and ~40% higher eutrophication potential than conventional septic tank, or septic tank + constructed wetlands. Finally, the cost analysis showed that the wastewater treatment cost of GDM (with recycled materials-based ceramic membranes) was ~0.213 EUR/m^3, which was comparable to those of conventional treatment processes.

Útdráttur

Til að uppfylla sífellt strangari losunarstaðla frárennslis er þörf á að þróa áreiðanleg dreifð hreinsunarferli frárennslis. Markmið þessarar rannsóknar var að besta þyngdardrifna himnu (GDM) síun og meta tæknilega, umhverfislega og hagkvæma möguleika hennar fyrir dreifða skólphreinsun í köldu loftslagi. GDM kerfin meðhöndluðu skólp frá sveitarfélögum við mismunandi hitastig (22°C og 8°C), mismunandi himnustillingar (lífræn himna hliðarstraums og keramikhimna á kafi) og mismunandi reglubundnar hreinsunaraðferðir. Niðurstöðurnar sýndu að (1) meðhöndluð vatnsgæði í GDM kerfunum uppfylltu losunarstaðla ESB, óháð hitastigi og himnustillingum; (2) Í GDM kerfunum hliðraðist ríkjandi gangverk óhreininda með síunartímanum og óhreinindalag varð ríkjandi þegar flæðið hafði náð jafnvægi (1.6-4.3 L/m^{2}klst); (3) Tveggja fasa skolun, efnahreinsun og hátíðnihreinsun bættu hreinsunina samanborðið við reglubundna skolun með því að þenja óhreinindalagið og losa um agnir og uppleyst lífræn efni úr himnunni; (4) Tilvist örplasts í vatninu leiddi til minni framleiðni vatns og meiri uppsöfnunar þungmálma í GDM kerfinu. Formgerð óhreinindalaga var mjög tengd stærð og magni örplasts. Til samanbrðar leiddi LCA greining í ljós að GDM kerfið gæti minnkað áhrif á hlýnun jarðar um ~90% jarðar og ~40% meiri ofauðgun en hefðbundin rotþró, eða rotþró + tilbúið votlendi. Að lokum sýndi kostnaðargreiningin að kostnaður við skólphreinsun með GDM (með keramikhimnum sem byggir á endurunnum efnum) var ~0.213 EUR/m^3, sem var sambærilegt við hefðbundna hreinsunarferla.

To my family.

Table of Contents

List of Figures ..... **xi**

List of Tables ..... **xiv**

List of Publications ..... **xvi**

Abbreviations ..... **xvii**

Acknowledgements ..... **xix**

1 Introduction **1**
1.1 Advances of Decentralized Wastewater Treatment in Cold Climate 1
1.1.1 Status and Challenges of Decentralized Wastewater Treatment 1
1.1.2 Status and Challenges of Wastewater Treatment in Cold Climate 2
1.2 Application of GDM for Wastewater Treatment 3
1.3 Research Questions 4
1.4 Thesis Organization 5

2 Combined Effect of Temperature and Periodic Cleaning on Gravity-Driven Membrane Filtration **7**
2.1 Abstract 7
2.2 Introduction 7
2.3 Materials and Methods 10
2.3.1 Experimental Setup 10
2.3.2 Wastewater and Geothermal Water 11
2.3.3 Filtration Experiments Protocol 11
2.3.4 Fouling Resistance Examination and Fouling Model Fitting 13
2.3.5 Cake Foulants Characterization 14
2.3.6 Water Quality Analysis 14
2.4 Results and Discussion 14
2.4.1 Water Quality of GDM Systems 14
2.4.2 Membrane Fouling Mechanism during Continuous Filtration (no Periodic Cleaning) 15
2.4.3 GDM Performance with Periodic Cleaning 20
2.5 Conclusions 28

3 Effect of Periodic Ultrasonication on Gravity-driven Membrane Filtration **29**
3.1 Abstract 29
3.2 Introduction 29
3.3 Materials and Methods 33
3.3.1 GDM Setup and Experimental Conditions 33
3.3.2 Direct Constant Flux Filtration Setup and Experimental Conditions 34
3.3.3 Analytical Methods 35
3.4 Results and Discussion 36

3.4.1 Ceramic Membrane Fouling Mechanisms 36
3.4.2 Ultrasonication-facilitated Fouling Control in GDM and Constant Flux Filtration Systems 39
3.4.3 Ultrasonication-facilitated Fouling Control Mechanisms 44
3.5 Conclusions 49

4 Effect of Microplastics on Gravity-driven Membrane Filtration 51
4.1 Abstract 51
4.2 Introduction 51
4.2.1 Mitigation of Microplastics in Wastewater Treatment 51
4.2.2 Mitigation of Microplastics in Decentralized Wastewater Treatment 53
4.2.3 Mitigation of Microplastics in Membrane-based Wastewater Treatment 54
4.3 Materials and Methods 56
4.3.1 Experimental Setup 56
4.3.2 Analytical Methods 56
4.4 Results and Discussion 57
4.4.1 Effect of Microplastics on Water Quality 57
4.4.2 Effect of Microplastics on Membrane Performance 58
4.5 Conclusions 63

5 Life Cycle Assessment and Cost Analysis of Decentralized Wastewater Treatment in Cold Climate 65
5.1 Abstract 65
5.2 Introduction 65
5.3 Materials and Methods 68
5.3.1 Recycled Construction Waste-based Constructed Wetlands 68
5.3.2 LCA Methodology 68
5.3.3 Life Cycle Inventory Data 69
5.3.4 Cost Analysis 71
5.4 Results and Discussion 72
5.4.1 Global Warming 72
5.4.2 Eutrophication 76
5.4.3 Cost Analysis 77
5.5 Conclusions 81

6 Conclusions and Outlook 83

References 85

Appendix 99

List of Figures

Figure 2.1. Schematic diagram of the biocarriers facilitated GDM system. 11

Figure 2.2. Water quality in feed, effluent and permeate (n=10-15). “p” represents p-value; TSS level in the permeate was ~ 0 mg/L, thus the column did not appear in the figure. 15

Figure 2.3. (a) Flux development, (b) resistance distribution (n=5), and (c) simulated filtration constants (n=5) in the GDM systems (no periodic cleaning). Stage 1 (S1) refers to the flux profile < ~1 day, Stage 2 (S2) refers to the flux profile during ~1-3 days; Stage 3 (S3) refers to the flux profile > ~3 days (the detailed simulation profiles for each phase were presented in Figure 2.5)..... 17

Figure 2.4. Permeate water productivity of GDM systems with/without periodic cleaning. 17

Figure 2.5. Membrane mechanism description based on the simulation profiles during continuous filtration (linear correlation coefficient $R^2 \geq 0.99$). Note: the dot red lines in the figure are used to indicate three stages, but the time duration of each stage for each stage for each flux simulation profile was dissimilar..... 19

Figure 2.6. (a) Soluble organics in the cake layers and cake foulant mass, and (b) Soluble inorganics in the cake layers on the membrane surface (no periodic cleaning). 20

Figure 2.7. Flux profiles of the GDM systems operated under different temperatures..... 21

Figure 2.8. (a) Fouling removal ratio, (b) water productivity, and (c) fouling resistance (non-fill symbols represent cake layer fouling, solid-fill symbols represent irreversible fouling) in the GDM systems with different periodic cleaning protocols. The dash line indicated the level in the control membrane module without periodic cleaning. “UGW” represents ultrasonicated geothermal water flushing; “US” represents ultrasonication; “U+GW” represents ultrasonication + geothermal water flushing. 23

Figure 2.9. (a) Foulant mass, and (b) specific cake resistance in the GDM systems with different periodic cleaning protocols. The dash line indicated the level in the control membrane module without periodic cleaning. “UGW” represents ultrasonicated geothermal water flushing; “US” represents ultrasonication; “U+GW” represents ultrasonication+ geothermal water flushing 24

Figure 2.10. Relationship between fouling removal effectiveness and deposited soluble organic foulants on the membrane surfaces in Phase VII..... 24

Figure 3.1. (a) GDM setup, (b) direct constant flux filtration setup, (c) side view, and (d) front view of membrane and ultrasonication probe when ultrasonication cleaning was employed. 33

Figure 3.2. The TMP increase rates under different filtration fluxes in the constant flux filtration system (filtration was performed for ~2 days). 35

Figure 3.3. (a) Flux development profiles in the GDM system during continuous filtration (Phase I), and (b) TMP development profiles in the constant flux filtration system. 37

Figure 3.4. Membrane mechanism description based on the simulation profiles during continuous GDM filtration (linear correlation coefficient $R^2 \geq 0.95$). 38

Figure 3.5. Simulated filtration constants during (a) GDM filtration (n=3, $R^2 \geq 0.95$) and (b) constant flux filtration (n=2, $R^2 \geq 0.95$). 38

Figure 3.6. Membrane mechanism description based on the simulation profiles during continuous constant flux filtration (linear correlation coefficient $R^2 \geq 0.95$). 39

Figure 3.7. (a) Flux development profiles in the GDM systems during Phases II and III; (b) TMP development profiles during constant flux filtration (red arrow pointed to ultrasonication cleaning). 40

Figure 3.8. Flux recovery ratio profiles in the GDM systems during Phases II and III. 40

Figure 3.9. Filtration resistances in the GDM and constant flux filtration systems (Note: under ultrasonication condition, the "cake layer resistance" = "cake resistance removed by US" + "remaining residual cake resistance after US"). 41

Figure 3.10. Photo of the fouled membrane during ultrasonication in the GDM system (after 3-h filtration). 43

Figure 3.11. Effect of ultrasonication duration on (a) foulant mass and (b) DOC content in the foulants from the GDM systems (3-h filtration and 2-day filtration) (n=2). The terms "center" and "side" refer to the foulant sampling locations; "Side" includes both right and left sides of the membrane (see Figure 3.1c). 46

Figure 3.12. Effect of ultrasonication duration on fouling resistance distribution (a) in the GDM system after 3-h filtration, (b) in the GDM system after 2-day filtration, (c) in the constant flux filtration (n=2-3) 48

Figure 4.1. Schematic diagram of GDM system with dosing different types and amounts of microplastics 56

Figure 4.2. The flux evolution profiles during GDM filtration of municipal wastewater with/ without dosed microplastics 58

Figure 4.3. Filtration resistance distribution and specific cake resistance during GDM filtration of municipal wastewater with/without dosed microplastics 59

Figure 4.4. The simulated filtration constants in the GDM systems (a) without dosed microplastics, and (b) with dosed microplastics. 60

Figure 4.5. A diagram showing the proposed cake morphology in the GDM systems in the absence and presence of dosed microplastics. 63

Figure 5.1. System boundaries in LCA analysis 69

Figure 5.2. Total impact in global warming (a) and eutrophication (b) categories. Contribution of each item to global warming (c & e) and eutrophication (d & f) during construction (c & d) and operation (e & f) phase. *GDCM methane emissions represent both methane and dinitrogen monoxide emissions; **Sludge treatment contribution was identical for all three scenarios. 73

Figure 5.3. Global warming potential under different scenarios when the sludge is landfilled in an unsanitary landfill site. 75

Figure 5.4. Economic analysis for GDM and constant flux filtration systems under different cleaning protocols. (a) Commercial ceramic membrane; (b) Recycled materials-based inorganic membrane. The cleaning duration was proposed as follows: GDM backwash: 30-min per week; GDM ultrasonication: 120 sec per 2-h filtration; constant flux backwash: 15-min (0.5% NaClO solution) per day; constant flux ultrasonication: 15-min per day..... 78

Figure 5.5. (a) and (c) Cost items in the GDM systems; (b) and (d) Cost items in the constant flux filtration systems with commercial ceramic membranes at different scales. “CF” refer to constant flux filtration. 79

Figure 5.6 Total costs of wastewater treatment scenarios 80

List of Tables

Table 2.1. Effect of periodic physical/chemical cleaning on membrane performance in GDM systems documented in literature. 8

Table 2.2. Geothermal water characteristics (Ionic concentration data were derived from literature (Gunnarsdottir et al., 2014; Kristmannsdóttir et al., 2010). 11

Table 2.3. A summary of membrane cleaning protocols in the GDM systems 12

Table 2.4. Dead-end filtration models for describing the membrane fouling mechanism under constant pressure condition (Ho & Zydney, 2000; Ye et al., 2005). 13

Table 2.5. Water quality in the GDM systems 15

Table 2.6. The density of soluble inorganics (mg/m^2) in the cake layers on the membrane surfaces (Phase VII) 25

Table 3.1. A summary of membrane cleaning protocols in the reported ceramic membrane-based wastewater treatment processes. 30

Table 3.2. A summary of filtration and physical cleaning protocols in the GDM and direct constant flux filtration systems 34

Table 3.3. Dead-end filtration models for describing the membrane fouling mechanism under constant flux condition (Ho & Zydney, 2002) 36

Table 3.4. Water quality in the GDM system 36

Table 3.5. Foulant mass, flux recovery and resistance reduction in the GDM systems with periodic cleaning 42

Table 3.6. Images of foulants remained on the membrane after ultrasonication cleaning. 45

Table 3.7. Effect of ultrasonication duration on soluble organic compositions in the foulants from the GDM systems (2-day filtration) (n=2). 46

Table 4.1. Water quality parameters of the biocarrier reactor effluent and GDM permeates 57

Table 4.2. TSS concentrations and removals in the GDM system 58

Table 4.3. The stabilized flux, deposited foulant mass, deposited soluble organics and estimated porosity in the GDM systems with/without dosed microplastics 59

Table 4.4. Metal and metalloid content in effluent and cake layers 61

Table 4.5. Divalent ion content in cake layers 62

Table 5.1. Life cycle inventory analysis for construction & operation phase 69

Table 5.2. A summary of capital and operational cost estimation 71

Table 5.3. Comparison of costs for septic tank and septic tank + wetland scenarios 77

List of Publications

1. Hube, S., Wu, B. 2021. Mitigation of emerging pollutants and pathogens in decentralized wastewater treatment processes: A review. *Science of the Total Environment, 779*, 146545. https://doi.org/10.1016/j.scitotenv.2021.146545

2. Hube, S., Lee, S., Chong, T.H., Brynjólfsson, S., Wu, B. 2022. Biocarriers facilitated gravity-driven membrane filtration of domestic wastewater in cold climate: Combined effect of temperature and periodic cleaning. *Science of the Total Environment, 833*, 155248. https://doi.org/10.1016/j.scitotenv.2022.155248

3. Hube, S., Hauser, F., Burkhardt, M., Brynjólfsson, S., Wu, B. 2023. Ultrasonication-assisted fouling control during ceramic membrane filtration of primary wastewater under gravity-driven and constant flux conditions. *Separation and Purification Technology*, *310*, 123083. https://doi.org/10.1016/j.seppur.2022.123083

4. Hube, S., Zaqout, T., Ögmundarson, Ó., Andradóttir, H., Wu, B. Constructed wetlands with recycled concrete for wastewater treatment in cold climate: Performance and life cycle assessment. *Science of the Total Environment*, *904*, 166778, https://doi.org/10.1016/j.scitotenv.2023.166778.

5. Hube, S., Burkhardt, M., Brynjólfsson, S., Wu, B. Influence of microplastics on gravity-driven membrane filtration performance during primary municipal wastewater treatment [In preparation]

Contributions of the author

Article 1: The author planned the scope of the article together with her supervisor, conducted a literature review, wrote the article, and discussed the results with the co-author.

Article 2: The author planned the experiments together with her supervisor, conducted the GDM experiments and data collection, analyzed the data, wrote the article, and discussed the results with the co-authors.

Article 3: The author planned the experiments together with her supervisor, conducted or supervised the experiments and data collection, analyzed the data, wrote the article, and discussed the results with the co-authors.

Article 4: The author planned the setup and experiments together with the co-authors, conducted or supervised the experiments and data collection, conducted the LCA, analyzed the data, wrote the article, and discussed the results with the co-authors.

Article 5: The author planned the experiments together with her supervisor, conducted or supervised the experiments and data collection, analyzed the data, wrote a part of the article, and discussed the results with the co-authors.

Abbreviations

A	Area
BOD_5	Biological Oxygen Demand
CF	Constant Flux
COD	Chemical Oxygen Demand
DOC	Dissolved Organic Carbon
EU	European Union
GDCM	Gravity-driven Ceramic Membrane Filtration
GDM	Gravity-driven Membrane Filtration
HRT	Hydraulic Retention Time
J	Flux
LCA	Life Cycle Assessment
LMH	L/m^2h
LMW	Low-molecular Weight
MBR	Membrane Bioreactor
MF	Microfiltration
PE	People Equivalent
PMS	Peroxymonosulfate
PVDF	Polyvinylidene Fluoride
P_w	Productivity
R	Resistance
R_c	Cake Layer Resistance
R_m	Membrane Resistance
R_t	Total Resistance
t	Time
TMP	Trans-membrane Pressure
TN	Total Nitrogen
TOC	Total Organic Carbon
TP	Total Phosphorus
TSS	Total Suspended Solids
UF	Ultrafiltration
V	Volume

Acknowledgements

First, I would like to express my deepest gratitude to my supervisor Prof. Bing Wu, for her encouragement, guidance, and support throughout my studies. This project would not have been possible without her, and I couldn't have wished for a more dedicated supervisor. I also thank my committee members Prof. Michael Burkhardt and Prof. Sigurður Brynjólfsson for their help and co-authoring my papers.

This project was made possible by grants from the University of Iceland Doctoral Fund, the Icelandic Road and Coastal Administration Research Fund (Vegagerðin), and the Energy Research Fund (Landsvirkjun).

I would like to offer my special thanks to Stefán Hansen Daðason, Hlöðver Stefán Þorgeirsson, and their team from the Veitur - Klettagarðar wastewater treatment plant, for their interest, for taking their time to continuously provide samples and for sharing their knowledge.

I would like to extend my sincere thanks to Prof. Ólafur Ögmundarson for his guidance with the LCA process. Several people supported my research by providing instrumental help: I want to thank our technician Vilhjálmur Sigurjónsson for helping to build the experimental setups, and our chemical supervisor Óskar Rudolf Kettler for providing chemicals and advice. Thank you Jóhann Gunnarsson Robin, Dr. Seonki Lee, Prof. Tzyy Haur Chong, Dr. Lee Nuang Sim, Dr. Liya Ge and Dr. Ke Zhao for analyzing my samples. Your support allowed me to improve my research and strengthen my results.

I would like to express the deepest appreciation to everyone, who helped with the experiments and kept me company in the lab and office: thank you Sigurður John Einarsson, Nicola Landolt, Megan Elizabeth Wiegmann, Fiona Hauser, Magnea Freya Kristjánsdottir, Dr. Tarek Zaqout, Lingxue Guan and my office mates. I also appreciate the motivation and work done by the students from the "*Environmental Engineering Lab*" class of Fall 2022.

Finally, I am deeply grateful to my family, my partner and my close friends for their unwavering support, patience, and advice. Thank you for your love, I wouldn't be where I am now without you.

1 Introduction

This chapter contains elements of all published articles presented in the list of publications.

1.1 Advances of Decentralized Wastewater Treatment in Cold Climate

1.1.1 Status and Challenges of Decentralized Wastewater Treatment

Globally, more than 80% of domestic wastewater is discharged into rivers or the sea without any treatment, majorly in rural areas for economic, topographic, demographic (e.g., scattered population), or climatic reasons (e.g., cold-climate regions) (United Nations, 2015). Towards achieving the United Nations Sustainable Development Goal 6 "Ensure access to water and sanitation for all" (United Nations, 2015), the implementation of wastewater treatment facilities in decentralized locations is necessary in the near future. Compared to centralized wastewater treatment systems, decentralization of wastewater treatment holds a large potential to reduce energy consumption for water transportation and allows more modularity and adaptation to the local situation, as it is located at the point of wastewater generation (Kobayashi et al., 2020; Longo et al., 2016). Generally, conventional activated sludge-based centralized wastewater treatment technologies require a stable operation temperature, organic content, and inflow rate. While small-scale on-site wastewater treatment facilities allow treating wastewater with specific characteristics or reclaiming wastewater for reuse in a closed-loop configuration. Therefore, decentralized wastewater treatment processes could significantly reduce the risk of system failures or insufficient treatment efficiency, and also displays greater technical flexibility (Wang, 2014).

Currently, several wastewater treatment techniques have been attempted in decentralized areas, such as septic tanks (Mac Mahon et al., 2022), aerobic/ anaerobic biological processes (Yang et al., 2021), constructed wetlands (Varma et al., 2021; Wang et al., 2017a), and membrane bioreactors (MBRs) (Arias et al., 2020). It is recognized that the selection of a suitable decentralized wastewater treatment technology relies on several prerequisites, such as treatment effectiveness, capital and operation costs, environmental impacts, geographic and climatic situation (Gallego-Schmid & Tarpani, 2019). For example, septic tanks and wetlands generally require large areas and present low treatment efficiencies. Biological processes and MBRs entail relatively high operation costs and require experienced operators, which may not always be feasible in rural areas. Additionally, these biological technologies require specific environmental conditions to ensure stable operation.

In recent decades, the occurrence of emerging pollutants (i.e., contaminants of emerging concern) in wastewater has received great attention because of their potentially negative impacts on human health and ecosystems (Lin et al., 2020; Ma et al., 2018; Sauve & Desrosiers, 2014). It has been recognized that wastewater treatment plants are the main barriers for mitigating the release of emerging pollutants and pathogens into the

environments. Towards diminishing the release of emerging pollutants and pathogens to the environments, stricter discharge standards of emerging pollutants in treated wastewater are being supplemented regionally and internationally. However, the creation of emerging pollutant discharge limits is confronted by their complex identification and quantification in water bodies (Kosek et al., 2020; Luo et al., 2014). Due to the complicated natures of emerging pollutants, hybrid decentralized wastewater treatment facilities (i.e., multiple treatment steps offering various microenvironments) displayed higher removal efficiencies of emerging pollutants and pathogens compared to the stand-alone facilities. However, this contradicts the philosophy of decentralized treatment, where systems should remain simple to operate and low-cost (Kobayashi et al., 2020). Considering increasingly stricter environmental regulatory standards and economic feasibility, great efforts on high-efficiency, low-cost, and compact decentralized wastewater treatment facilities are necessary (Kobayashi et al., 2020).

1.1.2 Status and Challenges of Wastewater Treatment in Cold Climate

The performances of conventional biological wastewater treatment processes in cold climate have been well investigated, as illustrated in a review article (Zhou et al., 2018). It was found that lower temperatures could lead to (1) significantly lower microbial activity, causing decreased organic degradation, nitrification & denitrification (Di Trapani et al., 2013; Kobayashi et al., 2020; Zhou et al., 2018); and (2) slower sludge settleability due to increased extracellular polymeric substances and increased viscosity of water (Zhou et al., 2018). Towards improving the performance, researchers have attempted to optimize operation conditions (such as increasing sludge retention time, hydraulic retention time, or dissolved oxygen level) or employ bioaugmentation. Moreover, it was reported that biofilm technologies (such as biological aerated filter, moving bed biofilm reactor, or hybrid sludge/biofilm reactor) could adapt better to cold climate than suspended growth biological processes. In detail, biocarriers can provide sufficient surface areas, which allows more biomass attachment and promotes the proliferation of slow-growing microorganisms. Specifically, decentralized wastewater treatment systems commonly suffer from construction mistakes, insufficient maintenance, pipe clogging, or irregular wastewater loading. Thus, when biological processes are applied for decentralized wastewater treatment in cold climate, high fluctuations in effluent quality are noticed, leading to frequent exceeding of national legal discharge limits (Kinnunen et al., 2023).

Alternatively, sand filtration, soil-based systems, package plants, septic tanks and constructed wetlands are commonly used as decentralized treatment technologies in cold climate, while the latter two are largely dominant (García et al., 2013; Hijosa-Valsero et al., 2010; Kinnunen et al., 2023; Kobayashi et al., 2020; Mac Mahon et al., 2022). In detail, septic tanks are passive wastewater treatment systems, which are mostly suitable for household-scale. Most commonly, they consist of two chambers, which can be considered as low-rate anaerobic digesters, where solids settle by gravity force and organics are biodegraded. However, the accumulated sludge requires regular emptying, and malfunctions in sludge settling or biodegradation efficiency (especially in cold climate) can lead to lower effluent quality (Mac Mahon et al., 2022). Nature-based constructed wetlands employ plants, packing materials (i.e., substrate, such as soil), and their associated microbial assemblages to treat wastewater, and displays advantages such as lower maintenance requirements, simple operation, low sludge production and cost (García et al., 2013; Hijosa-Valsero et al.,

2010; Kobayashi et al., 2020). In wetlands, several behaviours, such as aerobic/ anoxic/ anaerobic biodegradation, filtration, sorption, plant uptake, photodegradation, can simultaneously remove organics, nutrients, micropollutants, and pathogens from wastewater (Varma et al., 2021). The application of constructed wetlands for municipal wastewater treatment in cold climate has been systematically reviewed (Ji et al., 2020; Maucieri et al., 2017; Varma et al., 2021; Wang et al., 2017a; Werker et al., 2002), and several challenges have been addressed, such as ice formation and clogging, and reduced biological and plant activity (Varma et al., 2021). It was also illustrated that the effects of cold temperature on organic and nutrient removal efficiencies were highly associated with constructed wetland configuration and operation philosophy (Ji et al., 2020). On the other hand, lower greenhouse gas emissions were noticed in cold temperatures because of lower microbial activity, even though the reported greenhouse gas emission levels varied considerably as they highly depend on plant species, numbers and variety, as well as oxygen availability, wastewater loading and composition, wetland substrate and configuration (Maucieri et al., 2017).

In recent decades, membrane-based decentralized wastewater treatment technologies have received great attention, which could be attributed to their potentially less variable performance under low temperatures (Hube et al., 2020; Zhou et al., 2018). For example, in decentralized membrane bioreactors, excellent membrane separation performance allows achieving superior treated water quality in cold climate, although low temperatures could increase irreversible fouling due to the combined effects of lower biological degradation activity, higher water viscosity and reduced membrane pore sizes (Cui et al., 2017; Krzeminski et al., 2012; Ozgun et al., 2015; Tao et al., 2021a; van den Brink et al., 2011). However, membrane bioreactors present high operational costs due to high energy consumption and maintenance requirements, which limits their decentralized application (Zhou et al., 2018).

1.2 Application of GDM for Wastewater Treatment

Recently, gravity-driven membrane (GDM) filtration technique (driven by water head) for decentralized wastewater treatment has been well developed due to its advantages such as low energy consumption, easy maintenance, and little requirements on facility and auxiliary. In GDM systems, naturally present microorganisms in wastewater proliferate on the membrane surface to form a biofilm matrix, in which prokaryotes perform their roles in biodegradation of organics/nutrients and eukaryotic movement/predation behaviours result in porous cake morphology. Meanwhile, the membrane performs size-exclusion roles in retaining greater-sized substances, leading to superior permeate quality (Pronk et al., 2019).

However, a major challenge of GDM-based wastewater treatment process is its low permeate flux (< 5 L/m^2h without applying any cleaning protocols) due to limited driving force (< 1 m water head). Towards improving water productivity, researchers have attempted several approaches, for example, (1) employing periodic physical/chemical cleaning to remove foulants from the membrane and increase permeability (Derlon et al., 2022; Ding et al., 2016; Fortunato et al., 2020; Guðjónsdóttir et al., 2022; Lee et al., 2019; Oka et al., 2017; Peter-Varbanets et al., 2012; Shami & Wu, 2021; Shi et al., 2020; Stoffel et al., 2022; Tang et al., 2016); (2) combining GDM filtration with other process, such as biofilm pre-treatment (Feng et al., 2022a; Wu et al., 2016), activated carbon or sand filtration (Ding et al., 2018a; Ding

et al., 2018b; Feng et al., 2022b; Guo et al., 2022a; Lin et al., 2022), coagulation (Ding et al., 2017; Du et al., 2022; Huang et al., 2021), or vacuum ultraviolet light treatment (Feng et al., 2022a); (3) optimizing GDM configuration and operation condition, such as designing membrane modules for promoting biofilm growth (Stoffel et al., 2022), selecting appropriate membrane materials (Chawla et al., 2017), employing intermittent operation (Guo et al., 2022b). More details on the strategies for GDM performance improvement will be presented and discussed in the Introduction Sections of Chapters 2-4.

It has been predicted that the need for simple and stable decentralized wastewater treatment processes will increase. Thanks to low energy consumption, stable permeate quality and simple operation, GDM systems show great potential to be applied for decentralized wastewater treatment. To the best of our knowledge, employing GDM for wastewater treatment in cold climate has not been well studied yet. Therefore, there is a need for further research to examine technical, economical, and environmental feasibility of GDM-based wastewater treatment systems, especially in cold climate.

1.3 Research Questions

The research objective of this thesis is to examine the technical feasibility, economic benefit, and environmental impact of the GDM system for decentralized wastewater treatment in cold climate. The thesis addresses the detailed operation design and optimization of the GDM system, as well as the environmental and economic implications when employing the GDM system for real wastewater treatment. The overarching research question is:

How does GDM perform as a decentralized wastewater treatment process in cold climate?

The following questions are addressed to answer the main research question:

(1) How does temperature affect GDM performance and membrane fouling mechanisms (especially with different cleaning protocols)?

(2) How does periodic ultrasonication influence membrane cleaning effectiveness in a GDM system (especially with inorganic membrane)?

(3) How do emerging pollutants (microplastics) influence GDM performance and membrane fouling mechanisms?

(4) Can a GDM system compete with conventional decentralized wastewater treatment technologies in cold climate regarding environmental impact and economic benefit?

1.4 Thesis Organization

The thesis aims to address the above-mentioned research questions. First, in Chapter 1, status and challenges of decentralized wastewater treatment in cold climate are introduced, and the motivation for this research project is explained, followed by the research questions and thesis structure.

Research question 1 is addressed in Chapter 2. GDM technology has been well studied in warmer climates. As low temperatures could influence biological and physical separation behaviors in GDM systems, it is essential to understand detailed membrane filtration mechanisms in order to optimize GDM operation conditions. The results of extensive long-term GDM filtration of wastewater under different temperatures and various physical cleaning protocols are presented. The filtration performance was assessed by water quality testing, fouling resistance analysis, and fouling model simulation.

Research question 2 is addressed in Chapter 3. Organic membranes have been well adopted in GDM systems, however the application of inorganic membranes in GDM systems has not been well investigated yet. Note that ceramic membranes could be especially suitable for decentralized application because of their high stability and long lifespan. In this study, the performance of the GDM system with ceramic membranes in the absence and presence of periodic ultrasonication cleaning was examined, with a constant flux membrane filtration system as comparison.

Research question 3 is addressed in Chapter 4. Microplastics are widely found in the natural environment and present increasing challenges to wastewater treatment. It is crucial to know the influence of microplastics on decentralized wastewater treatment processes. In this study, the GDM systems fed with wastewater containing different amounts and sizes of microplastic beads were operated. The membrane fouling mechanisms and fouling resistance distribution were examined. The influence of microplastics on heavy metal accumulation in GDM systems was illustrated in detail.

Research question 4 is addressed in Chapter 5. To compare the GDM system with the conventionally used treatment systems in decentralized areas (septic tank and constructed wetlands as examples), (1) the recycled construction waste-based wetland was set up and its wastewater treatment performance at different temperatures was examined; and (2) a comparative life cycle assessment (LCA) and economic analysis for septic tank, septic tank + constructed wetlands, and a GDM system were performed.

Main findings and an outlook for future research are presented in Chapter 6.

2 Combined Effect of Temperature and Periodic Cleaning on Gravity-Driven Membrane Filtration

This chapter contains the Article 2:

Hube, S., Lee, S., Chong, T.H., Brynjólfsson, S., Wu, B. 2022. Biocarriers facilitated gravity-driven membrane filtration of domestic wastewater in cold climate: Combined effect of temperature and periodic cleaning. Science of the Total Environment, 833, 155248. https://doi.org/10.1016/j.scitotenv.2022.155248

2.1 Abstract

In this chapter, two lava stone biocarrier facilitated GDM reactors were operated at ~8°C and ~22°C in parallel for treating primary wastewater effluent. Although the biocarrier reactor at 8°C displayed less efficient removals of biodegradable organics than that at 22°C, both GDM systems (without cleaning) showed comparable fouling resistance distribution patterns, accompanied with similar cake filtration constants and pore constriction constants by modelling simulation. Compared to the GDM at 8°C, more foulants were accumulated on the GDM at 22°C, but they presented similar soluble organics/inorganics contents and specific cake resistances. This indicated the cake layers at 22°C may contain greater-sized foulants due to proliferation of both prokaryotes and eukaryotes, leading to a relatively less-porous nature. In the presence of periodic cleaning (at 50°C), the cleaning effectiveness followed a sequence as ultrasonication-enhanced physical cleaning > two-phase flow cleaning > chemical-enhanced physical cleaning > physical cleaning, regardless of GDM operation temperature. However, significantly higher cake resistances were observed in the GDM system at 22°C than those at 8°C, because shear force tended to remove loosely-attached foulant layers and may compress the residual dense cake layer. Nevertheless, operation temperature did not influence GDM permeate quality, which met EU discharge standards.

2.2 Introduction

The application of GDM for wastewater treatment is limited by its low productivity, caused by a low operation pressure (water head). As cake layer fouling was identified as the predominant fouling (55-85% of total fouling) in GDM systems (Lee et al., 2019; Shi et al., 2020; Tang et al., 2016), researchers have attempted to improve GDM permeate flux by employing periodic physical/chemical cleaning (details are summarized in Table 2.1), such as relaxation (Fortunato et al., 2020; Peter-Varbanets et al., 2012; Shi et al., 2020; Stoffel et al., 2022), physical flushing (Derlon et al., 2022; Peter-Varbanets et al., 2012; Shami & Wu, 2021; Shi et al., 2020; Stoffel et al., 2022), aeration (Ding et al., 2016; Fortunato et al., 2020; Lee et al., 2019; Oka et al., 2017; Tang et al., 2016), and chemical cleaning (Guðjónsdóttir et al., 2022; Shami & Wu, 2021).

Table 2.1. Effect of periodic physical/chemical cleaning on membrane performance in GDM systems documented in literature.

GDM system	Feed water	Cleaning protocol	Membrane performance	Reference
GDM bioreactor (UF) Water head: 25cm	Primary municipal wastewater	(1) Membrane relaxation (18 h filtration/6 h relaxation; 45 min filtration/15 min relaxation); (2) Aeration (continuous filtration): 5 min on/ 25 min off; 10 m^3/m^2h; (3) Aeration + relaxation: 30 min filtration/30 min relaxation and 5 min aeration at the end of relaxation	(1) Relaxation: No flux enhancement; (2) Aeration: 25% flux increase; (3) Air scouring + relaxation: 240% flux increase	(Fortunato et al., 2020)
GDM (UF) with biofilm pre-treatment Water head: 57.5 cm	Primary municipal wastewater	(1) Periodic geothermal flushing (50°C) at 6-30 min per 3-4 days; (2) Periodic chemical cleaning (50°C, with 0.5% NaClO or 100 mg/L persulfate) at 10-30 min per 3-4 days	(1) Geothermal flushing: ~15-16% flux recovery; (2) Chemical cleaning: ~31-58% flux recovery	(Guðjónsdóttir et al., 2022)
Granular activated carbon + GDM (UF) Water head: 30 cm	Primary municipal wastewater	Intermittent aeration: 60 min on/60 min off at 2 L/min; 30 min on/60 min off at 2 L/min; 30 min on/60 min off at 0.5 L/min	~130-300% flux increase compared to that without aeration	(Lee et al., 2019)
GDM (MF) with biocarriers Water head: 25 cm	Primary municipal wastewater	Periodical chemical cleaning (0.5% NaClO, 50°C) at 30/60 min every 3-4 days	Flux recovery at ~14.4 - 59.5% after cleaning	(Shami & Wu, 2021)
GDM bioreactor (UF) Water head: 50 cm	Greywater	(1) Direct aeration at 60 L/h with high shear stress on membranes; (2) Indirect aeration at 60 L/h with low shear stress on membranes	Increasing shear stress led to flux decline from 2 to 0.5 LMH (after 120-day operation)	(Ding et al., 2016)
GDM (UF) Water head adapted to achieve a flux of ~10 LMH	Pond water	Air sparging: 5 min on/ 24 h off and 5 min on/ 48 h off; Relaxation 0 h, 1 h, 4 h or 8 h	(1) Air sparging: permeability increased ~73-81% (2) Relaxation + air sparging: permeability increased ~68-123%	(Oka et al., 2017)
GDM (UF) Water head: 100 cm	River water	Periodic flushing for 5 min	More frequent shear led to slower flux decline	(Derlon et al., 2022)
GDM (UF) Water head: 40 cm	River water, Diluted primary	(1) Intermittent filtration (relaxation 3-312 h after 10-day filtration); (2) Intermittent filtration	(1) Flushing after relaxation resulted in higher flux recovery than only relaxation or	(Peter-Varbanets et al., 2012)

	municipal wastewater	(relaxation 3-19 h per day) with following 10 min flushing (0.01 L/min); (3) 10 min flushing per day (0.01 L/min)	only flushing; (2) An increase of daily relaxation time led to increased flux recovery	
GDM (UF) Water head: 110 cm	River water	(1) Flushing for 10 min per 4 h; (2) Flushing for 5 min after 55 min relaxation per day	~56%-67% flux increase compared to that without cleaning	(Stoffel et al., 2022)
GDM (UF) Water head: 65-200 cm	Reservoir water	Aeration: 10 min on/1 min off, 3 h on/21 h off, 6 h on/18 h off, and 12 h on/12 h off	~49-92% flux increase compared to that without aeration	(Tang et al., 2016)
GDM (UF) Water head: 55 cm	Lake water	(1) Relaxation (60 min per day); (2) Flushing (1 min at 0.1 m/s per day); (3) Relaxation (60 min per day) + flushing (1 min at 0.1 m/s per day)	(1) Relaxation or flushing alone did not increase flux; (2) Combined relaxation and flushing led to 70% flux increase	(Shi et al., 2020)

Theoretically, membrane relaxation allows cake layer foulants to diffuse back to the solution in the absence of pressure. Meanwhile, the biofilm layer remained active during standstill periods, in which eukaryotic predation/movement could enhance the formation of a porous and heterogeneous cake layer (Peter-Varbanets et al., 2012). Especially, under the optimal relaxation frequency, an increase of cake layer thickness with lessening specific cake resistance was observed in the GDM systems (Fortunato et al., 2020). However, merely employing membrane relaxation in the GDM systems did not always enhance permeate flux (Oka et al., 2017; Shi et al., 2020). Alternatively, introducing shear force along membrane surface via air scouring or liquid flushing was performed in the GDM systems, aiming to physically remove cake layers (Lee et al., 2019; Peter-Varbanets et al., 2012). When shear force was applied during membrane relaxation, the expanded cake layer could be more easily detached from the membrane surface, leading to flux enhancement (Fortunato et al., 2020; Guðjónsdóttir et al., 2022a; Shami & Wu, 2021). However, researchers noticed that employing shear force may increase irreversible fouling in GDM systems, possibly because (1) the residual biofilms were more resistant to erosion due to their elastic, cohesive and smooth properties, as a result, the subsequent filtration promoted to form a thinner, compressed, and more resistant irreversible foulant layer; (2) after the cake layer was detached, smaller-sized foulants may cause membrane pore constriction or blocking (Derlon et al., 2022; Ding et al., 2016; Fortunato et al., 2020; Lee et al., 2019; Shi et al., 2020). Thus, short-term chemical-enhanced physical cleaning was adopted in the GDM systems, resulting in more effective flux recovery (Guðjónsdóttir et al., 2022; Shami & Wu, 2021).

On the other hand, in membrane-based wastewater treatment processes (such as MBRs), it was found that temperature could affect the cake fouling layer morphology (Ma et al., 2013). In detail, lowering operation temperature led to increased irreversible fouling, which was mainly attributed to several facts, such as (1) lower biological degradation capability leading to more untreated organics and soluble extracellular polymeric substances available for membrane filtration; (2) higher water viscosity; and (3) reduced pore size and lumen diameter (hollow fiber) causing an increase of membrane resistance (Cui et al., 2017;

Krzeminski et al., 2012; Ozgun et al., 2015; Tao et al., 2021a; van den Brink et al., 2011). In our previous study (Shami & Wu, 2021), we found that lowering temperature from 21°C to 10°C caused a decline of permeate flux in the GDM reactor with synthetic fibre as biocarriers. Meanwhile, temperature had an insignificant impact on the permeate flux in the Icelandic lava stone or sand facilitated GDM reactor. However, there is still a lack of knowledge on the optimization of periodic cleaning protocols and fundamental mechanisms relating to flux enhancement in GDM systems operated under low-temperature conditions.

This chapter aims to investigate membrane performance and permeate quality in lava stone facilitated GDM systems under combined effects of temperature and periodic cleaning. Several cleaning strategies at various cleaning frequencies were applied, such as geothermal water flushing, two-phase flow cleaning, ultrasonication- and chemical-enhanced physical cleaning. The membrane fouling mechanism was illustrated by fitting experimental permeate flux data with a previously reported constant pressure filtration model. The effects of temperature on biodegradation behaviours of biofilms and membrane separation efficiency were illustrated by periodically examining water quality in the GDM reactor and permeate.

2.3 Materials and Methods

2.3.1 Experimental Setup

Two identical biocarriers facilitated GDM systems were set up (Figure 2.1) and operated at ~8°C (placed inside a temperature-controlled refrigerator) and ~22°C (placed in the lab at room temperature), respectively. In detail, Icelandic local lava stones (diameter: ~5-16 mm, density: ~2.33×10^3 kg/m^3) were used as biocarriers and packed (40% packing ratio) in the bottom of a tank (effective volume of 1 L). Four parallel membrane filtration cells were externally located under a constant water head of 60 cm, i.e., a trans-membrane pressure (TMP) at ~6 kPa. A piece of polyvinylidene fluoride (PVDF) microfiltration membrane (a nominal pore size of 0.08 μm and an effective membrane area of 24 cm^2) was placed in each filtration cell. The permeate was collected and weighted periodically by a digital balance (OHAUS, US). The feed water was delivered to the tank via a feed pump (Longer, China), and its flowrate was periodically regulated based on permeate flowrate. The average hydraulic retention time in the GDM systems was estimated at ~12 hr, which is calculated by dividing the bioreactor volume with the feed flowrate. The permeate flux (J, L/m^{2}h, LMH) was calculated as $J = \frac{\Delta V}{\Delta t \times A}$ (ΔV is the collected permeate water volume during filtration duration Δt, and A is membrane area). The water productivity (P_w, L/day) was calculated as $P_w = \frac{\sum \Delta V}{\sum \Delta t}$.

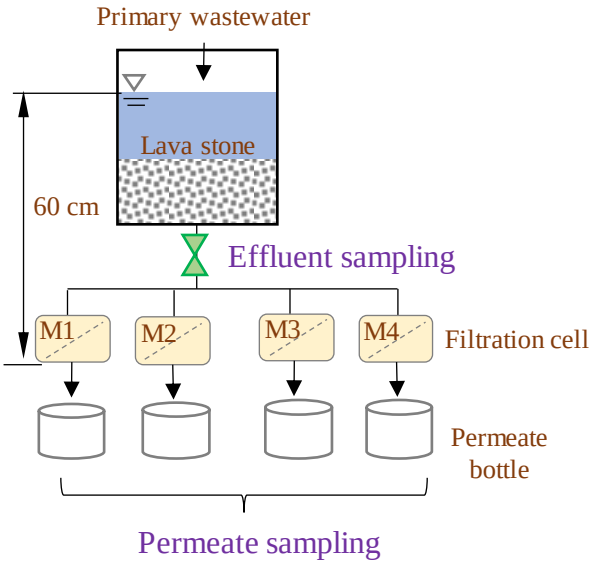

Figure 2.1. Schematic diagram of the biocarriers facilitated GDM system.

2.3.2 Wastewater and Geothermal Water

The feed wastewater was periodically collected from the primary settling tank in Veitur wastewater treatment plant at Klettagarður (Reykjavík, Iceland). The geothermal water (as cleaning water) was directly collected from the hot water tap and its characteristics were listed in Table 2.2.

Table 2.2. Geothermal water characteristics (Ionic concentration data were derived from literature (Gunnarsdottir et al., 2014; Kristmannsdóttir et al., 2010).

	Geothermal water
pH	7.82
Conductivity (μS/cm)	215
Si (mg/L)	64.78
Na (mg/L)	52.5
K (mg/L)	1.8
Ca (mg/L)	2.4
Mg (mg/L)	0.002
Fe (mg/L)	0.0015
Al (mg/L)	0.193
Cl (mg/L)	28.5
SO_4 (mg/L)	15.6

2.3.3 Filtration Experiments Protocol

The GDM systems were operated for ~ 128 days and their operations were divided into 7 phases as described in Table 2.3. In each phase, cleaned membranes with comparable membrane resistance were used after examining their clean water fluxes (J_0) at a water head of 60 cm. The clean membrane resistance was calculated as $R_m = \frac{TMP}{\mu \times J_0}$ (where TMP is 6 kPa,

μ is water viscosity at operation temperature). When membrane filtration was performed under no-cleaning conditions, the effluent from the biocarrier reactor was continuously delivered to the membrane filtration cell after it was installed in the GDM system.

Table 2.3. A summary of membrane cleaning protocols in the GDM systems

Biofilm reactor operation time	Membrane cleaning condition	Membrane module			
		M1	M2	M3	M4
Day 0-15	**Phase I:** Geothermal water flushing (50°C)	No cleaning	10 min	30 min	60 min
Day 16-32	**Phase II:** Air sparging + geothermal water flushing (50°C)	0.3 L/min (60 min)	0.3 L/min (30 min)	0.6 L/min (30 min)	0 L/min (30 min)
Day 35-52	**Phase III:** PMS in geothermal water (50°C) for 30 min flushing	10 mg/L PMS	50 mg/L PMS	100 mg/L PMS	0 mg/L PMS
Day 56-66	**Phase IV:** No cleaning	No cleaning	No cleaning	No cleaning	No cleaning
Day 70-86	**Phase V:** Ultrasonication (50°C)	10 min	30 min	60 min	No cleaning
Day 90-108	**Phase VI:** Ultrasonication with geothermal water flushing (50°C) for 30 min	Ultrasonication	Ultrasonication + geothermal water flushing	Ultrasonicated geothermal water flushing	No cleaning
Day 109-128	**Phase VII:** Comparison of physical and chemical cleaning (50°C, 30 min)	PMS (50 mg/L) in geothermal water flushing	Ultrasonication + geothermal water flushing	Air sparging (0.3 L/min) + geothermal water flushing	No cleaning

During periodic membrane cleaning (per 3-4 days of filtration), the individual influent line of the membrane filtration cell was clamped and the membrane cells were detached from the GDM setup to perform cleaning. In our previous studies (Guðjónsdóttir et al., 2022; Hube et al., 2021a; Hube et al., 2021b), it was found that cleaning water at a high temperature (50°C) displayed more effective fouling reduction. Thus, in this study, the cleaning temperature at 50°C was adopted for each cleaning protocol. In detail, (1) geothermal water flushing: ~300 mL of geothermal water (50°C) was recirculated along the membrane surface at a crossflow velocity of 0.01 m/s; (2) air sparging + geothermal water flushing (i.e., two-phase flow): an air pump was used to deliver air at a certain flowrate (controlled by a flow meter) into the geothermal (~300 mL, 50°C) flushing line (crossflow velocity of 0.01 m/s). The membrane was tilted by 20° during gas sparging in order to enhance shear force

(Mohamad Annuar et al., 2020); (3) chemical cleaning: potassium peroxymonosulfate (PMS; Sigma-Aldrich, US) solution was prepared by dissolving it into geothermal water. The PMS solution (~300 mL, 50°C) was recirculated along the membrane surface at a crossflow velocity of 0.01 m/s; (4) ultrasonication: the membrane cell was submerged in an ultrasonication bath (SONOREX RK 100 H, Germany; frequency: 35 kHz) and ultrasonication was performed at 50°C for a certain period of time; (5) ultrasonication + geothermal water flushing: the membrane cell was submerged in the ultrasonication bath and ~300 mL of geothermal water (50°C) was recirculated along the membrane surface at a crossflow velocity of 0.01 m/s during ultrasonication; (6) ultrasonicated geothermal water flushing: the membrane cell was located outside the ultrasonication bath, while the geothermal water (50°C) was ultrasonicated and recirculated along the membrane surface at a crossflow velocity of 0.01 m/s.

2.3.4 Fouling Resistance Examination and Fouling Model Fitting

To elucidate GDM fouling mechanisms, a series of fouling resistance distribution was examined based on the protocols in our previous studies (Lee et al., 2021; Lee et al., 2019). In detail, after each filtration, the final flux was recorded as J_1 and the total resistance (R_t) was calculated as $R_t = \frac{TMP}{\mu \times J_1}$ (where TMP is 6 kPa, μ is water viscosity at operation temperature). The fouling distribution was examined based on the protocol as follows: (1) the membrane module was detached from the reactor and the cake layer foulants were fully removed from the membrane surface with a cotton swab. Clean water filtration (under water head of 60 cm) was conducted with the physically cleaned membrane and the permeate flux (J_2) was recorded; (2) after chemical cleaning (0.5% NaOCl, soaking overnight), clean water filtration (under water head of 60 cm) was conducted and its permeate flux (J_3) was recorded. The cake layer resistance (R_c), irreversible fouling resistance, and irremovable fouling resistance were calculated as $(\frac{TMP}{\mu \times J_1} - \frac{TMP}{\mu \times J_2})$, $(\frac{TMP}{\mu \times J_2} - \frac{TMP}{\mu \times J_3})$, and $(\frac{TMP}{\mu \times J_3} - \frac{TMP}{\mu \times J_0})$, respectively. After each periodic cleaning, the fouling removal ratio (%) was evaluated as $(\frac{R_{fb} - R_{fa}}{R_{fb}}) \times 100\%$, in which R_{fb} represents the total fouling resistance before periodic cleaning and R_{fa} represents the total fouling resistance after periodic cleaning.

In addition, the membrane fouling mechanisms were illustrated based on mathematical simulation, i.e., the flux data (continuous filtration without any periodic cleaning) were fitted to the previously-reported constant pressure dead-end filtration equations (Table 2.4) (Ho & Zydney, 2000; Ye et al., 2005). The linear coefficient value of the simulation curve ($R^2 \geq 0.95$) was presented as the filtration constant.

Table 2.4. Dead-end filtration models for describing the membrane fouling mechanism under constant pressure condition (Ho & Zydney, 2000; Ye et al., 2005).

Governing equation	$\frac{d^2t}{dV^2} = k\left(\frac{dt}{dV}\right)^n$	t: filtration time; V: filtered water volume
$n = 0$	$t/V = aV + b$	Cake filtration
$n = 1$	$1/J = at + b$	Intermediate pore blocking
$n = 1.5$	$t/V = at + b$	Pore constriction
$n = 2$	$ln\ (J_0/J) = at + b$	Complete pore blocking

Note: “a” represents the constant value in each filtration equation.

2.3.5 Cake Foulants Characterization

The cake layer foulants were suspended with 10 mL clean water and their total suspended solids (TSS) concentration was measured using a spectrophotometer (Hach, US). The specific cake resistance (m/mg) was calculated by dividing the cake resistance (m^{-1}) with the foulants mass density (mg/m^2). The cake layer foulant solution was filtered through a 0.45 μm filter and the filtrate (i.e., soluble foulants) was collected for further analysis. The soluble organic foulant components in the cake layers were analysed by a liquid chromatography-organic carbon detection analyser (LC-OCD; DOC-Labor, Germany) following the details described in a previous study (Huber et al., 2011). The inorganic fraction of the soluble cake layer foulants was examined by inductively coupled plasma-optical emission spectroscopy (ICP-OES; Perkin Elmer, USA).

2.3.6 Water Quality Analysis

The feed, reactor effluent, permeate samples were collected periodically. The pH and conductivity were measured using a pH meter (Hach, US) and a conductivity meter (Hach, US), respectively. The total suspended solids (TSS), chemical oxygen demand (COD), and total nitrogen (TN) were measured using analysis kits (Hach, US) and a spectrophotometer (DR3900, Hach, US), according to the manufacturer's manual. Biological oxygen demand (BOD_5) was measured following standard methods (APHA, 1998). To examine the statistical significance of two different sets of data, the *p*-value was calculated based on a two-sample T-test (Microsoft Excel). The statistically significant difference was recorded when *p*-value was <0.05 (a confidence interval of 95%).

2.4 Results and Discussion

2.4.1 Water Quality of GDM Systems

The water qualities of feed, reactor effluent and membrane permeate are summarized in Table 2.5 and Figure 2.2. In detail, the two lava stone biofilm reactors produced effluents with comparable pH, conductivity, COD, TN, and TSS, regardless of operation temperature ($p>0.05$). Accordingly, both biofilm reactors achieved comparable COD removals, TN removals, and TSS removals. However, relatively lower BOD_5 levels (21.1 ± 8.8 mg/L) in the effluent of the biofilm reactor operated at 22°C were noticed compared to those at 8°C (27.6 ± 13.4 mg/L; $p<0.05$). This reveals that increasing temperature significantly promoted biodegradable organic (BOD_5) removals in the biofilm reactors (56 ± 27% at 22°C *vs.* 47 ± 26% at 8°C, $p<0.05$).

Furthermore, the GDM systems produced permeates with relatively comparable quality (Table 2.5 and Figure 2.2, $p>0.05$) in terms of pH, conductivity, COD, BOD_5, TN, and TSS. It is noted the permeates from the two GDM systems had relatively higher pH levels than the feed ($p<0.05$; Table 2.5). In our previous study (Guðjónsdóttir et al., 2022), it was found that the presence of MnOx in the lava stone facilitated nitrification by serving as oxidants. The subsequently produced Mn^{2+} promoted denitrification, leading to TN removal in the GDM system. Thus, the alkaline by-products generated during the denitrification process caused pH elevation. Nevertheless, the GDM systems could remove 67-71% of COD, 93-

96% of BOD_5, 27-32% of TN, and ~100% of TSS, regardless of the operation temperatures. Accordingly, the GDM permeates met European urban wastewater discharge standards (COD ≤ 125 mg/L; BOD_5 ≤ 25 mg/L; TSS ≤ 35 mg/L; TN <15 mg/L in sensitive areas) (European Union, 1991).

Table 2.5. Water quality in the GDM systems

	Feed	**Effluent (22°C)**	**Effluent (8°C)**	**Permeate (22°C)**	**Permeate (8°C)**
pH	7.70 ± 0.26	8.03 ± 0.25	7.99 ± 0.23	8.76 ± 0.29	8.73 ± 0.24
Conductivity (μS/cm)	1518 ± 308	1559 ± 254	1499 ± 289	1659 ± 237	1644 ± 252
COD (mg/L)	101.2 ± 54.8	36.4 ± 19.1 *(58 ± 19%)*	42.3 ± 13.9 *(51 ± 37%)*	25.8 ± 7.5 *(67 ± 21%)*	25.1 ± 8.6 *(71 ± 19%)*
BOD_5 (mg/L)	52.4 ± 30.0	21.1 ± 8.8 *(56 ± 27%)*	27.6 ± 13.4 *(47 ± 26%)*	2.0 ± 2.1 *(93 ± 10%)*	1.6 ± 1.8 *(96 ± 4%)*
TN (mg/L)	14.4 ± 3.5	14.4 ± 8.5 *(16 ± 12%)*	12.3 ± 2.3 *(15± 8%)*	10.1 ± 3.3 *(27 ± 10%)*	9.8 ± 2.7 *(32 ± 10%)*
TSS (mg/L)	32.2 ± 63.2	3.9 ± 7.5 *(79 ± 42%)*	3.6 ± 2.5 *(72 ± 38%)*	0	0

Note: The number in the bracket represents removal efficiency by comparing the levels in effluent and feed (i.e., removal efficiency in the biofilm reactor), or comparing the levels in the permeate and feed (i.e., removal efficiency in the biofilm-GDM system).

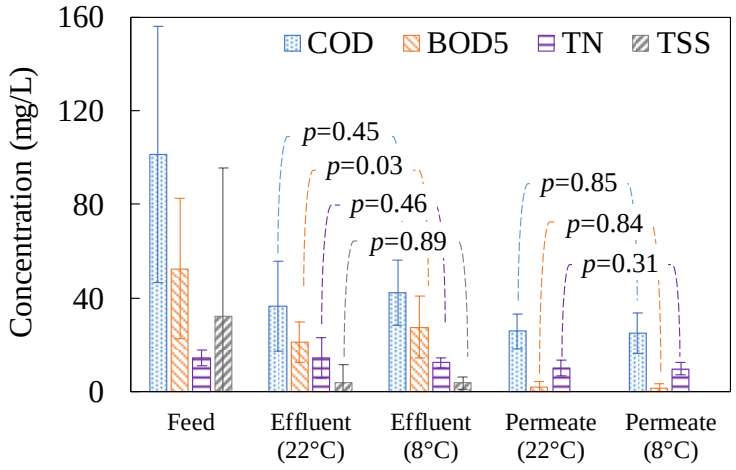

Figure 2.2. Water quality in feed, effluent and permeate (n=10-15). "p" represents p-value; TSS level in the permeate was ~ 0 mg/L, thus the column did not appear in the figure.

2.4.2 Membrane Fouling Mechanism during Continuous Filtration (no Periodic Cleaning)

Flux Development, Resistance Distribution, and Model Fitting

Figure 2.3a shows the GDM flux evolution (no periodic cleaning) with extending biofilm reactor operation time. In each phase, an obvious flux drop occurred during the initial several hours (>90% loss of initial flux), followed by a slow flux decrease within ~ 3 days. After that, the fluxes tended to be relatively stabilized or fluctuated slightly. It is noted that the

feed wastewater presented great temporal variations in its composition (e.g., COD ranging from ~30.6 to ~216.2 mg/L, TSS from ~2 to ~265 mg/L) throughout the GDM operation period. However, the biofilm reactor displayed efficient biodegradation and straining of larger-sized particles, accordingly, leading to relatively comparable stabilized flux level in each phase under both 22°C and 8°C.

Among the tested five phases, similar flux profiles were noticed in phases I and VII for the GDM systems receiving the effluents of biofilm reactors operated at 22°C and 8°C, while slightly higher (phases IV and V) or lower (phase VI) final fluxes were observed in the GDM system at 22°C compared to those at 8°C. To make a fair comparison, the average permeate water productivity in each GDM system (no periodic cleaning) was compared, as shown in Figure 2.4. On average, the biofilm GDM system operated at 22°C (~0.21 L/day) achieved ~24% higher water production compared to that at 8°C (~ 0.17 L/day).

At the end of the GDM filtration, resistance analysis was performed, and the averaged resistance levels were presented in Figure 2.3b. It was found that the cake layer resistance constituted more than 90% of the total fouling resistance (i.e., predominant fouling mechanism), regardless of biofilm operation temperature and time span. This was in accordance with the findings in previous GDM-based wastewater treatment processes (Fortunato et al., 2020; Guðjónsdóttir et al., 2022; Jin et al., 2019; Lee et al., 2021; Lee et al., 2019; Shami & Wu, 2021; Wang et al., 2017b). In addition, there were no significant differences of cake layer resistance (p=0.19), irreversible fouling resistance (p=0.70), and irremovable fouling resistance (p=0.78) in the GDM systems operated at 8°C and 22°C, respectively. This indicated that the operation temperature had an insignificant influence on filtration resistance and resistance distribution.

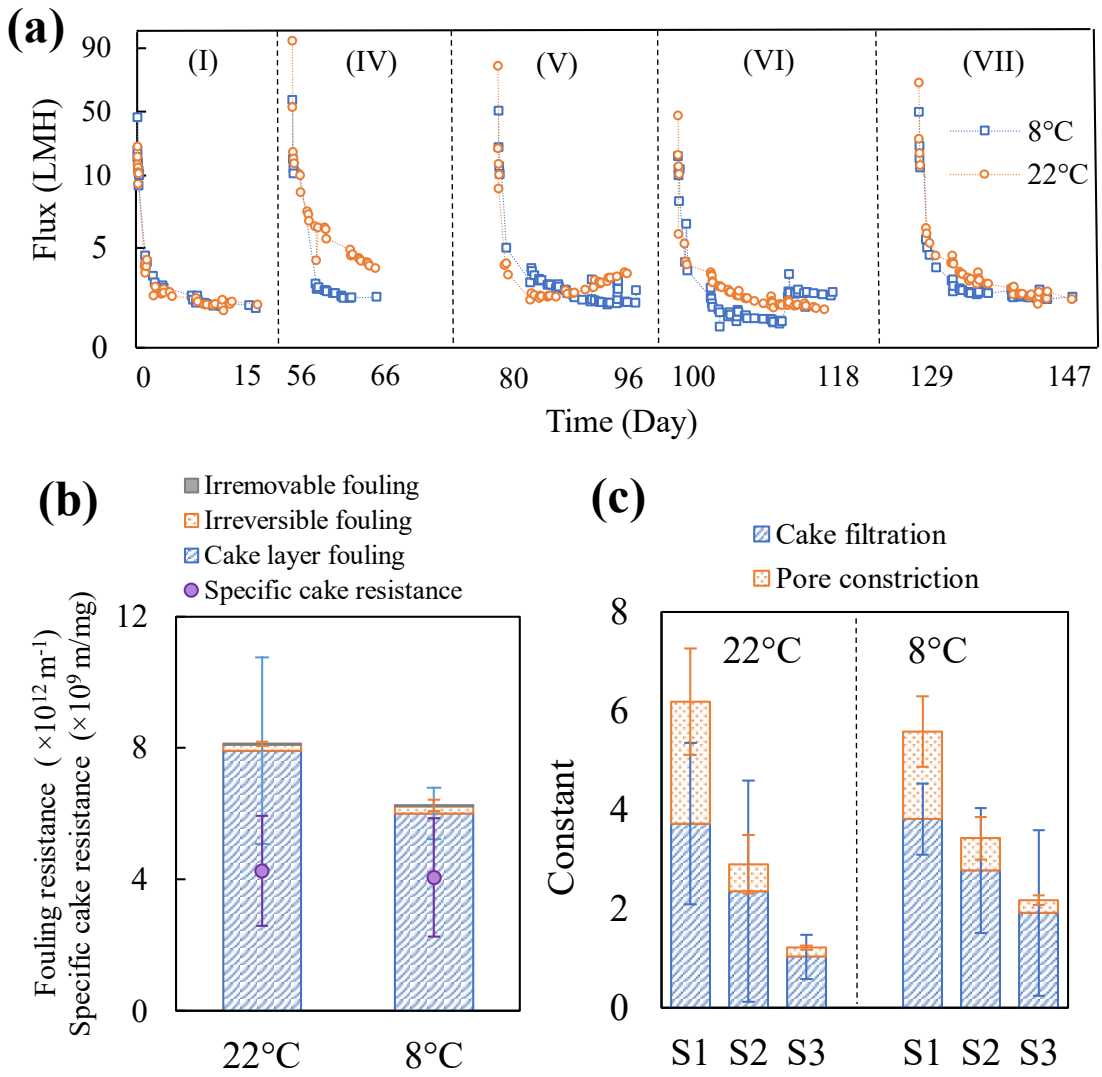

Figure 2.3. (a) Flux development, (b) resistance distribution (n=5), and (c) simulated filtration constants (n=5) in the GDM systems (no periodic cleaning). Stage 1 (S1) refers to the flux profile < ~1 day, Stage 2 (S2) refers to the flux profile during ~1-3 days; Stage 3 (S3) refers to the flux profile > ~3 days (the detailed simulation profiles for each phase were presented in Figure 2.5)

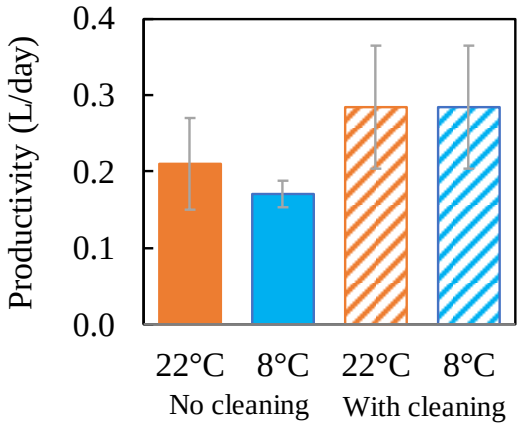

Figure 2.4. Permeate water productivity of GDM systems with/without periodic cleaning.

Meanwhile, filtration simulation was conducted based on the measured flux profiles and the previously-reported constant pressure dead-end filtration model (Table 2.4) (Ho & Zydney, 2000; Ye et al., 2005). As shown in Figure 2.3c, cake filtration and pore constriction were dominant fouling behaviours under different GDM operation durations and temperatures. This observation was similar to the findings in the previously reported GDM systems for seawater pre-treatment and wastewater treatment (Akhondi et al., 2015; Guðjónsdóttir et al., 2022; Wu et al., 2016). As demonstrated in all simulation profiles (Figure 2.5), the GDM filtration of wastewater followed a three-stage pattern in terms of filtration time, i.e., Stage 1 (S1): < ~1 day, Stage 2 (S2): ~ 1-3 days; Stage 3 (S3): > ~ 3 days. The simulated filtration constants for each stage were calculated according to the linearly fitting curves ($R^2 \geq 0.99$) and summarized in Figure 2.3c.

Clearly, both cake filtration and pore constriction constants decreased with extending filtration time, coinciding with GDM flux profiles under both temperature conditions (Figure 2.3a). In particular, at each stage, cake filtration/pore constriction constants were not influenced by operation temperature of GDM systems (all *p*-values >0.05). In detail, during the initial stage (i.e., Stage 1), the higher pore constriction constant may be associated with the effective interaction of smaller-sized foulants and a clean membrane via partially blocking membrane surface pores (Akhondi et al., 2015; Guðjónsdóttir et al., 2022). Our previous study (Guðjónsdóttir et al., 2022) also revealed that the lava stone biocarriers tended to release some fine particles, which could contribute to a rapid cake layer formation (i.e., higher cake filtration constant). As a result, the faster cake formation and pore constriction led to the rapid initial flux decline on the first day of GDM filtration. In the following Stage 2, the cake filtration constant displayed a slower drop trend (~28% drop at 8°C and ~42% drop at 22°C compared to the respective level in Stage 1) than the pore constriction constant (~63% drop at 8°C and ~78% drop at 22°C compared to the respective level in Stage 1). Similarly, in the Stage 3, both cake filtration and pore constriction continuously reduced, and the pore constriction constants were limited. It is recalled that the irreversible and irremovable fouling resistances contributed less than 10% to the total fouling (Figure 2.3b). Possibly, after cake layers covered the membrane surface, the smaller-sized foulants would contact the void openings in the top cake layers, performing pore constriction of the existing cake layers. With expanding filtration time, cake layers tended to be less porous, offering less chances for pore constriction (i.e., significant drop of pore constriction constants).

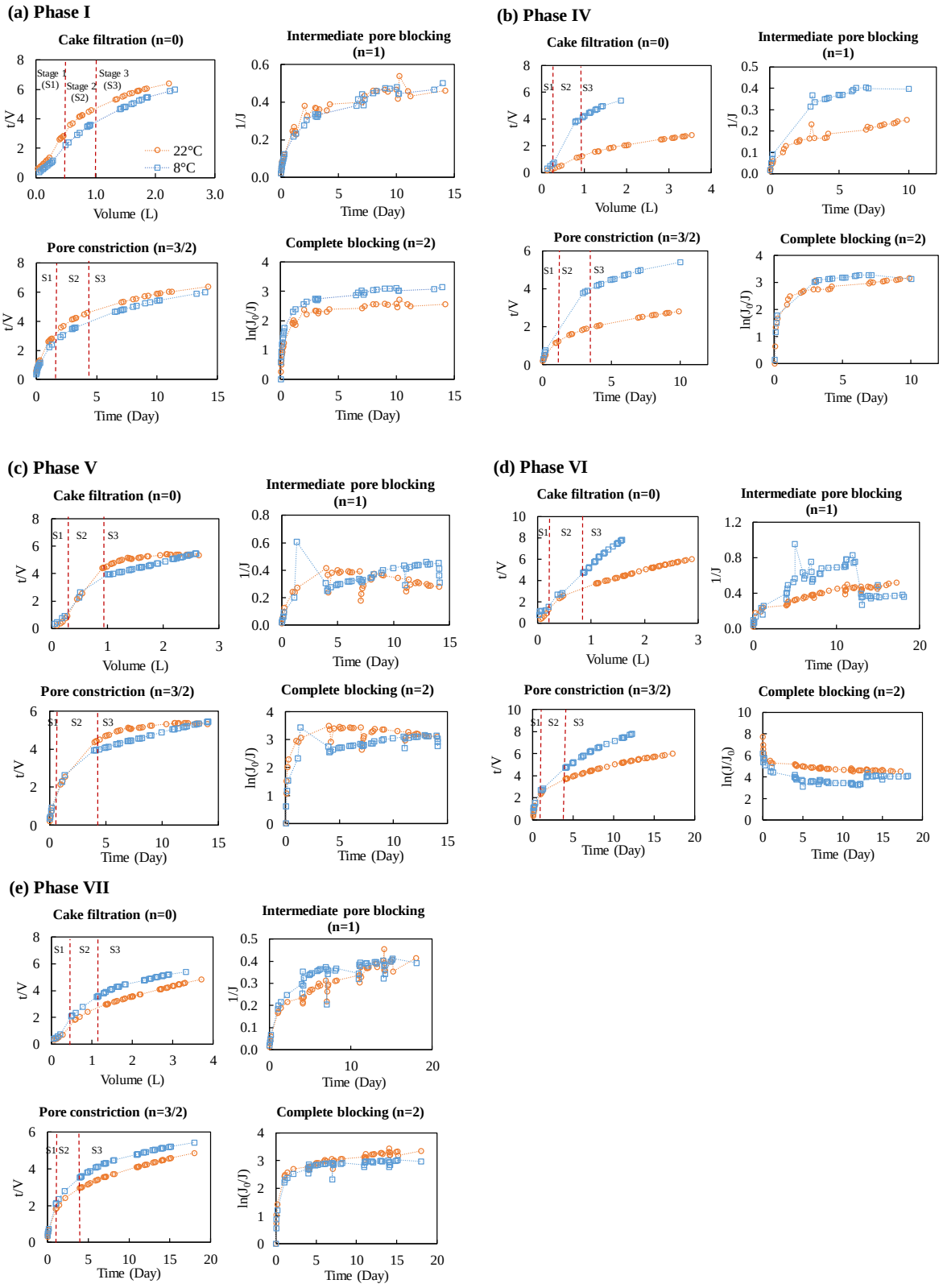

Figure 2.5. Membrane mechanism description based on the simulation profiles during continuous filtration (linear correlation coefficient $R^2 \geq 0.99$). Note: the dot red lines in the figure are used to indicate three stages, but the time duration of each stage for each stage for each flux simulation profile was dissimilar.

Cake Foulants Analysis

At the end of each phase, the cake layer foulants were collected and the soluble organic (biopolymers, humic substances, building blocks, and low molecular weight (LMW) neutrals) and inorganic components (Na, Si, Ca, Mg, Fe, SO_4, and PO_4) were analysed, as shown in Figure 2.6. Clearly, the biopolymers (typically MW > 10 kDa) performed as the dominant organic foulants in the cake layers, contributing 75 ± 12% (22°C) and 77 ± 7% (8°C) to the total dissolved organics (DOC) respectively. In the cake layer foulants, Si and Ca contents were comparable, representing the major divalent cations under both temperature conditions. The soluble organic and inorganic components in the cake layers were independent of the GDM operation temperature (p>0.05). Interestingly, the total cake foulant mass collected from the GDM at 22°C was significantly higher than that at 8°C (2.03 ± 0.71 g/m^2 *vs.* 1.54 ± 0.50 g/m^2; p<0.05). Such observations revealed that the GDM operation temperature could influence the surface density of cake foulants developed on the membrane, which was majorly attributed to the particulate foulants having sizes greater than 0.45 µm (such as microbial flocs) instead of soluble foulants.

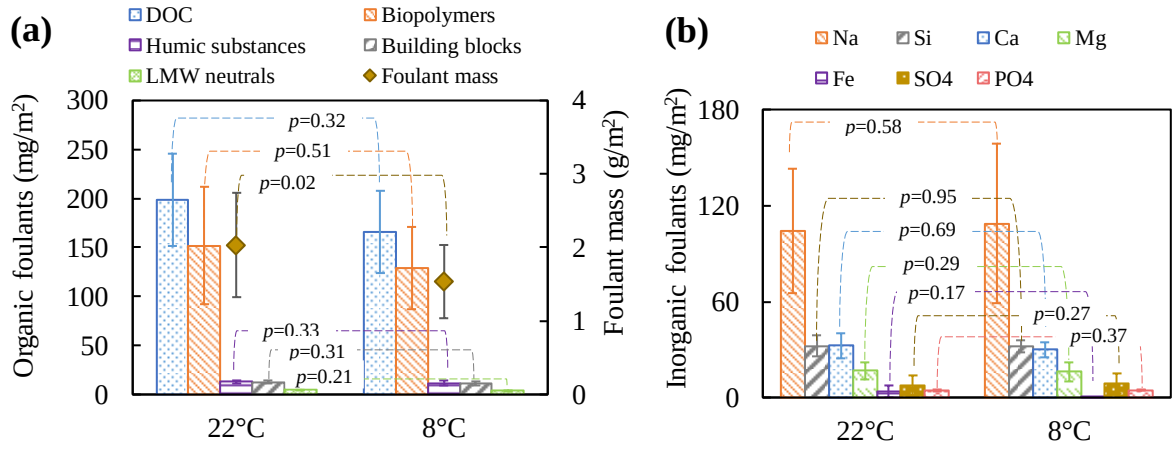

Figure 2.6. (a) Soluble organics in the cake layers and cake foulant mass, and (b) Soluble inorganics in the cake layers on the membrane surface (no periodic cleaning).

2.4.3 GDM Performance with Periodic Cleaning

Flux Development, Fouling Mechanisms, and Cake Layer Properties

To improve permeate water productivity of the GDM systems, periodic physical/chemical-enhanced physical cleaning was performed per 3-4 days (i.e., before flux stabilization). The flux development profiles of the GDM systems with different cleaning protocols were plotted in Figure 2.7. After cleaning, the flux was improved, but it appeared to drop promptly and then followed a similar flux profile as that under the control condition (no periodic cleaning).

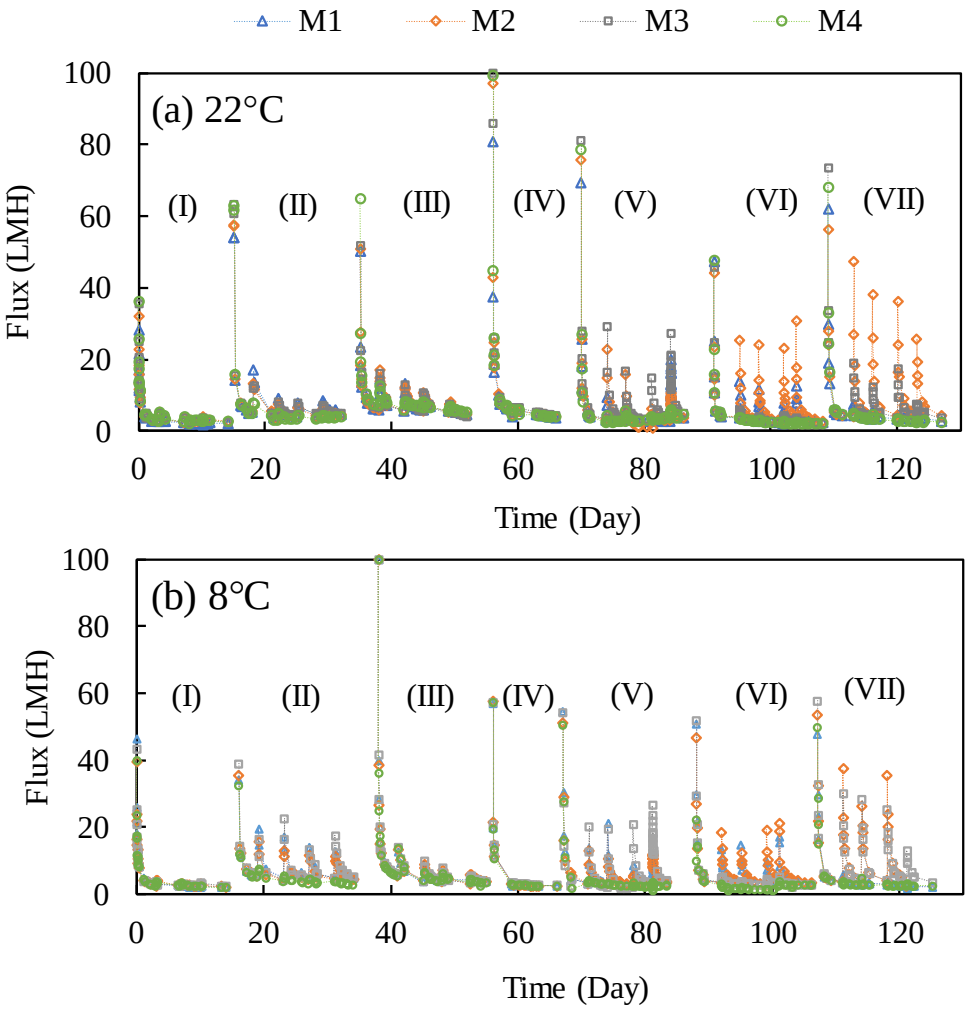

Figure 2.7. Flux profiles of the GDM systems operated under different temperatures.

To optimize the cleaning protocol, the cleaning effectiveness (i.e., fouling removal ratio) under each phase was illustrated in Figure 2.8a. In phase I, geothermal water (50°C) was used to periodically flush the membranes at a duration of 10, 30, and 60 min per 3-4 days, respectively. Under both temperature conditions, increasing cleaning duration from 10 to 60 min did not significantly improve fouling removal ratio (from ~20 to ~35%). This was possibly associated with limited shear force induced by a crossflow velocity of 0.01 m/s. Furthermore, air bubbles (0.3 and 0.6 L/min) were introduced into the geothermal water (50°C) flushing line to perform two-phase flow cleaning (Phase II). Clearly, the additional shear benefited to remove foulants, leading to ~46-57% and ~62-70% fouling removal for the GDM system at 22°C and 8°C, respectively. However, both increasing air flowrate from 0.3 to 0.6 L/min (duration at 30 min) and extending cleaning duration from 30 min to 60 min (air flowrate of 0.3 L/min) led to comparable flux recovery.

In phase III, PMS-enhanced geothermal water (50°C) flushing was applied for periodic membrane cleaning. The presence of PMS slightly improved fouling removal, e.g., the fouling removal ratio improved from ~22% to ~46% (22°C) and from ~37% to ~51% (8°C) when the PMS concentration increased from 0 to 50 mg/L; while further increasing PMS concentration to 100 mg/L did not further reduce fouling. This finding was in accordance with our previous study (Guðjónsdóttir et al., 2022), in which there were no great differences

in flux recovery between geothermal water flushing and Persulfate (100 mg/L)-enhanced geothermal water flushing. It is recalled that cake layer fouling was predominant, and their contribution to the total fouling increased with extending filtration duration (Figure 2.3c). Possibly, PMS merely interacted with the top fouling layer due to their greater molecular size with lower diffusion rate, leading to limited contribution to irreversible fouling removal.

In recent years, ultrasonication has been reported as an alternative physical membrane fouling control strategy, by which ultrasonication-induced cavitation bubbles facilitate detaching the foulants from the membrane surface (Kan et al., 2016; Luo & Wang, 2022). In phase V, ultrasonication cleaning (50°C) via submerging membrane cells into an ultrasonication bath was performed for 10, 30, and 60 min, respectively. Obviously, increasing ultrasonication duration from 10 to 60 min slightly benefited for fouling removal (~20% enhancement). Furthermore, the fouling control effectiveness of ultrasonication, ultrasonicated geothermal water flushing, and combined ultrasonication with geothermal water flushing (ultrasonication-enhanced physical cleaning) was compared in Phase VI. The ultrasonication-enhanced physical cleaning resulted in the most effective fouling reduction (~86% at 22°C and ~78% at 8°C), slightly higher than those only with ultrasonication (~75% at 22°C and ~74% at 8°C) and much more efficient than those with ultrasonicated geothermal water flushing (~34% at 22°C and ~28% at 8°C). It was believed that ultrasonication-induced cavitation locally offered much stronger shear force to dislodge the foulants from the membrane surface (i.e., cavitation bubbles could reach the membrane module). Especially, when additional crossflow shear force was combined with ultrasonication, it did help to efficiently remove the loosened foulants from the membrane surface, leading to enhanced fouling mitigation.

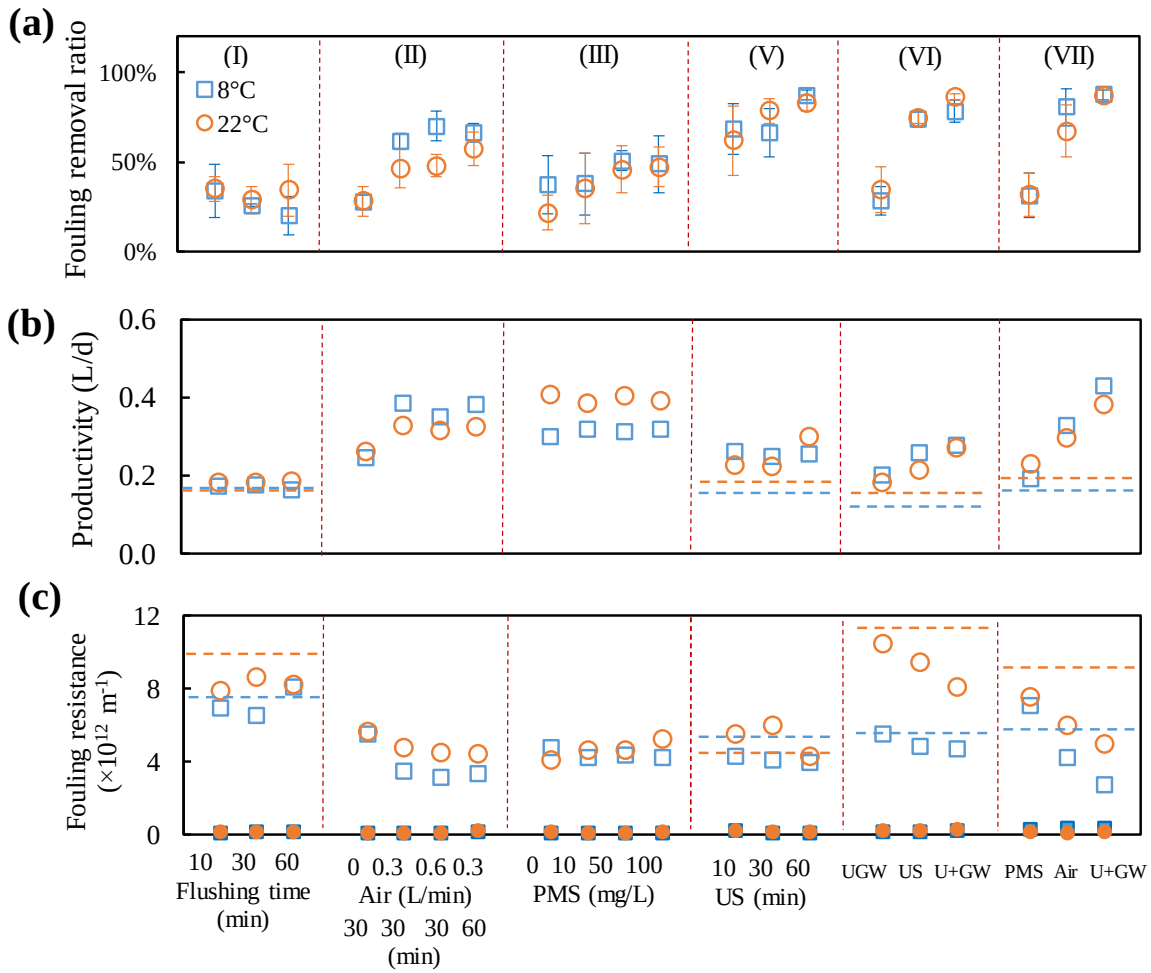

Figure 2.8. (a) Fouling removal ratio, (b) water productivity, and (c) fouling resistance (non-fill symbols represent cake layer fouling, solid-fill symbols represent irreversible fouling) in the GDM systems with different periodic cleaning protocols. The dash line indicated the level in the control membrane module without periodic cleaning. "UGW" represents ultrasonicated geothermal water flushing; "US" represents ultrasonication; "U+GW" represents ultrasonication + geothermal water flushing.

It is noted that the cleaning effectiveness may be influenced by the biofilm reactor effluent quality due to variable feed wastewater characters. To make a fair comparison of various types of cleaning protocols, PMS (50 mg/L)-enhanced geothermal water flushing, two-phase flow cleaning (0.3 L/min air with geothermal water flushing), and ultrasonication+ geothermal water flushing (ultrasonication-enhanced physical cleaning) methods were applied in parallel for the GDM systems in Phase VII (50°C, 30 min). Overall, the cleaning effectiveness followed a sequence as "ultrasonication-enhanced physical cleaning" (~87% at 22°C and ~88% at 8°C) > "two-phase flow cleaning" (~67% at 22°C and ~81% at 8°C) > "chemical-enhanced physical cleaning" (~32% at 22°C and ~31% at 8°C) under both GDM operation temperatures. It was also noticed that with periodic ultrasonication-enhanced physical cleaning, less foulants (Figure 2.9) containing lower amounts of soluble organic foulants (Figure 2.10) and inorganic foulants (

Table 2.6) were accumulated on the membrane surfaces, almost regardless of operation temperature.

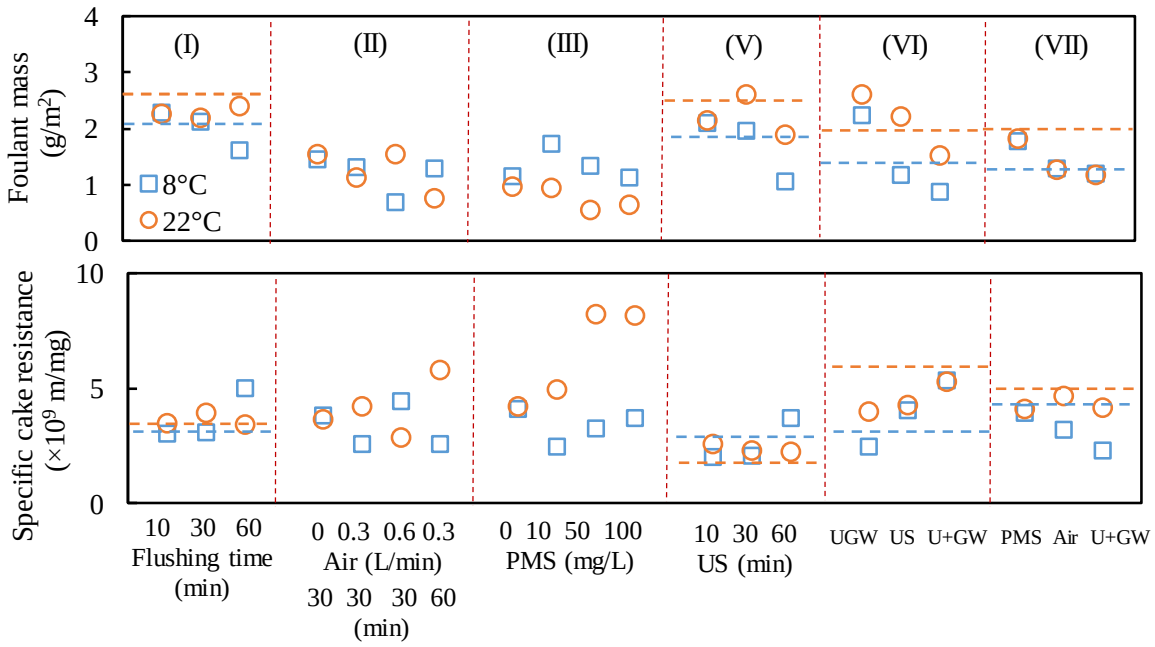

Figure 2.9. (a) Foulant mass, and (b) specific cake resistance in the GDM systems with different periodic cleaning protocols. The dash line indicated the level in the control membrane module without periodic cleaning. "UGW" represents ultrasonicated geothermal water flushing; "US" represents ultrasonication; "U+GW" represents ultrasonication+ geothermal water flushing

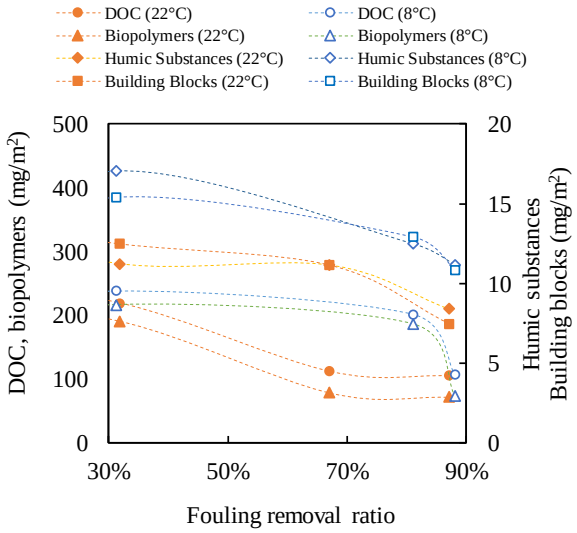

Figure 2.10. Relationship between fouling removal effectiveness and deposited soluble organic foulants on the membrane surfaces in Phase VII.

Table 2.6. The density of soluble inorganics (mg/m^2) in the cake layers on the membrane surfaces (Phase VII)

		Na	Si	Ca	Mg	Fe	SO_4	PO_4
22°C	PMS (50 mg/L) in geothermal water flushing	313.2	34.8	28.1	15.9	16.9	3.1	0.3
	Air sparging (0.3 L/min) + geothermal water flushing	86.4	32.2	31.5	13.9	2.3	3.5	0.4
	Ultrasonication + geothermal water flushing	73.7	29.8	19.0	8.4	3.7	2.1	0.2
8°C	PMS (50 mg/L) in geothermal water flushing	79.6	28.1	27.5	13.8	13.1	3.1	0.3
	Air sparging (0.3 L/min) + geothermal water flushing	71.2	28.8	30.5	11.0	13.7	3.4	0.4
	Ultrasonication + geothermal water flushing	71.3	27.5	31.5	12.3	3.2	3.5	0.4

In addition, the water productivity of the GDM systems under each phase was presented in Figure 2.8b, which almost followed the same pattern as the fouling removal ratio (Figure 2.8a). Overall, the operation temperature of the GDM system displayed insignificant effects on the fouling removal ratio (52 ± 21% at 22°C and 54 ± 23% at 8°C; p>0.05) and water productivity (0.28 ± 0.08 L/day at 22°C and 0.28 ± 0.08 L/day at 8°C; p>0.05). Figure 2.8c shows the cake layer fouling and irreversible fouling resistances in the GDM systems with various cleaning protocols. Similar to continuous filtrations (i.e., no cleaning, Figure 2.3b), cake layer resistances were dominant (>95%) in the GDM systems with periodic cleaning. In each phase, the cake layer fouling resistance almost followed an inverse relationship with the cleaning effectiveness (Figure 2.8a), revealing the cleaning protocols effectively controlled cake development. Overall, during filtrations with periodical cleaning, the cake resistance in the GDM system at 22°C was significantly greater than that at 8°C (p<0.05), while the irreversible fouling resistances under both temperatures were comparable (p>0.05).

Effect of Temperature on GDM Performance and Cake Layer Properties

Temperature is an important operation parameter in biological-based membrane processes as it could influence biological degradation capability and membrane fouling behaviours (Cui et al., 2017; Krzeminski et al., 2012; Ma et al., 2013; Ozgun et al., 2015; Tao et al., 2021a; van den Brink et al., 2011). In this study, the two lava stone biofilm reactors operated at 22°C and 8°C produced the effluents with comparable levels of total solids, total organics (i.e., COD), or total nitrogen, but less biodegradable organics (i.e., BOD_5) was present in the effluent at 22°C (Figure 2.2). As illustrated in previously reported studies (How et al., 2020; Krzeminski et al., 2012; Ozgun et al., 2015; Tao et al., 2021a), warmer operation temperatures could promote hydrolysis of particulate organics and microbial oxidation of bioavailable soluble organics (such as biopolymers). Meanwhile, the slowly-biodegradable and biologically recalcitrant components (such as humic acid-like substances) may be produced during faster decomposition of such organics, which could be detected by COD measurement instead of BOD_5 measurement (Lee et al., 2019; Tao et al., 2021b).

Interestingly, both GDM systems (22°C and 8°C, no cleaning) had indistinguishable cake fouling resistance, irreversible fouling resistance, and irremovable fouling resistance, as well as similar cake filtration constants and pore constriction constants in modelling simulation (Figure 2.3). This was not in agreement with the observations in several previously reported studies (Ma et al., 2013; Ozgun et al., 2015; Tao et al., 2021a), where a higher filtration resistance was identified at a lower temperature. These documented findings emphasized that a lower temperature could cause higher levels of organics or fine particles in the biological treatment effluent, leading to either enhanced cake resistance or irreversible fouling resistance in the following membrane filtration process. In this study, the operation temperature appeared not to influence the total organics and solid contents in the effluent of the lava stone biofilm reactors, which was thought to be associated with their approximately similar fouling resistance distribution. Meanwhile, the dissimilar biodegradable organic levels (i.e., BOD_5) in the reactor effluents at 22°C and 8°C displayed insignificant effects on fouling resistance patterns.

Further analysis of the cake foulants revealed that the soluble organic and inorganic components deposited on the membrane surface were independent with the feed water quality (i.e., the effluent from the biofilm reactor) and membrane filtration temperature (Figure 2.6). However, the foulant mass density in the GDM operated at 22°C was greatly higher than that at 8° (Figure 2.6a). Possibly, the biodegradable organics available for the GDM at 22°C (even lower than that at 8°C) were sufficient for the microbial growth on the membrane surface, so the organic level was not a limiting growth factor. Indeed, the higher operation temperature (22°C) promoted faster development of biofilm on the membrane surface compared to the lower operation temperature (8°C), leading to higher cake foulant density.

On the other hand, the specific cake resistances (i.e., cake resistance per foulant mass density) of the GDM systems at 22°C and 8°C appeared to be at a relatively close level (Figure 2.3b). According to the Carman-Kozeny equation (Ghaffour & Qamar, 2020), $\alpha = \frac{180\ (1-\varepsilon)}{\rho_p d_p^2 \varepsilon^3}$, (in which α is specific cake resistance, d_p is particle size, ρ_p is particle density, ε is cake porosity), the specific cake resistance was strongly associated with the foulant size and cake porosity. It has been well documented that the cake porosity in the GDM system was associated with a combined effect of (1) the accumulation of organics/ inorganics and development of prokaryotic biofilms on the membrane surface (contributing to form dense cake layers) and (2) eukaryotic movement and predation behaviours (contributing to form heterogeneous fouling layer with high porosity nature) (Akhondi et al., 2015; Ayache et al., 2013; Derlon et al., 2012). As mentioned above, the deposition amounts of soluble organics/inorganics on the membrane surface in the GDM systems at 22°C and 8°C were not significantly different (Figure 2.6), but a higher temperature (22°C) led to more biofilm accumulation on the membrane surface (Figure 2.6a). Possibly, compared to the GDM at 8°C, the proliferation of both prokaryotic and eukaryotic microorganisms in the GDM at 22°C may lead to larger foulant particle sizes (higher d_p), but they tended to develop the cake with a relatively lower porosity (higher $\frac{(1-\varepsilon)}{\varepsilon^3}$, i.e., lower ε), possibly due to prokaryotes contributing more to the cake formation than eukaryotes. As a result, the specific cake resistances under both temperature conditions were insignificantly dissimilar.

It is noted that the GDM system operated at 22°C could produce ~24% more permeate water than that at 8°C (Figure 2.4). As the GDM systems at both temperatures displayed similar

fouling resistances, this could be mainly attributed to a lower water viscosity under a higher temperature (~26% lower viscosity level at 22°C than that at 8°C), facilitating water passing through the membrane and foulant layers.

Combined effect of temperature and cleaning effectiveness

Although GDM-based wastewater treatment processes display an extremely lower energy consumption and operation costs, their water treatment capacity is limited due to a lower driving force. Several periodic physical and chemical cleaning protocols have been attempted for the GDM systems, and improved water productivity was achieved (Guðjónsdóttir et al., 2022; Shami & Wu, 2021). Similarly, in this study, compared to the GDM without cleaning, periodic physical or chemical-enhanced physical cleaning (10-60 min per 3-4 days) benefited to improve water productivity in each phase (Figure 2.8b). Under each cleaning protocol, increasing cleaning intensity (such as longer cleaning duration, higher aeration flowrate, higher concentration of chemical solution) to a certain optimal level could benefit to improve water productivity of the GDM systems. Overall, periodic cleaning in the GDM systems appeared to increase total water productivity by ~35% (at 22°C) and ~67% (at 8°C) throughout the operation period compared to respective control group (Figure 2.4), showing the importance of employing periodic cleaning in GDM systems under cold climate.

With periodic cleaning, the temperature had an insignificant effect on the water productivity (p>0.05), which showed a dissimilar pattern as that without periodic cleaning (higher water productivity at a higher temperature). As discussed in the previous sub-chapter, the morphologies of cake layers (without cleaning) were associated with filtration temperatures, e.g., more cake matrix developed at 22°C that could possibly have greater-sized foulants with less-porous nature. In several previously-documented GDM systems (Derlon et al., 2022; Ding et al., 2016; Fortunato et al., 2020; Shi et al., 2020), it has been illustrated that the presence of shear force could compress the cake layers due to their elastic, cohesive and smooth characteristics, as a result, modifying cake layer morphology and promoting to form a thinner and more resistant fouling layer against erosion. Probably, under the same shear force, more foulants could be detached from the cake layers developed at 22°C, leading to comparable foulant mass (Figure 2.9). However, the shear force may facilitate compressing the residual dense-nature cake layer that was developed at 22°C. Thus, significantly higher cake resistances were observed in the GDM system at 22°C than those at 8°C (Figure 2.8b, p<0.05). As a result, the positive contribution of lower water viscosity at 22°C to water productivity was compromised by the negative role of higher cake resistance. In addition, the intensity of shear force may determine the extent of cake morphology change after experiencing shear force, influencing specific cake resistance (Figure 2.9b).

Under the same cleaning condition (50°C, 30 min), ultrasonication-enhanced physical cleaning performed more effectively in enhancement of water productivity compared to physical cleaning, two-phase flow cleaning, and chemical-enhanced physical cleaning. As periodic cleaning would increase operation cost of the GDM system, but benefit for reducing capital cost (e.g., less membrane and tank costs due to improved water productivity) (Shami & Wu, 2021), further cost estimation was performed for a pilot-scale GDM system with optimized cleaning protocols and presented in the Chapter 5.

2.5 Conclusions

This chapter illustrated the effects of operation temperature (22°C *vs.* 8°C) and periodic cleaning protocols on the performance of GDM reactors in treating primary wastewater effluent. The main findings are as follows:

(1) Under control condition (without cleaning), the operation temperature did not significantly influence fouling mechanisms (both experimental fouling resistance analysis and mathematical modelling simulation) of the GDM reactors. However, a higher operation temperature (22°C) promoted the formation of cake layers with more foulant mass but containing similar amounts of soluble organics/inorganics compared to a lower temperature at 8°C. Specific cake resistance analysis of both GDM systems revealed that the cake layers developed at 22°C may have greater-sized foulants with less porosity.

(2) In the presence of periodic cleaning, the operation temperature did not impact flux recovery, water productivity, and foulant deposition mass, but significantly higher cake resistances were observed at 22°C than those at 8°C. Possibly, the shear force could remove the loosely attached cake layers and subsequently cause more compression of the residual dense-nature cake layers at 22°C.

(3) The operation temperature did not influence COD, TSS, and TN removals in the biocarrier reactors, except higher BOD_5 removal at 22°C. Nevertheless, both GDM systems produced superior permeate quality that could meet EU discharge standards, regardless of temperature.

3 Effect of Periodic Ultrasonication on Gravity-driven Membrane Filtration

This chapter contains parts of Article 3:

Hube, S., Hauser, F., Burkhardt, M., Brynjólfsson, S., Wu, B. 2023. Ultrasonication-assisted fouling control during ceramic membrane filtration of primary wastewater under gravity-driven and constant flux conditions. Separation and Purification Technology, 310, 123083. https://doi.org/10.1016/j.seppur.2022.123083

3.1 Abstract

This chapter investigated the feasibility of using ultrasonication as a ceramic microfiltration membrane fouling control strategy during GDM filtration of primary municipal wastewater, with constant flux filtration for a comparison. The fouling model fitting curves revealed that initial intermediate pore blocking was dominant in the GDM system, followed by cake filtration; while cake filtration was dominant during constant flux filtration with a continuously increasing pattern. In the GDM system, periodic ultrasonication cleaning achieved higher cake resistance reduction (~60% *vs.* ~26%) and led to lower specific cake resistances ($0.2\text{-}2.0\times10^7$ *vs.* $29.6\text{-}59.3\times10^7$ m/mg) compared to periodic backwash. Ultrasonication-facilitated fouling mitigation effectiveness was related to cake properties (such as cake foulant density and porosity) and improved with extending ultrasonication duration. The foulant examination indicated that ultrasonication may result in porous cake nature by cake expansion and facilitate detaching particulate foulants and soluble organics (such as biopolymers) from the membrane.

3.2 Introduction

Conventional organic membranes have limited mechanical, chemical, and thermal stability and need to remain a wet once in use, which are challenges for their applications in decentralized wastewater treatment processes. To improve the sustainability of membrane-based wastewater treatment systems during their long-term operation in cold climate, ceramic membranes have been considered as a feasible option due to several advantages, such as greater mechanical, chemical and thermal stability, longer lifespan, and higher recoverability (Asif & Zhang, 2021; Li et al., 2021c; Niwa et al., 2016; Zhao et al., 2019b).

However, membrane fouling is still a major challenge in ceramic membrane-based wastewater treatment processes (Kramer et al., 2020; Zhu et al., 2012). Several studies have highlighted that cake layer fouling was predominant (Im et al., 2019; Li et al., 2021c; Ninomiya et al., 2020; Song et al., 2020; Zhao et al., 2019a), while other researchers noticed irreversible fouling contributed majorly (Kramer et al., 2020) or both cake layer fouling and irreversible fouling dynamically changed with filtration duration (Zhu et al., 2012). Such

inconsistent findings may be associated with different types of ceramic membranes, dissimilar wastewater properties, and operation conditions. Thus, identification of suitable ceramic membrane fouling control strategies with regards to various operation philosophies is paramount. As reported in the previous studies, several solutions have been attempted to mitigate fouling and increase productivity during ceramic membrane filtration of wastewater, such as coagulation pretreatment (Zhao et al., 2019a; Zhao et al., 2019b; Zhu et al., 2012), physical cleaning (backwash, forward flushing, air sparging, particle scouring, brushing, ultrasonication) (Im et al., 2019; Kramer et al., 2020; Zhao et al., 2019a; Zhao et al., 2019b; Zhu et al., 2012), chemical cleaning (NaOCl, acid, alkali, ozonation) and chemical-enhanced physical cleaning (Ninomiya et al., 2020; Song et al., 2020; Zhang et al., 2020; Zhao et al., 2019a; Zhao et al., 2019b) (details in Table 3.1).

Table 3.1. A summary of membrane cleaning protocols in the reported ceramic membrane-based wastewater treatment processes.

Membrane system	Feed water	Cleaning protocol	Membrane performance	Reference
Tubular ceramic membrane (pore size of 0.1, 0.5 and 1.0 µm) Constant flux (3 m^3/m^2d)	Coagulated (PACl) municipal wastewater	Periodic backwash with permeate (500 kPa) and subsequent air blowing	Stable operation for 95, 78 and 6.2 h for the 0.1, 0.5 and 1.0 µm membrane, respectively	(Zhu et al., 2012)
Tubular ceramic membrane (pore size of 0.9 nm) Constant flux (15, 40 or 50-60 LMH)	Synthetic sewage (0.8 g/L sodium alginate)	(1) Backwash for 5 min at 1, 2 and 6 bar when permeability reached 10 L/m^2h bar (2) Forward flushing for 3 min at a crossflow velocity of 0.4, 1.1, 2.2 and 4.3 m/s per 20 min filtration	(1) Backwash at 1 and 2 bar did not affect the permeability, while permeability increased 25-42% at 6 bar (2) Forward flushing slightly improved permeability, regardless of crossflow velocity	(Kramer et al., 2020)
Combined ozone, biological activated carbon, coagulation, ceramic membrane filtration (pore size 0.1 µm)	Secondary municipal wastewater (conventional activated sludge effluent)	Backwash with permeate for 30 sec per 1 h filtration (300 kPa), and subsequent air sparging (300 kPa)	Limited flux reduction after 305 h operation	(Im et al., 2019)
Flat sheet ceramic membrane (Al_2O_3) (pore size of 100 nm Constant flux (41.7 LMH)	Pre-coagulated ($FeCl_3$/PACl) domestic sewage	(1) Continuous filtration with/ without coagulation pre-treatment (2) Intermittent filtration: 144s filtration, 16s backwash with filtrate & aeration; then 13s of idling with aeration	(1) Without coagulation: max TMP reached before 30 min. With coagulation: max TMP reached within 1 d	(Zhao et al., 2019b)

		(3) Chemical cleaning per 3-5 d (at TMP = 35kPa) (4) Alternative cleaning: 4h soaking in chemical baths (alkalic/ acid)	(2) Max TMP reached every 3-5 days (3) Permeability almost completely restored with diluted acidic, alkaline, chlorine or H_2O_2 solution (87-98%) (4) 95% flux recovery	
Tubular ceramic membrane (pore size of 20 & 50 nm)	Secondary municipal wastewater effluent	(1) Pre-ozonation: 8, 20 or 40 min (~2 mg/L dissolved O_3) and periodical backwash and chemical cleaning (0.03 M NaOH) (2) In-situ ozonation (8, 20 or 40 min for 90 min filtration) and periodical backwash and chemical cleaning (0.03 M NaOH)	(1) 29-32% flux increase after backwash, 47-50% flux increase after chemical cleaning (2) 33-57% flux increase after backwash, 48-63% flux increase after chemical cleaning	(Song et al., 2020)
Flat sheet ceramic membrane (pore size of 0.1 µm) Constant flux (50 LMH)	Municipal wastewater	(1) Intermittent filtration (1 min off - 11 min on) (2) Mechanical scouring with granules and chemical (NaOCl: 50, 200 and 1000 ppm) enhanced backwash for 10, 30 or 60 min per 120, 24 or 6 h	Permeability recovery at ~20%, ~40% and ~60% for 15-, 30- and 60-min backwash with 50 ppm NaOCl; ~10%, ~35% and ~60% with 200 ppm NaOCl; ~20% and ~80% (15 and 60 min) with 1000 ppm NaOCl	(Ninomiya et al., 2020)
Flat sheet ceramic membrane (pore size of 0.1 µm) Constant flux (60/80 LMH)	Municipal wastewater: effluent from denitrification filters	(1) In-situ ozonation (5mg/L) (2) Ex-situ ozonation (5 mg/L) (3) Air bubbling (without ozone), backwash for 40 sec per 30 min filtration (backwash flux = 3 times filtration flux)	(1) TMP increase by 2.9-4.9 kPa in 15-21 d (2) TMP increase by 10 kPa in 2 d (3) TMP increase by 30 kPa in 60 h	(Zhang et al., 2020)
Flat sheet ceramic membrane (pore size of 0.1 µm) Constant flux (41.7 LMH)	Coagulated ($FeCl_3$/PACl) municipal wastewater	(1) Chemical soaking for 2 h (0.1 M NaOH followed by 0.1 M HCl) (2) Brushing (3) Backwash with 0.1 M NaOH (5 min) followed by 0.1 M HCl (5 min) (4) Backwash with 0.1 M HCl (5 min) followed by 0.1 M NaOH (5 min), and brushing (5) Backwash with NaOCl (1.1-1.4%) or H_2O_2 (1.5%)	Membrane filterability recovery at (1) 80% (2) 86.7% (3) 95% (4) 60.5% (5) ~100% (6) 70.0% (7) 77.6%	(Zhao et al., 2019a)

		(6) Hot water (80-90°C) and HCl backwash (7) Ultrasonication (3 min)		
MBR, flat-sheet Al_2O_3 (pore size of 0.1 μm) Constant flux (50 to 60 LMH)	Real domestic wastewater	Intermittent filtration: 11 min filtration, 1 minute relaxation, membrane scouring with granules. (1) Backwash (tap water) (2) Backwash (chemical enhanced) (3) Backwash (nanobubbles)	(2) & (3) Comparable performance & irreversible fouling was controlled (3) Better cleaning performance and reversible fouling mitigation than tap water.	(Fernandes et al., 2023)
Conductive ceramic membrane Constant flux (~62.5 LMH)	Synthetic wastewater with organics (oil emulsion) and inorganics (kaolin solution)	Application of negative charge (2.0 V)	Fouling was reduced by ~50%	(Li et al., 2021c)

Among the reported membrane fouling control strategies, ultrasonication appeared to be an effective physical cleaning method, in which cavitation bubbles induced by high-frequency sound waves could loosen the interactions of foulants with the membrane and allow the foulants being detached from the membrane (Aghapour Aktij et al., 2020; Kan et al., 2016; Luo & Wang, 2022). It is noted that ultrasonication has a high energy footprint for wastewater treatment and may induce membrane damage during long-term (Aghapour Aktij et al., 2020; Kan et al., 2016; Luo & Wang, 2022; Reuter et al., 2017; Wang et al., 2016). However, economic analysis for ultrasonication-facilitated membrane cleaning in ceramic membrane-based wastewater treatment systems is lacking (Aghapour Aktij et al., 2020), especially when the wastewater treatment plants are driven by renewable energy (e.g., Icelandic scenario). Additionally, ultrasonication cleaning protocols during ceramic membrane filtration of wastewater have not been well optimized, and relevant membrane fouling control mechanisms have been little investigated. Such information is crucial for achieving sustainable operation of ceramic membrane-based decentralized wastewater treatment facilities in cold climate.

This chapter aims to investigate the feasibility of using ultrasonication as a fouling control strategy during direct ceramic membrane filtration of primary municipal wastewater under gravity-driven and constant flux-driven conditions. The membrane performance and water quality under various operation conditions were monitored. The detailed membrane fouling and mitigation mechanisms were elucidated by experimental analysis and model simulation. The economic analysis of the direct ceramic membrane filtration systems with ultrasonication as a fouling control method was performed, with geothermal water backwash as a baseline for comparison.

3.3 Materials and Methods

3.3.1 GDM Setup and Experimental Conditions

As shown in Figure 3.1a, the GDM system consisted of a biofilm reactor and a submerged GDM filtration tank. In the biofilm reactor (10 L), lava stones (diameter: ~5-16 mm, density: ~2.33 × 10^3 kg/m^3) were used as biocarriers at a 40% packing ratio. The GDM tank had an effective volume of 44 L, in which 4 pieces of ceramic membranes (silicon carbide, pore size of 0.1 µm, membrane area of 0.06525 m^2/piece; Cembrane, Denmark) were placed vertically. The biofilm reactor was fed with primary wastewater by a peristaltic pump (Longer, China) and had a hydraulic retention time of ~26 h. The effluent of the biofilm reactor directly flowed to the GDM tank by gravity force. A constant water level (water head at 0.23 m) in the GDM tank was maintained by an overflow line, i.e., a constant transmembrane pressure (TMP) at ~2.3 kPa. The permeate water was collected and weighed by a digital balance (OHAUS, USA) periodically. The permeate flux and productivity were calculated as explained in Chapter 2.3.1.

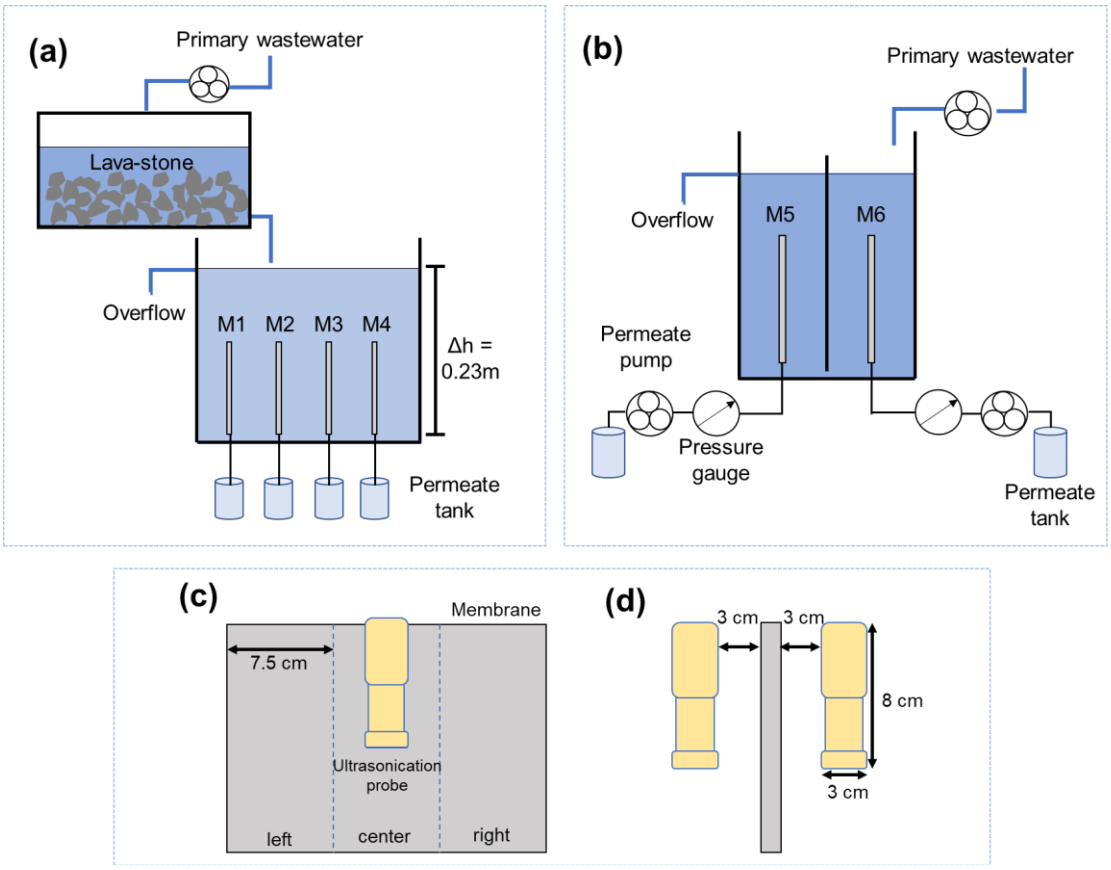

Figure 3.1. (a) GDM setup, (b) direct constant flux filtration setup, (c) side view, and (d) front view of membrane and ultrasonication probe when ultrasonication cleaning was employed.

The GDM system was operated in two phases as described in Table 3.2. In Phase I, long-term (~20 d) GDM filtration with/without periodic physical cleaning was performed (geothermal water backwash or ultrasonication per 3-4 days, i.e., before flux stabilization, in order to maximize overall water productivity with limited energy consumption). In detail,

(1) geothermal water backwash: geothermal water (60°C) was delivered from the permeate side through the membrane at a flux of 3 LMH for 10, 30 or 60 min. (2) Ultrasonication: Ultrasonication probes (50±5 kHz, power output 70W, TTLIFE, China) were located between two membranes in the GDM tank (their installation was described in Figure 3.1c and d). During ultrasonication, the permeation stopped. In phase II, the GDM filtration was continuously conducted for 3 h and 2 days, respectively. Then the membranes were taken out of the GDM tank and placed in a clean water tank mounted with ultrasonication probes (their installation was described in Figure 3.1c and d) for ultrasonication at different durations (5, 30 or 120 sec). Under each experimental condition, cleaned membranes were used.

Table 3.2. A summary of filtration and physical cleaning protocols in the GDM and direct constant flux filtration systems

GDM system	**Biofilm reactor operation time**	**Membrane cleaning condition**	**Membrane module**			
			M1	**M2**	**M3**	**M4**
Phase I	Day 0-23		No cleaning			
	Day 27-40	Geothermal water (60°C; 3 LMH) backwash duration per 3~4 day-filtration	0 min	10 min	30 min	60 min
	Day 42-60	Ultrasonication duration per 3~4 day-filtration	0 min	7.5 min	15 min	37.5 min
Phase II operation	Day 74-80	Ultrasonication duration after 3 h- and 2 d- filtration	0 sec	5 sec	30 sec	120 sec

Direct constant flux filtration	**Membrane cleaning condition**	**Membrane module**	
		M5	**M6**
Phase I: 45 min filtration (10 LMH) -15 min relaxation	Periodic ultrasonication	No cleaning	15 min-ultrasonication per 12 h-operation
Phase II: Continuous filtration (10 LMH)	Ultrasonication duration after TMP reached a certain level	5 sec/30 sec/120 sec	5 sec/30 sec/120 sec

3.3.2 Direct Constant Flux Filtration Setup and Experimental Conditions

Figure 3.1b shows the direct constant flux filtration setup. Two ceramic membranes (silicon carbide, pore size of 0.1 µm, membrane area of 0.06525 m^2/piece; Cembrane, Denmark) were submerged in the tank, which was fed with primary treated wastewater by a peristaltic pump (Longer, China). The water level in the tank was maintained by an overflow line and the constant permeate flow was collected by a peristaltic pump (Longer, China). A constant flux of 10 LMH was set in order to simulate long-term operation scenario (i.e., above critical flux, Figure 3.2). The permeate pressure was measured by a pressure gauge and the total TMP was calculated as the difference between the water head and the permeate pressure.

The TMP induced by fouling (TMP_f) was obtained by deducting the clean membrane TMP (TMP_0, which was measured with clean water at the same operation condition) from total TMP.

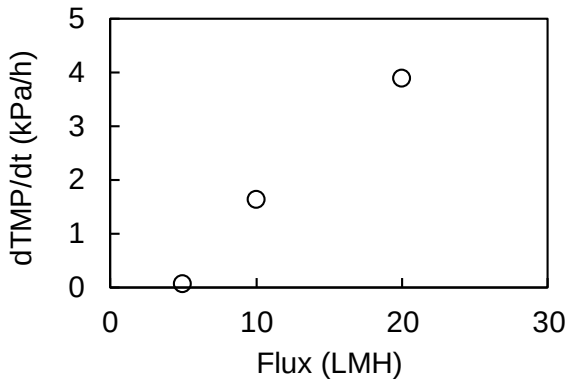

Figure 3.2. The TMP increase rates under different filtration fluxes in the constant flux filtration system (filtration was performed for ~2 days).

During ultrasonication cleaning, two ultrasonication probes were submerged in the tank and located on both sides of the membrane (their installation was described in Figure 3.1c and d). The experimental conditions in the constant flux filtration system were illustrated in Table 3.2. Under intermittent filtration condition (45 min filtration-15 min relaxation, flux of 10 LMH, Phase I), ultrasonication was applied for 15 min per 12 h of operation to examine whether periodic ultrasonication benefited fouling mitigation. Under continuous filtration condition (Phase II), when the TMP level reached to a certain level, ultrasonication at different durations (5, 30, or 120 sec) were performed in order to illustrate the effect of ultrasonication duration on fouling mitigation effectiveness.

3.3.3 Analytical Methods

The fouling resistance distribution profiles in both GDM and direct constant flux filtration systems were examined as illustrated in previously reported studies (Broeckmann et al., 2006; Lee et al., 2021; Lee et al., 2019) and as described in Chapter 2.3.4. It is noted that in the GDM system, the TMP level was maintained at 23 cm water head; while in the direct constant flux filtration system, the permeate flux was kept at 10 LMH.

The collected flux data during continuous GDM filtration and the collected TMP data during constant flux filtration were fitted to previously reported constant pressure (see Chapter 2.3.4) and constant flux (

Table 3.3) (Ho & Zydney, 2002) dead-end filtration equations, respectively. The linear coefficient value of the simulation curve ($R^2 \geq 0.95$) was presented as the filtration constant.

Table 3.3. Dead-end filtration models for describing the membrane fouling mechanism under constant flux condition (Ho & Zydney, 2002)

Governing equation $\frac{dP}{dt} = kP^n$	P: TMP; V: filtered water volume	
$n = 0$	$P = a + bV$	Cake filtration
$n = 1$	$1/P = a - bV$	Intermediate pore blocking
$n = 1.5$	$1/P^{1/2} = a - bV$	Pore constriction
$n = 2$	$1/P^2 = a - bV$	Complete pore blocking

The water samples were periodically collected from the feed tank, biofilm reactor effluent, and permeate tank. Water quality analysis was conducted as explained in Chapter 2.3.5 and 2.3.6. The DOC in the filtered foulants was measured by a TOC/TN analyzer (Shimadzu, Japan).

3.4 Results and Discussion

3.4.1 Ceramic Membrane Fouling Mechanisms

In this study, the water quality in the GDM systems was monitored and presented in Table 3.4. Clearly, the permeate quality met the requirement of EU urban wastewater discharge standards (COD ≤ 125 mg/L; BOD_5 ≤ 25 mg/L; TSS ≤ 35 mg/L) (European Union, 1991).

Table 3.4. Water quality in the GDM system

	Feed	Effluent	Permeate
pH	7.1 ± 0.1	7.3 ± 0.6	7.9 ± 0.2
Conductivity (μS/cm)	1865 ± 383	1881 ± 353	1819 ± 324
COD (mg/L)	87.6 ± 36.0	46.0 ± 12.4 *(44 ± 28%)*	24.7 ± 2.3 *(65 ± 17%)*
BOD_5 (mg/L)	53.3 ± 21.4	46.9 ± 21.5 *(18 ± 19%)*	7.7 ± 4.9 *(82 ± 16%)*
TN (mg/L)	21.7 ± 3.1	18.2 ± 1.7 *(15 ± 11%)*	16.4 ± 1.6 *(22 ± 14%)*
TSS (mg/L)	96.9 ± 20.1	60.9 ± 32.6 *(43 ±28%)*	0.9 ± 1.3 *(99 ± 1%)*

Note: The number in the bracket represents removal efficiency by comparing the levels in effluent and feed (i.e., removal efficiency in the biofilm reactor), or comparing the levels in the permeate and feed (i.e., removal efficiency in the biofilm-GDM system).

In the GDM system, the ceramic membrane flux development profiles under continuous filtration (i.e., Phase I) were described in Figure 3.3a. The flux dropped significantly (>90%) during the first ~2 days and then stabilized at a lower level (~1.6 LMH), showing a typical flux pattern during GDM filtration of wastewater (Guo et al., 2022b; Pronk et al., 2019). The water permeability of the ceramic membrane (~70 LMH/bar) was comparable to those in the

previously-reported GDM systems with organic membranes for wastewater treatment (44-150 LMH/bar) (Ding et al., 2017; Lee et al., 2021; Lee et al., 2019; Peter-Varbanets et al., 2010; Wang et al., 2017b).

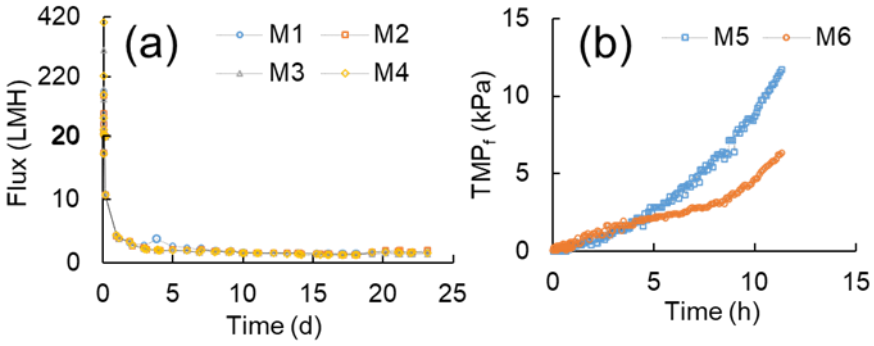

Figure 3.3. (a) Flux development profiles in the GDM system during continuous filtration (Phase I), and (b) TMP development profiles in the constant flux filtration system.

Subsequently, the collected GDM flux data were fitted to the previously reported constant pressure dead-end filtration model (Hermia, 1982; Ho & Zydney, 2000; Ye et al., 2005) as illustrated in Figure 3.4. The filtration constants were summarized in Figure 3.5a, displaying a three-stage pattern. In detail, in stage I (< 1 day), intermediate pore blocking was the dominant fouling mechanism, followed by pore constriction, which was attributed by direct interactions between the foulants and the clean membrane before a cake layer was formed (Lee et al., 2019; Wu et al., 2016). In the Chapter 2 pore constriction and cake filtration were found to be initially dominant with organic microfiltration membranes (PVDF, 0.08 μm; packed in filtration cells). It was observed that the lava stone biocarriers could release fine particles, which may contribute greatly to the initial cake formation due to their greater-sized nature (Guðjónsdóttir et al., 2022). These dissimilar fouling mechanisms may be associated with several facts, e.g., (1) compared to the filtration cell configuration (the lava stones could be limited in the filtration cell and had to be accumulated on the organic membrane surface), the vertically submerged ceramic membrane experienced less opportunities in contacting these high density lava stone particles due to their settling behaviors; (2) the organic and inorganic membrane properties, such as surface characteristics, pore size distribution and morphology, were different.

In stage II (Day 1-7), intermediate pore blocking constant significantly reduced, while pore constriction constant stayed constant. Possibly, the available membrane pores were blocked by the larger-sized foulants, and continuous accumulation of foulants could lead to cake layer formation (at a filtration constant of ~0.004 day/L^2). Meanwhile, the smaller-sized particles could continuously fill in the pores between the foulants, at a similar pore constriction rate as that in stage I. In stage III (>7 days), both pore constriction and intermediate pore blocking constants decreased, while cake filtration displayed its dominance. This was consistent with the observation in the GDM systems with organic membranes (Chapter 2). Notably, with development of biofouling cake layer on the membrane, cake compaction may occur due to their elastic nature (Derlon et al., 2022), leading to less porosity in the foulant layer, i.e., limited pore blocking or constriction. Additionally, the dominance of cake layer corresponded to the fouling resistance distribution

pattern (examined at the end of wastewater filtration), in which irreversible and irremovable resistance contributed less than 2% to the total fouling resistance (data not shown).

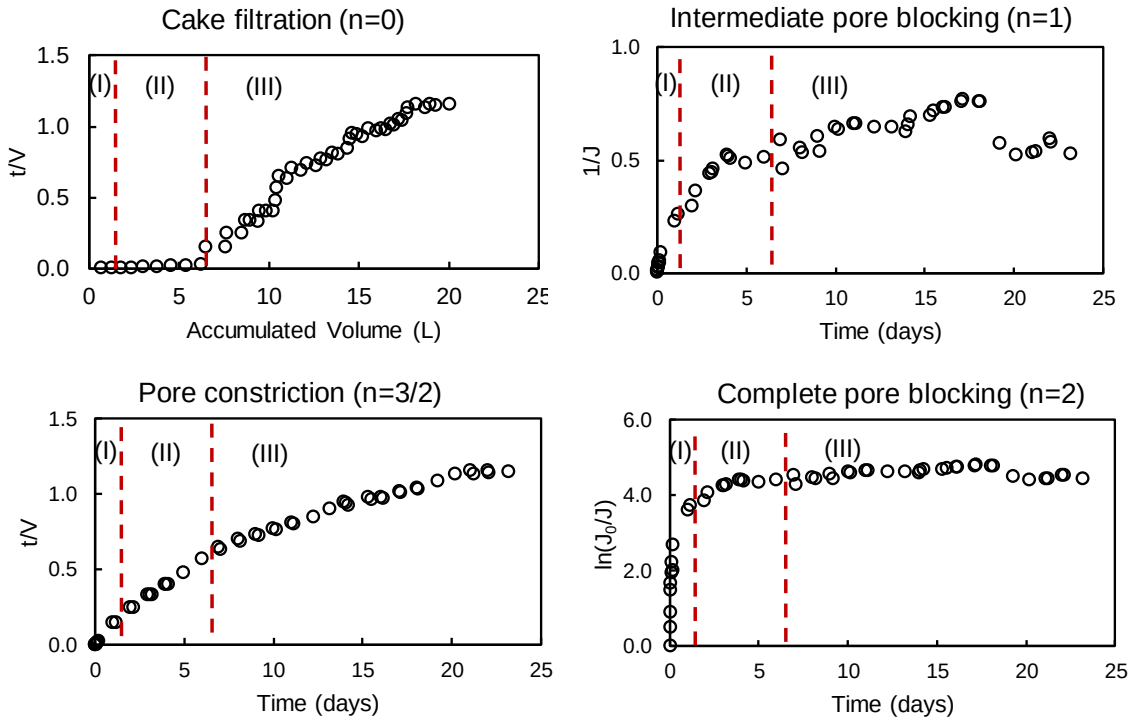

Figure 3.4. Membrane mechanism description based on the simulation profiles during continuous GDM filtration (linear correlation coefficient $R^2 \geq 0.95$).

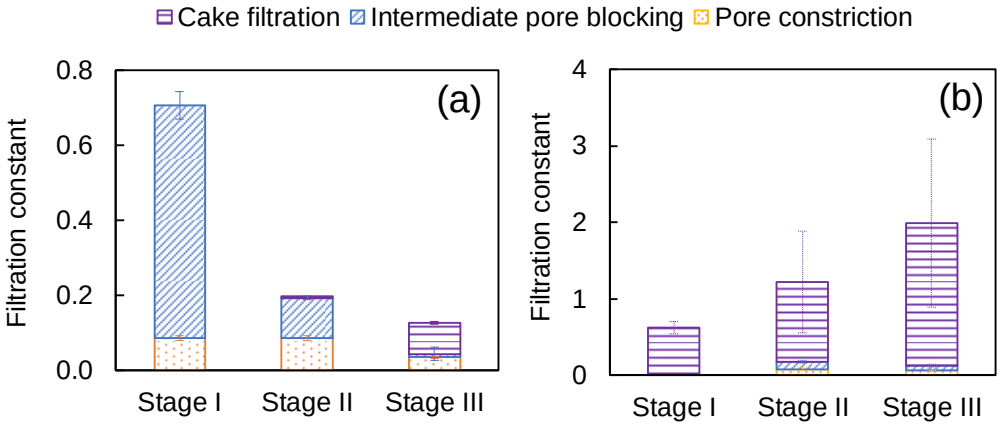

Figure 3.5. Simulated filtration constants during (a) GDM filtration (n=3, $R^2 \geq 0.95$) and (b) constant flux filtration (n=2, $R^2 \geq 0.95$).

During direct constant flux filtration of municipal wastewater, an almost linear TMP increase was noticed within the initial ~8 h, followed by a sharp increase of TMP (Figure 3.4b). Subsequently, the fitted constant flux filtration model profiles were plotted in Figure 3.6 and the filtration constants were presented in Figure 3.5b. The membrane fouling mechanisms followed a three-stage pattern, coinciding with the slope change of TMP increase. In stage I, cake filtration was solely present, indicating a rapid cake formation on the inorganic

membrane surface at a flux of 10 LMH (above critical flux). In a previous study (Nascimento & Miranda, 2021), it was also found that the initial TMP increase was attributed by cake layer formation on the membrane during long-term direct membrane filtration of municipal wastewater. Meanwhile, in our previous studies on direct constant flux microfiltration (organic membranes) of municipal wastewater under crossflow conditions, intermediate pore blocking was dominant during the initial stage (Hube et al., 2021a; Hube et al., 2021b). Possibly, the shear force induced by crossflow could prevent foulant deposition; however, under such non-shear condition in this study, permeation force efficiently enhanced foulant depositions for cake formation. In stages II and III, cake filtration maintained its predominance and its constant increased with extending filtration duration, revealing continuous accumulation of cake foulants and/or compaction of cake layers. Meanwhile, pore constriction and intermediate blockage constants were limited. Possibly, the formed cake layers had a dense nature, so that the foulants could not penetrate to the pores in the cake layer matrix, indeed continuously contributing to cake formation. This phenomenon was similar to our previous observation with organic membranes under crossflow conditions (Hube et al., 2021a; Hube et al., 2021b).

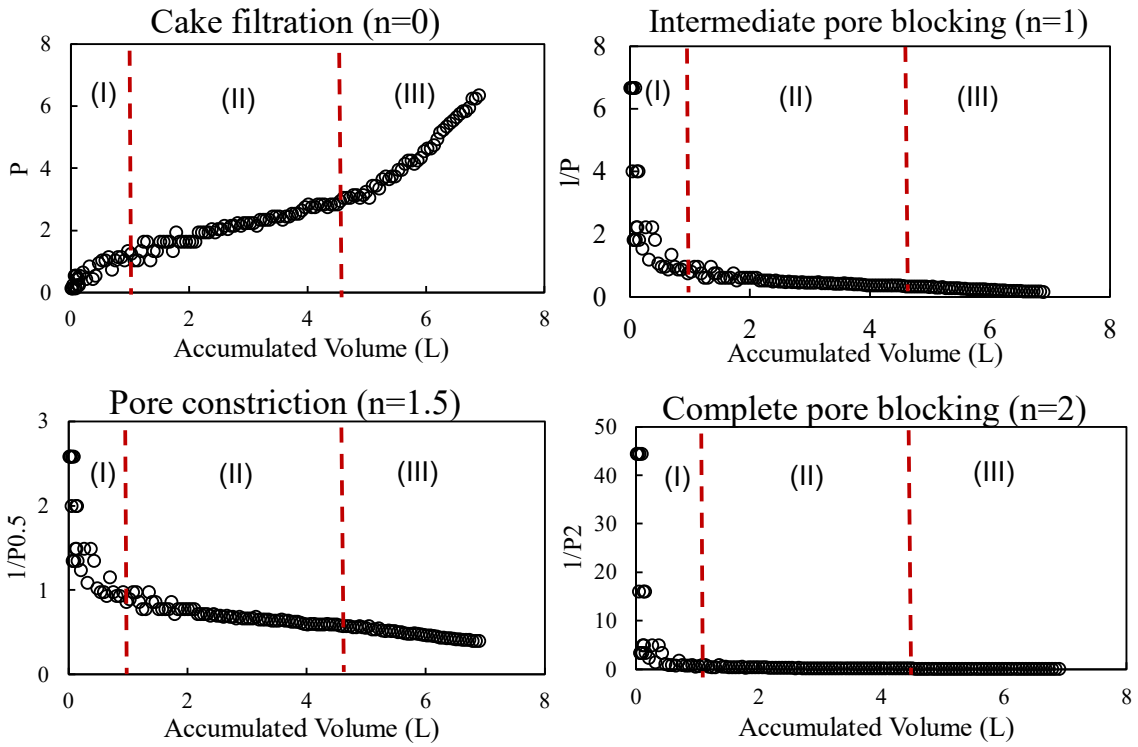

Figure 3.6. Membrane mechanism description based on the simulation profiles during continuous constant flux filtration (linear correlation coefficient $R^2 \geq 0.95$).

3.4.2 Ultrasonication-facilitated Fouling Control in GDM and Constant Flux Filtration Systems

GDM System

To improve water productivity of GDM systems, periodic cleaning was employed for flux recovery per 3-4 days (i.e., before flux stabilization). Figure 3.7 shows the flux development profiles of GDM systems with periodic geothermal water backwash and ultrasonication.

Clearly, in the presence of geothermal water backwash, the flux recovery was limited (<6%) and tended to decrease with extending cleaning cycle, regardless of cleaning duration. As discussed previously, after the initial 3–4 day GDM filtration, intermediate pore blocking and pore constriction were predominant, so that high temperature (60°C) backwash water allowed such fine foulants partially being diffused/detached. Meanwhile, with the foulants continuously accumulating on the membrane (i.e., shifting to cake filtration), the employed backwash force was not sufficient to overcome foulants-foulants interaction, leading to limited fouling mitigation. Averagely, with 10, 20, and 60 min periodic geothermal water backwash, fouling resistance reduced ~21±9%, ~21±13%, and ~35±10%, respectively. It appears that increasing backwash duration from 10 to 60 min (6-fold), merely 1.7-fold fouling reduction was achieved.

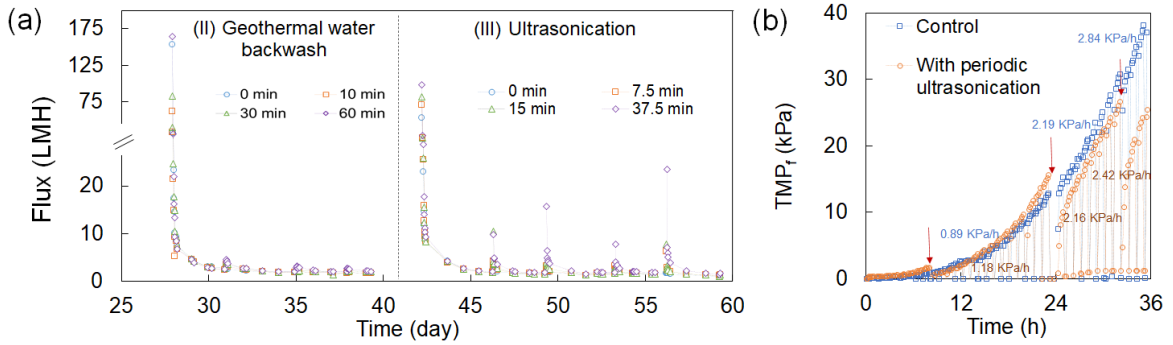

Figure 3.7. (a) Flux development profiles in the GDM systems during Phases II and III; (b) TMP development profiles during constant flux filtration (red arrow pointed to ultrasonication cleaning).

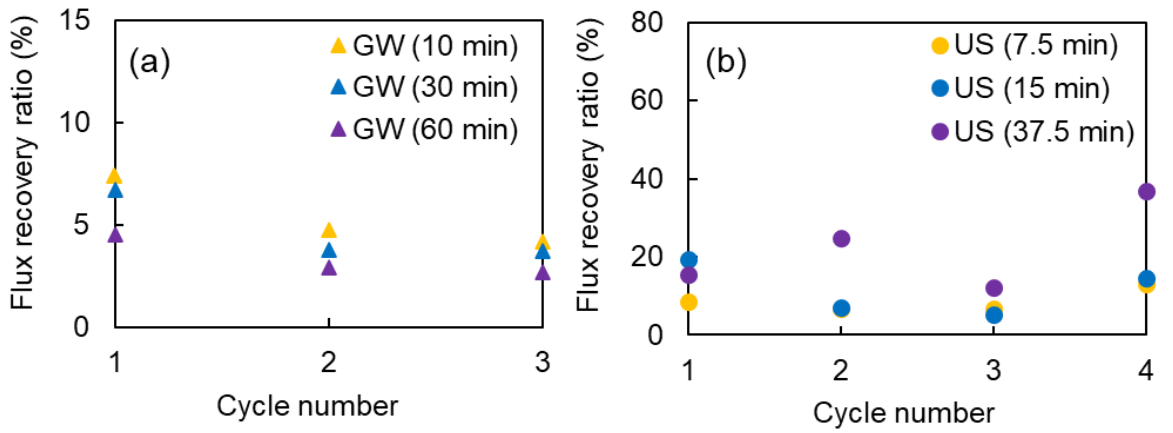

Figure 3.8. Flux recovery ratio profiles in the GDM systems during Phases II and III.

At the end of filtration, the GDM systems displayed comparable permeate fluxes (~1.8-2.3 LMH), which were not significantly affected by the presence/absence of backwash and backwash duration. Additionally, as shown in Figure 3.9, the cake layer resistance was dominant (contributing to ~95% to the total resistance) during the GDM filtration, implying that high temperature geothermal water backwash did not influence the fouling mechanism, especially not causing significant increases of irreversible or irremovable fouling. This finding was in accordance with our previous studies on the GDM systems with organic membranes (Guðjónsdóttir et al., 2022; Hube et al., 2022; Hube et al., 2021b; Shami & Wu,

2021) and Chapter 2. It was thought that the high temperature condition (60°C) may prevent potential inorganic scaling (caused by geothermal water) from the membrane pores. In the presence of geothermal water backwash, the specific cake resistances slightly decreased with extending cleaning durations, which were lower than that without backwash. On the other hand, the presence of backwash led to more foulant density on the membrane (Table 3.5). This suggests that backwash force may expand the cake layer and then allow the smaller-sized particles (from wastewater) to be filled into the cake matrix during the following filtration cycle (i.e., leading to more cake foulants).

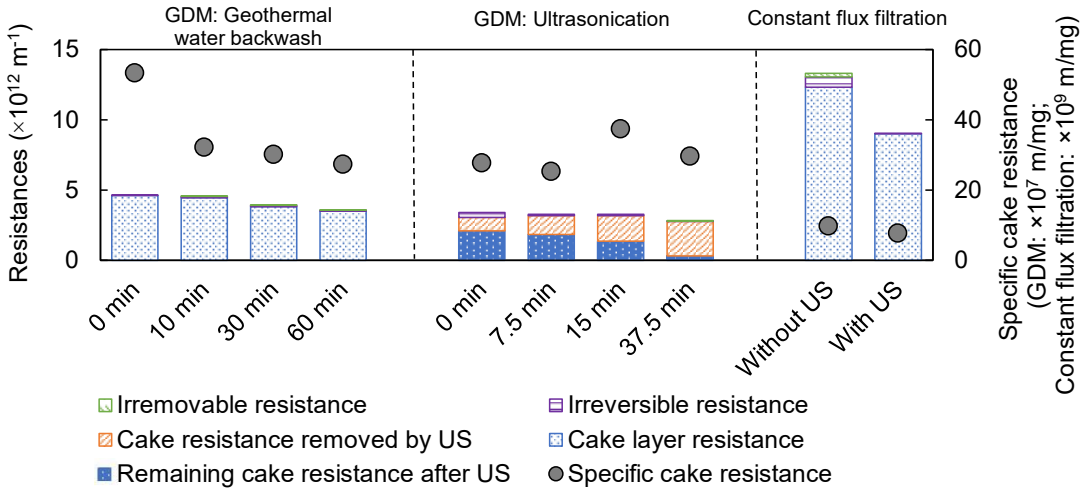

Figure 3.9. Filtration resistances in the GDM and constant flux filtration systems (Note: under ultrasonication condition, the "cake layer resistance" = "cake resistance removed by US" + "remaining residual cake resistance after US").

In the presence of periodic ultrasonication cleaning, it was observed that ~9%-22% permeate flux was recovered after periodic ultrasonication (Table 3.5); Note: as the four membrane modules were in the same tank without separation device, the membrane modules without direct ultrasonication also experienced turbulences induced by the cavitation bubbles). It appears that flux recovery did not compromise with increasing ultrasonication cleaning cycles, showing dissimilar behaviors as those with geothermal water backwash (Figure 3.8). This was attributed to the strong force induced by the ultrasonication and additional membrane relaxation during permeation-off period, which could help detach the deposited foulants and transport them away from the membrane (Guo et al., 2022b; Reuter et al., 2017). Nevertheless, the permeate flux tended to decrease within 1-day after ultrasonication (Figure 3.7a), leading to comparable flux levels at the end of filtration (~1.6-1.9 LMH).

Table 3.5. Foulant mass, flux recovery and resistance reduction in the GDM systems with periodic cleaning

Geothermal water backwash duration	***0 min***	***10 min***	***30 min***	***60 min***
Foulant mass (g/m^2)	8.6±3.0	13.9±0.0	12.7±0.4	12.8±3.6
Flux recovery	-	2.6±0.7%	1.7±0.5%	2.1±0.5%
Resistance reduction	-	21.2±7.4%	21.2±10.7%	34.6±7.8%
Ultrasonication duration	***0 min***	***7.5 min***	***15 min***	***37.5 min***
Foulant mass (g/m^2)	17.6±1.9	20±2.8	13.5±1.9	14.9±0.4
Flux recovery	5.9±1.0%	8.8±2.6%	9.4±5.8%	22.3±9.6%
Resistance reduction	27.4±13.2%	59.1±11.5%	66.0±19.5%	84.3±7.3%

As shown in Figure 3.9, the presence of ultrasonication could effectively alleviate cake fouling as the cavitation bubbles could trespass and move underneath the cake layer (Reuter et al., 2017), as a result, the cake layer could be loosened and expanded, and then detached from the membrane surface (Figure 3.10). In addition, ~32%, ~42%, ~58%, and ~89% of cake layer resistance was reduced by employing ultrasonication for 0, 7.5, 15, and 37.5 min respectively, showing that the mitigation effectiveness was improved with extending ultrasonication duration. This finding was consistent with those in the previous studies (Aghapour Aktij et al., 2020; Kan et al., 2016; Luo & Wang, 2022). Furthermore, extending ultrasonication cleaning duration led to increased specific cake resistances ($\alpha = \frac{180(1-\varepsilon)}{\rho_p d_p^2 \varepsilon^3}$, α is specific cake resistance, d_p is particle size, ρ_p is particle density, ε is cake porosity (Ghaffour & Qamar, 2020), which was possibly related to less cake foulants (Table 3.5) and re-compaction of cake layer during filtration after cleaning.

Figure 3.10. Photo of the fouled membrane during ultrasonication in the GDM system (after 3-h filtration).

Constant Flux Filtration System

The TMP evolution profiles during direct filtration (45 min on-15 min off) of primary wastewater with/without periodic ultrasonication are depicted in Figure 3.7b. Clearly, the presence of periodic ultrasonication (15 min per 12 h of operation) benefited to decrease the initial TMP level in the following cycle. For example, at a lower TMP_f level (i.e., first cycle), 15-min ultrasonication could fully remove the foulants, leading to the initial TMP_f at ~ 0 kPa in the second cycle; while when the TMP_f level increased to >15 kPa, residual foulants may be present after ultrasonication, causing the initial TMP_f at ~ 0.8-1.2 kPa. This implies that the ultrasonication cleaning effectiveness may be associated with the fouling situation. However, periodic ultrasonication could not facilitate delaying the TMP increase rate (Figure 3.7). Possibly, (1) after ultrasonication, certain cleaned membrane area was exposed to the foulants and the membrane-foulant interactions were stronger than the foulants-foulants interactions (without cleaning). (2) The periodic ultrasonication may render the cake layer with more porous nature, as indicated by a lower specific cake layer resistance (Figure 3.9). It is believed that such porous cake layer could be readily compacted when the filtration

force was employed, as a result, leading to comparable TMP increase rate in the presence/absence of ultrasonication cleaning.

As illustrated in Figure 3.9, periodic ultrasonication could alleviate cake fouling, irreversible fouling, and irremovable fouling during direct constant flux filtration. This phenomenon was dissimilar with observations in the previous studies, in which ultrasonication cleaning appeared not to reduce pore constriction and blocking (Kan et al., 2016; Reuter et al., 2017). This may be attributed to different cleaning protocols (probe distance and ultrasonication duration) and ceramic membrane properties such as pore size. During constant flux filtration, periodic ultrasonication contributed to reduce ~27% of cake fouling resistance, which was significantly lower than those in the GDM systems (42-89%). This was associated with the higher operation pressure in the constant flux filtration, which enhanced the interaction of cake foulants with the membranes and limited cake layer removal by ultrasonication (Aghapour Aktij et al., 2020).

3.4.3 Ultrasonication-facilitated Fouling Control Mechanisms

Effect of Ultrasonication Duration on Foulant Compositions

To further elucidate the effectiveness of ultrasonication duration on fouling alleviation, short-term GDM (3-h and 2-d, presenting intermediate pore blocking- and cake layer-dominant fouling behavior, respectively) and constant flux filtration experiments (fouling resistance was ~5-7×10^{12} m^{-1}) were performed, followed with ultrasonication for 5, 30 or 120 sec (with no ultrasonication as control). The images of remaining foulant morphology were taken and presented in Table 3.6. In this study, the ultrasonication probes were placed close to the center of the membrane sheet. Clearly, it appeared that the residual foulants on the membrane surface displayed an uneven distribution on the membrane surface. This phenomenon was associated with the fact that circular movement of ultrasonication waves could enhance the removals of cake layers within cavitation domain (Bazan et al., 2020); once certain cake layers were detached from the membrane surface, the cavitation-induced bubbles could easily penetrate these areas and further remove cake layer components (Reuter et al., 2017).

Table 3.6. Images of foulants remained on the membrane after ultrasonication cleaning.

After 3-h GDM filtration			
0 sec	5 sec	30 sec	120 sec
			
After 2-day GDM filtration			
0 sec	5 sec	30 sec	120 sec
			
After resistance reached ~5-7×10^{12} m^{-1} during constant flux filtration			
0 sec	5 sec	30 sec	120 sec
Not taken			Not taken

To illustrate the effectiveness of ultrasonication-facilitated fouling removal along the membrane, the remaining foulants were sampled from the membrane at different locations in the GDM system (Figure 3.1c). As shown in Figure 3.11a, there was almost no significant difference of foulant mass in the center and side of the membrane (p>0.05), regardless of GDM filtration duration and ultrasonication cleaning duration. For both GDM filtration scenarios (after 3-h or 2-day filtration), with increasing ultrasonication cleaning duration from 0 to 30 sec, an almost linear reduction of the residual foulant mass was noticed (R^2=0.97

and 0.93 for 3-h or 2-day filtration respectively), while further extending ultrasonication duration to 120 sec, almost no additional foulants were removed from the membrane surface.

The amounts and composition of soluble organics in the residual foulants from the GDM systems were examined, as shown in Figure 3.11b and Table 3.7. The soluble organic contents (i.e., DOC) followed the similar trend as the residual foulant mass. In detail, the DOC contents in the foulants after 3-h GDM filtration was significantly lower than those after 2-day GDM filtration. With increasing ultrasonication cleaning duration, the DOC contents in the foulants decreased. This indicated that both particulate and soluble foulants were readily detached from the membrane by ultrasonication. As illustrated in Table 3.7, among the remaining soluble foulants (after 2-day GDM filtration), the biopolymers greatly reduced with extending ultrasonication time from 0 to 30 sec, and no further reduction was noticed with increasing ultrasonication duration from 30 to 120 sec, which was in accordance with the trend of cake foulant mass (Figure 3.11a). However, humic acid, building blocks, and low molecular weight (LMW) neutral organics were not significantly affected by ultrasonication duration.

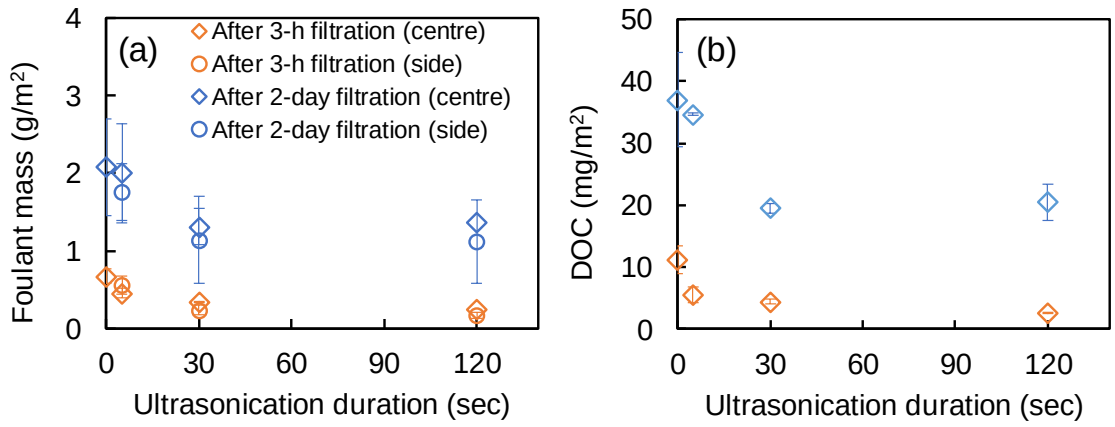

Figure 3.11. Effect of ultrasonication duration on (a) foulant mass and (b) DOC content in the foulants from the GDM systems (3-h filtration and 2-day filtration) (n=2). The terms "center" and "side" refer to the foulant sampling locations; "Side" includes both right and left sides of the membrane (see Figure 3.1c).

Table 3.7. Effect of ultrasonication duration on soluble organic compositions in the foulants from the GDM systems (2-day filtration) (n=2).

Ultrasonication duration (sec)	Biopolymers (mg/m^2)	Humic acids (mg/m^2)	Building blocks (mg/m^2)	LMW neutral (mg/m^2)
0	12.28±3.63	4.07±0.17	3.70±0.15	3.33±0.93
5	11.12±1.24	3.90±0.42	3.35±0.17	2.89±0.13
30	7.08±0.74	3.86±0.30	2.53±0.35	2.02±0.25
120	6.36±1.29	3.95±0.26	2.83±0.20	2.42±0.00

3.3.2 Effect of Ultrasonication Duration on Fouling Resistance Distribution

Furthermore, the fouling resistance distributions were analyzed and presented in Figure 3.12. After 3-h GDM filtration (i.e., initial stage of GDM filtration), cake fouling, irreversible fouling, and irremovable fouing contributed to ~55%, ~38%, and ~8% of the total fouling resistance (Figure 3.12a). When employing ultrasonication cleaning at 5 sec, 30 sec, and 120 sec, cake fouling was reduced by ~41%, ~31%, and ~100% respectively, while irreversible fouling was reduced by ~47%, ~51%, and ~100% respectively. However, ultrasonication cleaning could not alleviate irremovable fouling, i.e., the foulants that were strongly attached on the membrane and resistant to chemical cleaning. After 2-day GDM filtration (i.e., the flux tended to be stable), cake fouling was predominant with ~94% contribution ratio to the total fouling (Figure 3.12b). Extending ultrasonication cleaning from 5 sec, to 30 sec, to 120 sec, cake fouling reduction ratio increased from ~56%, to ~81%, to ~100%, respectively; while, the employed ultrasonication did not alleviate irreversible and irremovable fouling.

In addition, the specific cake resistances of the residual cake foulants were compared after different ultrasonication durations (Figure 3.12). Here, the specific cake resistance after 2-day filtration was almost ~10 time of that after 3-h filtration (without ultrasonication), indicating a denser nature of cake layer after a longer filtration time (assuming the foulant particle size/density was relatively comparable as the foulants could be majorly derived from wastewater during such short-term filtration duration). After 3-h GDM filtration, a shorter ultrasonication duration (5-30 sec) did not lead to lower specific cake resistances, even though both particular and soluble foulants were partially removed from the membrane (Figure 3.11). However, when ultrasonication duration was set at 120 sec, a greatly lower specific cake resistance was observed. It is noted that the amounts of the remaining foulants on the membrane after 30 sec and 120 sec ultrasonication were comparable (Figure 3.11a). This implies that longer ultrasonication duration could not only remove the foulants from the membrane surface; but also faciliate expanding the residual cake layers, leading to be relatively more porous (i.e., lower specific cake layer resistance).

After 2-day GDM filtration, increasing ultrasonication cleaning duration also led to reduction of the specific cake resistance (Figure 3.12b), but followed a dissimilar pattern as that after 3-h GDM filtration. This implies that the effect of ultrasonication on specific cake resistance was associated with the initial cake foulant properties (such as morphology, mass). When greater amount of foulants with denser nature were deposited on the membrane, extending ultrasonication duration (even at a shorter time) could significantly increase the cake porosity by expanding the cake layer and reducing biopolymers accumulated in the residual cake foulants (Table 3.7).

In the constant flux filtration system, cake layer fouling was clearly dominant (>90% of total fouling resistance) and its reduction was improved with increasing ultrasonication duration, showing a similar pattern as those in GDM filtration. However, with a longer ultrasonication duration (i.e., 120 sec), the cake layer reduction was less effective than that in the GDM system. This could be attributed to the higher operating pressure during constant flux filtration, which would compact the cake foulants and facilitate forming a dense cake layer with a higher specific cake layer resistance (~ 4.9×10^{15} m/mg without ultrasonication). The ultrasonication-induced cavitation bubbles may offer insufficient force to detach the foulants from such dense cake matrix.

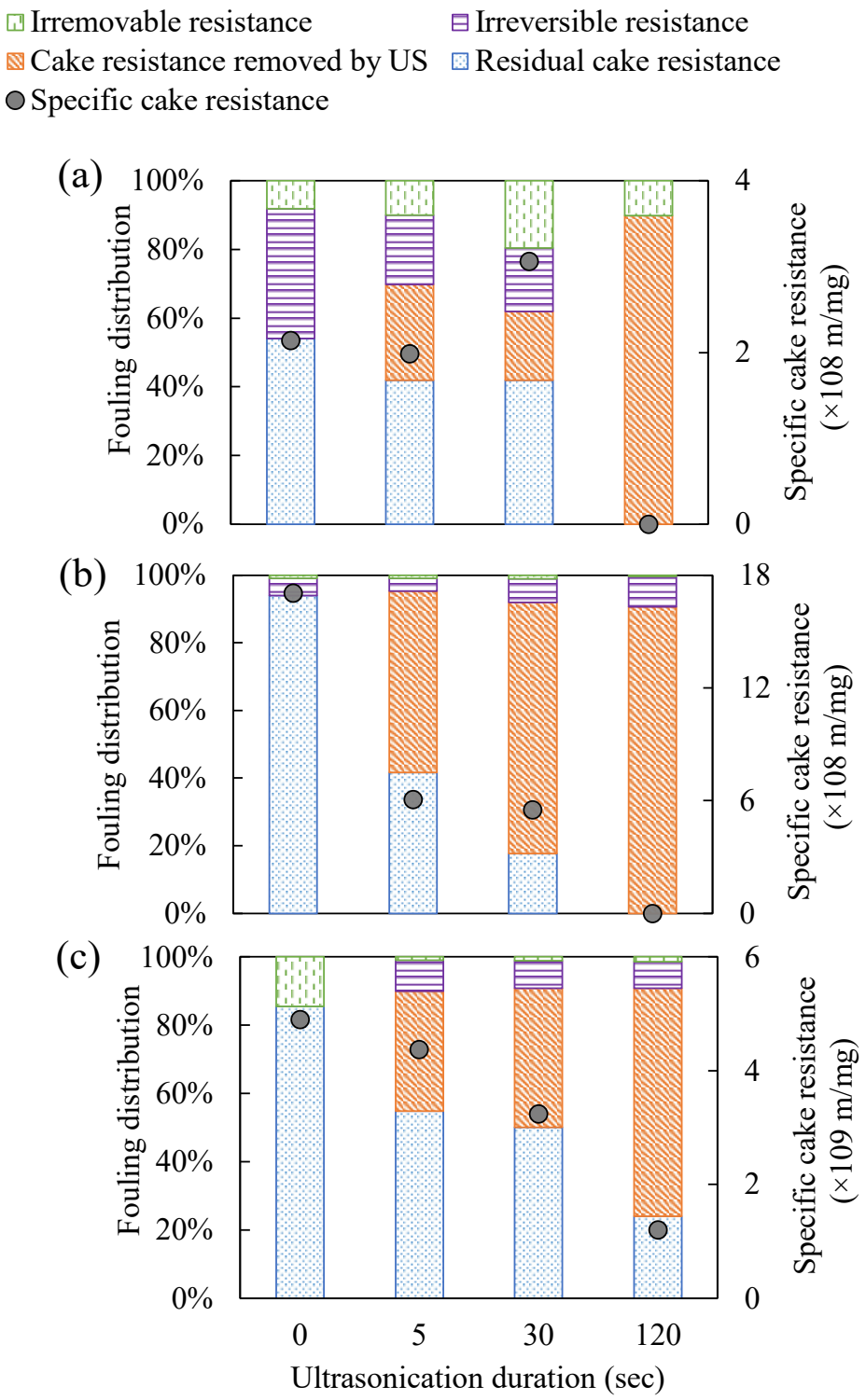

Figure 3.12. Effect of ultrasonication duration on fouling resistance distribution (a) in the GDM system after 3-h filtration, (b) in the GDM system after 2-day filtration, (c) in the constant flux filtration (n=2-3).

3.5 Conclusions

This chapter investigated the feasibility of ultrasonication-assisted GDM and constant flux filtration with ceramic membranes for decentralized wastewater treatment. The main findings are:

(1) During GDM filtration of wastewater, the dominant fouling mechanisms shifted with filtration time, i.e., initially intermediate pore blocking, followed by cake filtration after flux stabilization. Meanwhile, during constant flux filtration of wastewater, cake filtration was predominant, and the filtration constant increased with filtration time.

(2) In the GDM system with periodic geothermal water backwash, cleaning efficiency was not greatly improved by increasing cleaning duration. Meanwhile, the GDM system with periodic ultrasonication achieved more effective cake fouling reduction with extending cleaning duration, and cleaning efficiency was independent with cleaning cycle.

(3) During constant flux filtration, ultrasonication led to less cake fouling reduction than that in the GDM systems. In addition, periodic ultrasonication could not facilitate delaying the TMP increase rate due to compaction behavior of the residual cake layer at a higher pressure.

(4) Resistance analysis revealed that ultrasonication could mostly reduce cake layer resistance in both GDM and constant flux filtration systems. This could be linked to a reduction of foulant mass and biopolymers in the foulants.

4 Effect of Microplastics on Gravity-driven Membrane Filtration

This chapter contains parts of the contents in Articles 1 and 5:

Hube, S., Wu, B. 2021. Mitigation of emerging pollutants and pathogens in decentralized wastewater treatment processes: A review. Science of the Total Environment, 779, 146545. https://doi.org/10.1016/j.scitotenv.2021.146545

Hube, S., Burkhardt, M., Brynjólfsson, S., Wu, B. Influence of microplastics on gravity-driven membrane filtration performance during primary municipal wastewater treatment [In preparation]

4.1 Abstract

Microplastic is an emerging pollutant which is often released to the environment through wastewater streams. While its implications in centralized wastewater treatment have been well studied, its influence on small-scale decentralized treatment systems remains largely unknown. This chapter investigated the influence of accumulating microplastics in GDM for decentralized wastewater treatment. Microplastic beads of different sizes and in different amounts were periodically added to real primary treated wastewater before continuous GDM filtration was conducted for one month. Water quality and permeate volume were analyzed weekly, and resistance analysis and fouling model fitting and heavy metal analysis was conducted. The presence of microplastics led to a flux stabilization at a lower level than the control filtration, while amount and size of microplastic had less influence. Cake layer filtration was largely dominant in the presence of microplastics; however, pore constriction was initially dominant and decreased over time with the cake layer building up in the control filtration. Specifically, larger microplastic beads led to a more porous cake layer, while the high concentration of divalent ions in the control and small microplastic in low amounts filtration led to dense cake layers. Finally, heavy metal analysis showed increased concentrations of most measured elements in the microplastic cake layer.

4.2 Introduction

4.2.1 Mitigation of Microplastics in Wastewater Treatment

Microplastics (< 5 mm) are omnipresent as primary material in products in different forms, including fibers, fragments, and beads, or is produced as secondary microplastics by plastic degradation. They enter wastewater streams through various sources, including laundry processes, cosmetics and personal care products, cleaning products, paints, tire abrasion, and industrial activity (Bayo et al., 2020b; Bui et al., 2020; Enfrin et al., 2019; Hou et al., 2021;

Jiang et al., 2022; Zhou et al., 2021). Microplastics have been found in seafood, terrestrial animals and plants, tap water, soil, beaches, and freshwater systems (Bayo et al., 2020b; De Silva et al., 2021; Vitali et al., 2022; Zhou et al., 2021). The toxicity of microplastics seems to be dependent on size, polymer type, additives and surface chemistry (Okeke et al., 2022). In particular, pharmaceuticals or heavy metals easily adsorb onto the hydrophobic microplastics, increasing the toxicity of the microplastics (Bayo et al., 2020b; Dhineka et al., 2021; Zhou et al., 2021). Although research on the impact of microplastics on human health is limited, it is believed that microplastics can affect human health in three ways: physical damage (i.e. accumulation in internal organs, causing oxidative stress), toxic chemical components (i.e. additives could leach from plastics), and vectors of contaminants (i.e. persistent pollutants or heavy metals get adsorbed by microplastics and could desorb once ingested) (Krishnan et al., 2023; Mohana et al., 2022; Okeke et al., 2022; Yang et al., 2022).

Wastewater is an entry pathway of microplastic pollution to aquatic environments, and wastewater treatment plants serve as the primary barriers for their release to the environment (Jiang et al., 2022). Although the detection of microplastics in wastewater matrix remains challenging, many studies have shed light on their transportation and fates in conventional centralized wastewater treatment processes and explored their impacts on the treatment performance, as summarized in several recently-published review articles (Bui et al., 2020; Enfrin et al., 2019; Hou et al., 2021; Zhang & Chen, 2020). The removal of microplastics in wastewater treatment plants is highly dependent on treatment method and microplastic characteristics (Bui et al., 2020; Enfrin et al., 2019; Hou et al., 2021; Zhang & Chen, 2020). Several studies reported high microplastic removal efficiencies (>90%) in conventional pre-treatment processes (sedimentation/grit chamber), especially for larger microplastics (>100 µm), which can aggregate with activated sludge flocs to facilitate their settling (Bakaraki Turan et al., 2021; Bui et al., 2020; Dhineka et al., 2021; Enfrin et al., 2019; Talvitie et al., 2017). Meanwhile, fibers and low-density microplastics were more easily removed in the aeration tanks (up to 95%), as they attached to air bubbles, which allowed their transport to the water surface (Bui et al., 2020; Enfrin et al., 2019; Hou et al., 2021; Talvitie et al., 2017).

However, microplastics can also negatively affect microbial activity in degrading organics/nutrients by introducing toxic pollutants and foreign microorganisms (attached on their surfaces), or indirect by leaching additives (Bui et al., 2020; Enfrin et al., 2019; Fu et al., 2018; Sun et al., 2018; Wei et al., 2019; Zhang & Chen, 2020). In detail, microplastics could (1) influence microbial ammonization, nitrification and denitrification processes, accordingly, limiting nitrogen removal from the wastewater; (2) promote sludge production: Microplastics offer great surface for microbial immobilization, which would result in enhanced microbial growth; (3) lead to a decreasing number of microbial species and shifts of dominant microbial community compositions (Zhang & Chen, 2020). In addition, the presence of microplastics in the settled sludge may further negatively influence sludge post-treatment, especially when microplastics potentially leach hazardous components during sludge digestion (Enfrin et al., 2019; Fu et al., 2018; Sun et al., 2018). For example, released Bisphenol A from microplastics could inhibit sludge hydrolysis and acidification processes (Wei et al., 2019).

Alternatively, microplastics have hydrophobic surface characteristics, which allow their removals from the wastewater matrix via physical sorption. However, regeneration of adsorbents is still the bottleneck of this approach. In a recently-reported study (Tang et al., 2021), magnetic carbon nanotubes were developed, which displayed strong sorption behaviors to both nonpolar microplastics (via hydrophobic interactions) and polar

microplastics (via electron, electrostatic and hydrogen-bond interactions, and complexation). Thus, microplastics in wastewater might be removed by magnetic carbon nanotube sorption. Importantly, the microplastics removal efficiency was independent of organic and nutrient concentrations in the kitchen wastewater. The process therefore presents an efficient, economic, and eco-friendly alternative for microplastic removal from wastewater.

4.2.2 Mitigation of Microplastics in Decentralized Wastewater Treatment

In decentralized wastewater treatment processes, the investigation on microplastics mitigation has recently gained attention. Note that most of research focused on their mitigation in constructed wetlands (Bydalek et al., 2023a; Bydalek et al., 2023b; Long et al., 2022; Lu et al., 2022; Rozman et al., 2023; Wang et al., 2020; Wei et al., 2020; Xu et al., 2022), and only a few studies focused on their removals from household wastewater in a combined biological treatment with constructed wetlands. Clearly, such combined systems could achieve high removal efficiencies of microplastics (up to 98%) (Wang et al., 2020; Wei et al., 2020). However, these removal values didn't represent additives, which could leach into the water and thus not be removed with the microplastics.

In detail, in the biological treatment processes, it was found that the removal efficiency of microplastics was highly dependent on several factors, such as (1) microplastic size; The larger microplastics were mainly removed by sedimentation and smaller ones by sludge sorption (Wei et al., 2020); (2) microplastic shape; Notably, the removal of fibers in the biological steps was found to be inefficient compared to that of fragments and particles (Wang et al., 2020). This is because the fibers had smooth surfaces, accordingly, presenting less resistance in water than those with other irregular shapes (Wei et al., 2020); (3) operation mode of biological process; It was noticed that ~73% of microparticles (0.1 to 5 mm) could be removed from the water phase in anaerobic systems, while only ~46% of those were mitigated in the combined anaerobic/anoxic/oxic processes. This could be attributed to turbulences and lifting force created by aeration, which reduced the settling velocity of microplastics (Wei et al., 2020).

In constructed wetland processes, high microplastic retention rates were reported (>95%) (Bydalek et al. 2023a). In detail, the main removal mechanisms of microplastics were interception and sorption by the filling materials and sedimentation. Further development of biofilm on the filling materials (reducing void space to facilitate rejection) and plant roots (improving biosorption) could contribute to enhanced removals of microplastics (Wang et al., 2020). Accordingly, more smaller-sized microplastics could be removed compared to larger-sized microplastics (Wei et al., 2020). While, microplastic size distribution and microplastic shape were also important parameters that were associated with their removal efficiencies in the wetland (Wang et al., 2020). For example, lower removal ratios of fibers were noticed compared to those of fragments and particles because fibers had a high length-to-width ratio and thus easily passed through the filling materials (Wei et al., 2020). Nevertheless, it has been highlighted that the constructed wetlands displayed great buffering capacity in treating peak concentrations of microplastics in the raw wastewater (e.g., feed: 21.9-102.3 pieces/L; effluent: 0.10-1.22 pieces/L) (Wang et al., 2020).

4.2.3 Mitigation of Microplastics in Membrane-based Wastewater Treatment

Due to the physical barrier behavior of membranes, superior microplastic removals in MBRs with real wastewater have been reported (e.g., >99.9% removal for 0.005 to 6.9 microplastics/L (Talvitie et al., 2017); >99.4% removal for 57.6 microplastics/L using a 0.4 μm pore size membrane (Lares et al., 2018)). Generally, microplastic removal was dependent on membrane pore size, as the main removal mechanism was size exclusion. Pramanik et al. added polyethylene, polyvinyl chloride and polyester (75, 150 and 300 μm) to a lab-scale membrane filtration (pore sizes 0.1 μm and 100 kDa) with clean water to examine the influence of particle size of microplastics on their removal efficiencies. Due to the smaller pore size of the UF membrane (100 kDa), it achieved higher removals (96% vs. 91% with the MF) (Pramanik et al., 2021). However, in real wastewater microplastics are prone to agglomerate with organic matter and thus form larger particles, which could be more easily removed (Bui et al., 2020; Enfrin et al., 2019). Moreover, the shape and size of microplastics influenced their removals in MBRs. For example, in a full-scale MBR (pore size 0.4 μm) for real wastewater treatment, it was found that the microplastic beads were more easily removed than the fibers (98.83% vs. 57.65%) because of the high operation pressure forcing the thin fibers through the membrane pores (Bayo et al., 2020a). Additionally, high pressure could break microplastics into smaller fragments with sharp edges, causing damages to the membrane (Mohana et al., 2022). Thus, researchers attempt to fabricate novel membranes that could enhance microplastic removal by favoring electrostatic repulsion or increase membrane stability to avoid abrasion (Dey et al., 2023; Mohana et al., 2022).

On the other hand, the presence of microplastics in wastewater could influence performances of membrane-based wastewater treatment system. First, the presence of microplastics could decrease operation flux or increase TMP through creating additional filtration resistance. For example, in a dead-end constant pressure membrane filtration process, the membranes with smaller pore sizes experienced higher flux declines in the presence of microplastics, likely due to the microplastics blocking membrane pores (Pramanik et al., 2021). Second, the presence of microplastics could impact the pollutant removal. For example, when large amount of synthetic polypropylene beads in the wastewater (0.5 g/L), ~91% of COD and ~77% of NH_4^+-N removals were noticed, which were higher than those without microplastics (~89% of COD and ~71% of NH_4^+-N removals) and low amount of microplastics (0.3 g/L: ~88% of COD and ~71% of NH_4^+-N removals) (Wang et al., 2022). This was in accordance with the finding in the work conducted by Hyeon et al., in which it was found ~50-70% of TOC removals by the MF membrane in treating laundry wastewater with microplastic fibers. This could be attributed to enhanced adsorption processes between organics and the hydrophobic microplastics (Hyeon et al., 2023). Thirdly, the presence of microplastics could also influence the microbial behaviors. For example, in an aerobic MBR for municipal wastewater treatment, the microplastics (polypropylene) at lower concentrations (0.14-0.30 g/L) could negatively affect the microbial diversity and enhance extracellular polymeric substances (EPS) production, leading to higher membrane fouling potential; while the microplastics at high concentrations (2.34-5 g/L) showed the opposite trend, resulting in less membrane fouling (Wang et al., 2022).

Towards improving microplastic mitigation, multi-stage wastewater treatment processes are usually adopted. Zhou et al. (Zhou et al., 2020) analyzed the occurrence and elimination of

microfiber (100-500 µm; low density) in on-site three-stage textile wastewater treatment systems, i.e., different combinations of biological treatment, air flotation, and membrane technologies (MBR and reverse osmosis). Compared to the biological treatment process, the air flotation and reverse osmosis process showed highly effective behaviors in mitigating microplastics from textile wastewater. Unexpectedly, the reverse osmosis membrane did not completely reject microplastics, which could be attributed to impaired membranes and non-favorable operating conditions. In terms of the overall microplastics removal efficiency, a combination of biological treatment with air flotation was adopted as the preferable treatment process. However, even excellent microplastics removal ratios (85- 99%) could be achieved by coupling different technologies, the textile industry still releases greater amounts of microfibers to the environments compared to domestic wastewater treatment plants. Especially, the microplastics derived from the textile industry contain chemicals, which raise their negative environmental concerns.

In GDM-based filtration systems, microplastic mitigation in surface water treatment (using synthetic water) has been reported in several articles (Chen et al., 2022; Kim et al., 2022; Wan et al., 2022). Depending on membrane and operation conditions, ~67.5% to >92% microplastic removals were achieved (Kim et al., 2022; Wan et al., 2022). In detail, when the feed water only contained microplastics (5 µm), almost no fouling occurred in a UF GDM system as the rejected microplastics formed a permeable cake layer (Chen et al., 2022). In a GDM system in treating surface water with a large amount of polystyrene beads (100 mg/L; 50-100 nm, 200-500 nm, and 1000-1900 nm) (Wan et al., 2022) or with polyethylene beads (1 mg/L; 40.48 µm) (Kim et al., 2022), the microplastics were primarily removed through size-exclusion which resulted in cake layer fouling and/or pore blocking. In detail, the removal of smaller-sized microplastics were majorly attributed by their electrostatic and hydrophobic interactions with the membranes, therefore, limited microplastic mitigation was present once the adsorption sites were occupied. While the larger-sized microplastics tended to be deposited on the membrane surface to form a dynamic cake layer, which led to a decrease of the flux by ~70% and improved the rejection of smaller-sized microplastics (Wan et al., 2022). Moreover, compared to the GDM system without dosing microplastics, the presence of microplastics in the cake layer rendered it more uniform and facilitated flux stabilization. It was therefore proposed to use the naturally present microplastics in surface water for cake layer conditioning to reduce maintenance during decentralized application of GDM systems (Chen et al., 2022).

As GDM systems are gaining popularity, and the concern on the transport and fate of microplastics in wastewater treatment processes is growing, detailed knowledge on the microplastic mitigation in the GDM-based wastewater system is of paramount importance. However, so far, such work has not been reported. This chapter investigates the influence of microplastics on the GDM performances in treating primary municipal wastewater. The treated water productivity (flux) and quality were monitored when the GDM systems were fed with the wastewater containing different types and amounts of microplastics. The detailed membrane fouling mechanisms were explored by experimental analysis and fouling model simulation. The heavy metals in raw and treated water as well as in the membrane foulants were examined to investigate their interactions with microplastics.

4.3 Materials and Methods

4.3.1 Experimental Setup

The experimental setup was illustrated in Figure 4.1.Totally, 5 GDM systems were operated in parallel, in which the filtration cell was connected to a feed container. The biocarrier reactor (HRT of ~26 h; as described in the Chapter 2.3.1) effluent was employed as the feed water for the GDM systems and certain amount of microplastics were dosed into the feed water as illustrated in Figure 4.1. Two types of microplastics were used in this study, i.e., large microplastics with particle size of 40-48 µm (Polyethylene, Merck, Germany, herein defined as L) and small microplastics with particle size of 0.022-0.027 µm (Polyethylene, Merck, Germany, herein defined as S). In detail, R1 was operated without dosing microplastic beads as control; R2, R3, R4, and R5 were operated with microplastics at 0.1 g/L (S), 0.1 g/L (L), 0.2 g/L (S), and 0.1 g/L (S) + 0.1 g/L (L), respectively. The high microplastic concentration was chosen to represent microplastic accumulation over time in a continuously operating GDM system. The feed containers were placed on magnetic stirrers, which prevented settling/floating of microplastics. The GDM systems were operated continuously without cleaning.

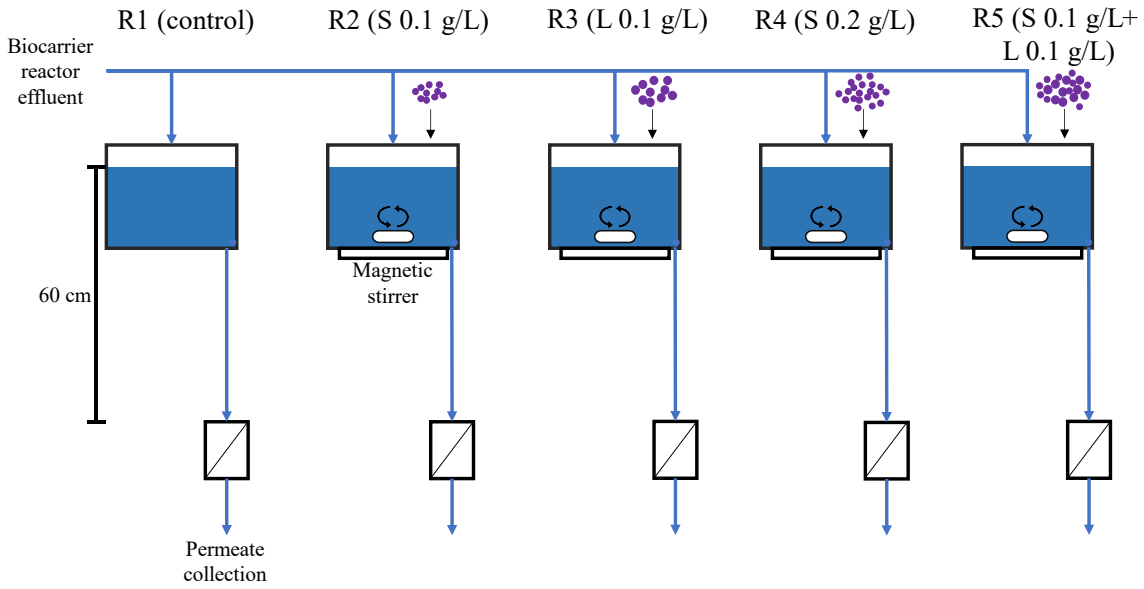

Figure 4.1. Schematic diagram of GDM system with dosing different types and amounts of microplastics

4.3.2 Analytical Methods

The fouling resistance distribution analysis and fouling model simulation followed the methods as described in the Chapter 2.3.3. Water quality analysis was conducted as explained in the Chapters 2.3.5 and 2.3.6. In terms of heavy metal analysis, the samples were digested with 2% nitric acid overnight before being filtered through a membrane filter (0.45 µm, Millipore, US). The metal elements in the filtered samples were analyzed by an inductively coupled plasma-mass spectrometry (ICP-MS, iCAP-Q, Thermo Scientific, US). For soluble organic measurement, the solids were separated from the foulant samples through centrifugation and the supernatant was collected for total organic carbon (TOC)

analysis with the TOC analysis kit (HACH, US) and a spectrophotometer (DR3900, Hach, US), according to the manufacturer's manual.

4.4 Results and Discussion

4.4.1 Effect of Microplastics on Water Quality

Table 4.1 and Table 4.2 show the water quality parameters of the biocarrier reactor effluent (i.e., GDM feed) and GDM permeates. The treated water met the European discharge standards for non-sensitive areas, except the TN values slightly higher than that for sensitive areas (15 mg/L) (European Union, 1991). Compared to the previous experiments presented in the Chapter 2.4.1, the higher COD and TN removal ratios in the GDM systems were noticed. This could be attributed to the longer HRT in the biofilm pre-treatment of the present study (26 h vs. 12 h in the previous study), which led to the effluent containing relatively lower COD concentrations. Moreover, the collected wastewater (the biocarrier reactor feed) presented higher TN values than those in our previous study (~30 mg/L vs. ~14 mg/L), due to seasonal fluctuations. As the MF membrane did not retain soluble nutrients, the higher TN concentrations in the permeate was observed. In addition, the BOD_5 removal ratios increased with more dosed microplastics in the feed water, which may be attributed to increased sorption amounts of organics with more microplastics (Table 4.3) (Chen et al., 2022; Wan et al., 2022).

Table 4.1. Water quality parameters of the biocarrier reactor effluent and GDM permeates

	COD (mg/L) (n=4-8)	TN (mg/L) (n=4-8)	BOD_5 (mg/L) (n=3-8)	pH (n=4-8)	Conductivity (µS/cm) (n=4-8)
Effluent	34.6±6.9	16.3±2.3	18.3±7.7	7.6±0.3	3268.7±1380.5
Permeate (control)	33.4±4.5*	15.8±3.1*	6.7±4.8	7.8±0.2	2552.6±1023.7
Permeate (S 0.1 g/L)			4.5±6.0	7.0±0.3	1230.0±1230.0
Permeate (L 0.1 g/L)			6.9±4.9	7.6±0.4	1295.5±1295.5
Permeate (S 0.2 g/L)			0.6±1.1	7.3±0.5	1303.1±1303.1
Permeate (S 0.1 g/L + L 0.1 g/L)			1.1±1.2	7.2±0.7	1735.9±1735.9
Removal ratios					
Permeate (control)	0±6%	0±15%	57±29%		
Permeate (S 0.1 g/L)			75±34%		
Permeate (L 0.1 g/L)			67±25%		
Permeate (S 0.2 g/L)			92±14%		
Permeate (S 0.1 g/L + L 0.1 g/L)			86±14%		

*The permeate samples were mixed and measured.

As shown in Table 4.2, the GDM systems with dosed microplastics achieved higher TSS removals (>94%) than the control GDM system (86%±15%) This reveals that the microplastics may allow smaller-sized particles being attached on their surfaces and forming agglomerates, thereby preventing them passing through the membranes.

Table 4.2. TSS concentrations and removals in the GDM system

	GDM system	TSS Concentration (mg/L)	Removal ratio
Effluent (GDM feed)	Control	10.7±4.7	
	S 0.1 g/L	20.5±6.0	
	L 0.1 g/L	50.5±5.4	
	S 0.2 g/L	30.5±6.0	
	S 0.1 g/L + L 0.1 g/L	52.3±15.0	
Permeate	Control	1.6±2.8	86%±15%
	S 0.1 g/L	0.0±0.0	100%±0%
	L 0.1 g/L	0.3±0.4	100%±1%
	S 0.2 g/L	1.5±1.5	95%±6%
	S 0.1 g/L + L 0.1 g/L	2.5±2.6	94%±7%

4.4.2 Effect of Microplastics on Membrane Performance

Flux development, fouling resistance distribution, and fouling simulation

The flux evolution profiles for the GDM systems with and without dosed microplastics are shown in Figure 4.2 and their stabilized fluxes were summarized in Table 4.3. It was observed that the initial flux decreased by >90% within the first day, after which the decrease of flux slowed down and tended to be stabilized after ~15 days. Clearly, the GDM system without the dosed microplastics (i.e., control) had a higher stabilized flux (~1.9 LMH) compared to those with the last days fluxes of the filtrations with dosed microplastics (~0.9-1.2 LMH). This was in accordance with a previous study, where the presence of microplastic led to an increased fouling tendency in an MBR for surface water treatment (Li et al., 2020).

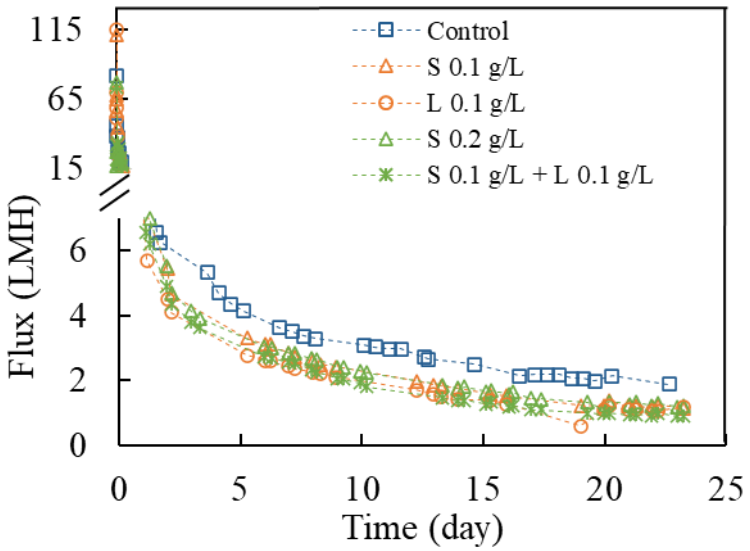

Figure 4.2. The flux evolution profiles during GDM filtration of municipal wastewater with/ without dosed microplastics

Table 4.3. The stabilized flux, deposited foulant mass, deposited soluble organics and estimated porosity in the GDM systems with/without dosed microplastics

Condition	Control	S 0.1 g/L	L 0.1 g/L	S 0.2 g/L	S 0.1 g/L + L 0.1 g/L
Stabilized flux (LMH)	1.93±0.10	1.13±0.06	1.11±0.18	1.20±0.10	0.88±0.08
Deposited foulant mass (g/m^2)	3.53±0.54	5.57±0.45	21.89±0.53	15.39±0.72	35.83±1.17
Deposited soluble organic contents (g/m^2)	0.30±0.06	0.33±0.03	0.32±0.04	0.73±0.08	0.68±0.02

At the end of GDM filtration, the fouling resistance distribution was analyzed and presented in Figure 4.3. In detail, (1) cake layer fouling was largely dominant for all the tested GDM systems (>98%). It is noted that the membrane had a pore size of 0.08 µm, which was greater than the small-sized microplastics (0.022-0.027 µm). Possibly, the small-sized microplastics could interact with organic foulants to form greater-sized aggregates through hydrophobic interactions, which tended to deposit on the membrane surface (Bui et al., 2020; Enfrin et al., 2019). This was confirmed by similar COD level in permeates and effluent, indicating the retention of all microplastic particles (Table 4.1; Note that the microplastics contained ~470 mg COD/g microplastics). (2) The presence of microplastics in the feed water led to a 56-117% increase in cake fouling resistance but did not cause a significant effect on irreversible and irremovable fouling resistance. This revealed that the majority of microplastics were deposited on the membrane surface instead of narrowing/blocking membrane pores. (3) Increasing microplastic size (S 0.1 vs. L 0.1 and S 0.2 vs. S 0.1+L 0.1) led to a slight increase in cake resistance (18% and 32% respectively). (4) Increasing microplastic amount (S 0.1 g/L vs. S 0.2 g/L) resulted in a similar cake resistance.

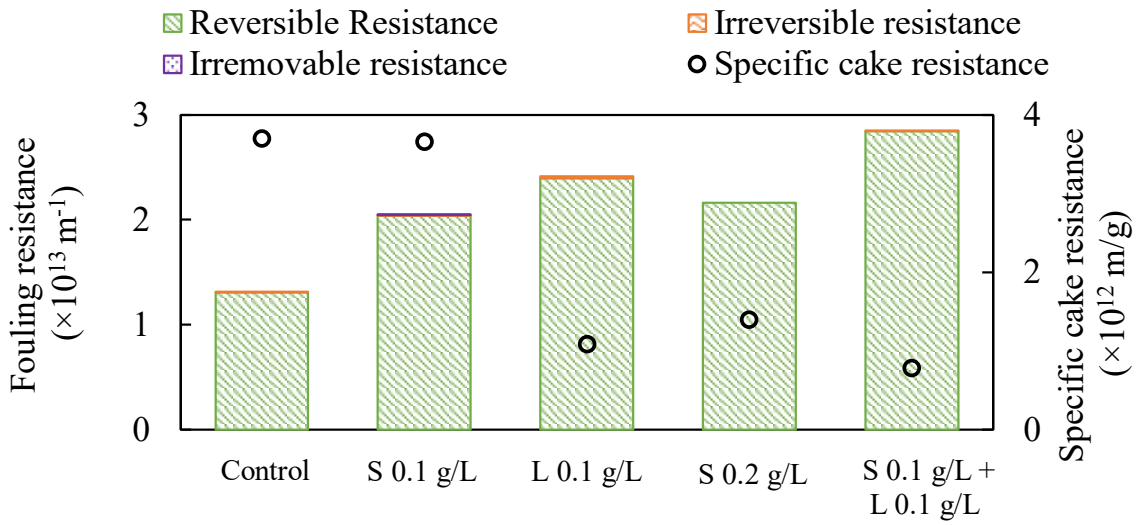

Figure 4.3. Filtration resistance distribution and specific cake resistance during GDM filtration of municipal wastewater with/without dosed microplastics

The filtration constants derived from fitting the flux data to the fouling model were shown in Figure 4.4. The GDM system without dosed microplastics (i.e., control) followed a three-stage fouling pattern. In detail, during initial filtration (within 1 h), the pore constriction was dominant; with extending filtration time, the pore constriction constants decreased, and the

contribution of cake filtration increased (Figure 4.4a). This was in accordance with the results presented in the Chapter 2.4.2. Compared to the control GDM system, the GDM filtration of wastewater with microplastics resulted in greatly lower pore constriction constants and higher cake filtration constants, regardless of microplastic type and dosed amount (Figure 4.4b). This could be explained by the rapid cake layer formation in the presence of microplastics, which could prevent smaller-sized foulants from entering the membrane pores.

When the wastewater contained 0.1 g/L of small- or large-sized microplastics, the membrane fouling displayed a two-stage pattern, in which the pore constriction constant reduced significantly while cake filtration constant remained constant with extending filtration time. However, in the GDM systems dosed with 0.2 g/L of microplastics, both pore constriction and cake filtration constants remained almost constant through the overall filtration period, showing a one-stage fouling pattern. The pore constriction constant was very limited, indicating a rapid cake layer proliferation on the membrane surface, possibly the presence of a greater amount of microplastics in the feed led to increased interactions with organic foulants, allowing them being deposited on the membrane surface (Table 4.3) instead of blocking/narrowing the pores.

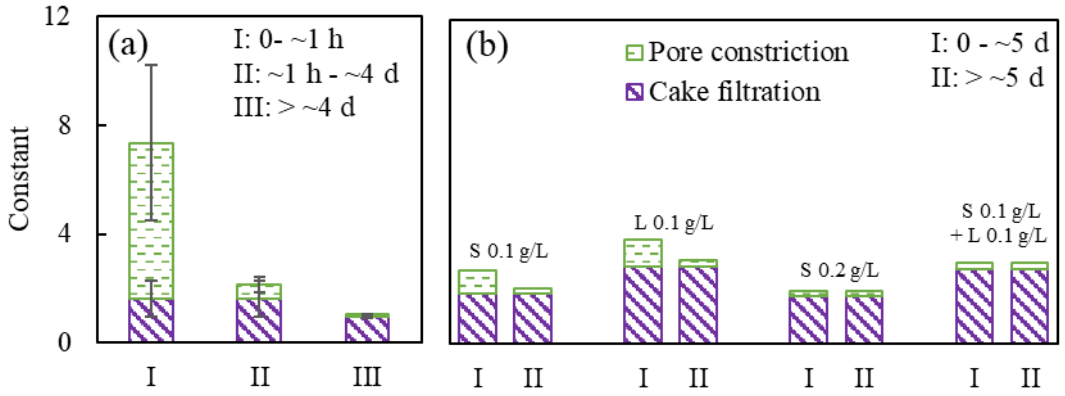

Figure 4.4. The simulated filtration constants in the GDM systems (a) without dosed microplastics, and (b) with dosed microplastics.

Cake layer Foulant analysis

The cake foulants that were deposited on the membrane surfaces were sampled for analysis of the cake mass density and soluble organic deposition density, as shown in Table 4.3. The results revealed that (1) increasing microplastic size (S 0.1 vs. L 0.1 and S 0.2 vs. S 0.1+L 0.1) led to higher foulant mass depositions (293% and 133% respectively) but did not influence the amount of organic deposition. Possibly, larger microplastics were fully retained by the membrane, and the cake layer structure allowed the development of prokaryotes and eukaryotes while smaller microplastics may form the cake layer structure that was not suitable for biofilm development. (2) increasing microplastic amount (S 0.1 g/L vs. S 0.2 g/L) led to a significant increase in foulant mass depositions (176%), due to increased depositions of microplastics and soluble organics (119%). As reported previously, the presence of more microplastics in the cake layer could facilitate organic accumulation due to increased interactions between organics and microplastics (Hyeon et al., 2023). Meanwhile, the GDM system without dosed microplastics showed slightly lower foulant

mass depositions than that with S 0.1 g/L, possibly due to dissimilar cake morphology influencing microbial community development.

Table 4.4 shows the metal and metalloid concentrations in effluent and cake layer foulants. Compared to the control, the GDM systems with the dosed microplastics tended to form cake layers embedded with greater contents of most measured elements. In particular, the cake layers with the dosed microplastics contained 47-144 times higher concentrations of Pb than that in the control system. The metal contents in the cake layers had a similar pattern as the foulant mass depositions (Table 4.3). In detail, increased microplastic amounts offered more opportunities for retention in the cake layer, which led to more metal accumulation. Specifically, no clear trend on metal deposition could be found between the different microplastic sizes. Generally smaller microplastics present higher surface areas, which is favorable for sorption processes (Qiao et al., 2019). Possibly, the divalent ions (Table 4.5) may compete with the metal elements presented in Table 4.4 for the sorption sites by microplastics.

Table 4.4. Metal and metalloid content in effluent and cake layers

	Effluent (μg/L)	Foulants (μg/m^2)				
		Control	S 0.1 g/L	L 0.1 g/L	S 0.2 g/L	S 0.1 g/L + L 0.1 g/L
Ti	7.6±1.7	374.42	1212.18	1549.54	1248.73	2259.01
V	3.1±1.3	405.57	275.20	483.72	541.94	789.81
Cr	1.0±0.3	92.63	100.28	234.94	193.10	280.67
Mn	408.3±214.1	4978.04	2442.94	6281.94	5951.71	13056.44
Co	12.6±9.3	315.98	112.13	546.99	281.60	854.09
Ni	25.4±13.9	177.34	149.25	307.55	378.48	615.67
As	1.0±0.4	24.85	17.25	23.83	47.76	58.91
Rb	8.9±1.8	13.23	11.67	18.97	27.47	34.82
Sr	245.9±64.3	1666.35	1128.70	1297.87	2756.01	2756.34
Mo	8.6±4.0	74.57	82.22	46.68	112.09	79.52
Cd	0.2±0.1	4.82	10.41	13.95	25.63	25.26
Sn	0.2±0.1	10.68	12.83	17.25	24.16	44.41
Sb	0.6±0.1	8.67	15.21	13.28	19.59	19.36
Ba	24.5±3.5	938.19	721.97	1016.79	1485.20	2627.00
W	2.1±1.6	5.81	8.93	21.09	16.18	43.52
Hg	2.3±3.0	0.64	0.80	1.14	1.57	2.14
Pb	2.0±0.4	110.63	5173.98	5068.77	15900.31	15198.31

As well documented, divalent metal ions can enhance aggregation of organics, which leads to a dense cake layer and strong fouling potential (Aoustin et al., 2001; Peter-Varbanets et al., 2011; Yuan & Zydney, 1999). Thus, the divalent ion contents (i.e., the mass of the ion accumulated on the membrane surface divided by the total foulant mass) in the cake layers were measured and presented in Table 4.5. Clearly, the divalent ion contents were independent of the amount and size of the dosed microplastics. Compared to the control, higher divalent contents in the cake layers with smaller microplastic at lower concentration (0.1 g/L) were noticed, while those in the other conditions were lower than the control.

Table 4.5. Divalent ion content in cake layers

Element	Unit	Control	S 0.1 g/L	L 0.1 g/L	S 0.2 g/L	S 0.1 g/L + L 0.1 g/L
Mg	mg/g	9.58	12.88	2.87	7.07	1.95
Si	mg/g	8.66	17.35	2.43	5.81	1.69
Ca	mg/g	21.64	32.32	4.34	15.85	3.25
Total	**mg/g**	**39.88**	**62.55**	**9.65**	**28.73**	**6.88**

Cake Fouling mechanism

To further explore the impact of accumulated microplastics on the cake layer fouling mechanism, the specific cake resistance was calculated and presented in Figure 4.3. It was noticed that (1) in the presence of a large-sized microplastics (L 0.1 g/L), the specific cake layer resistance was lower than that in the control, although more foulants accumulated on the membrane surface (Table 4.3). This indicated a more porous cake layer, which could be attributed to the larger-sized microplastics allowing more space between them (Li et al., 2021b), meanwhile the deposited organics appeared not to form a dense aggregate layer due to less divalent ions present in the cake layer (Table 4.5; as illustrated in Figure 4.5). (2) In the presence of small-sized microplastics (S 0.1 g/L), the specific cake resistance was comparable to that in control, possibly due to their similar foulant (especially organics) deposition (Table 4.3). Meanwhile, with increasing small-sized microplastic amounts from 0.1 g/L to 0.2 g/L in the feed water, the specific cake resistance decreased. It is noted that increasing microplastic amount led to increases of foulant mass depositions and organic density (i.e., more foulants accumulated), but with a lower divalent ion content in the cake layer, as a result, weaker bridging between organics occurred and thus a more porous cake layer (as illustrated in Figure 4.5). (3) In the presence of the same amount of microplastics with different sizes (S 0.1 g/L vs. L 0.1 g/L and S 0.2 g/L vs. S 0.1 g/L+ L 0.1 g/L), the larger microplastics led to a lower specific cake resistance, which indicated a more porous cake layer. Possibly, the presence of larger microplastics facilitated more foulant accumulation, but with less divalent ions, creating a porous cake layer (as illustrated in Figure 4.5).

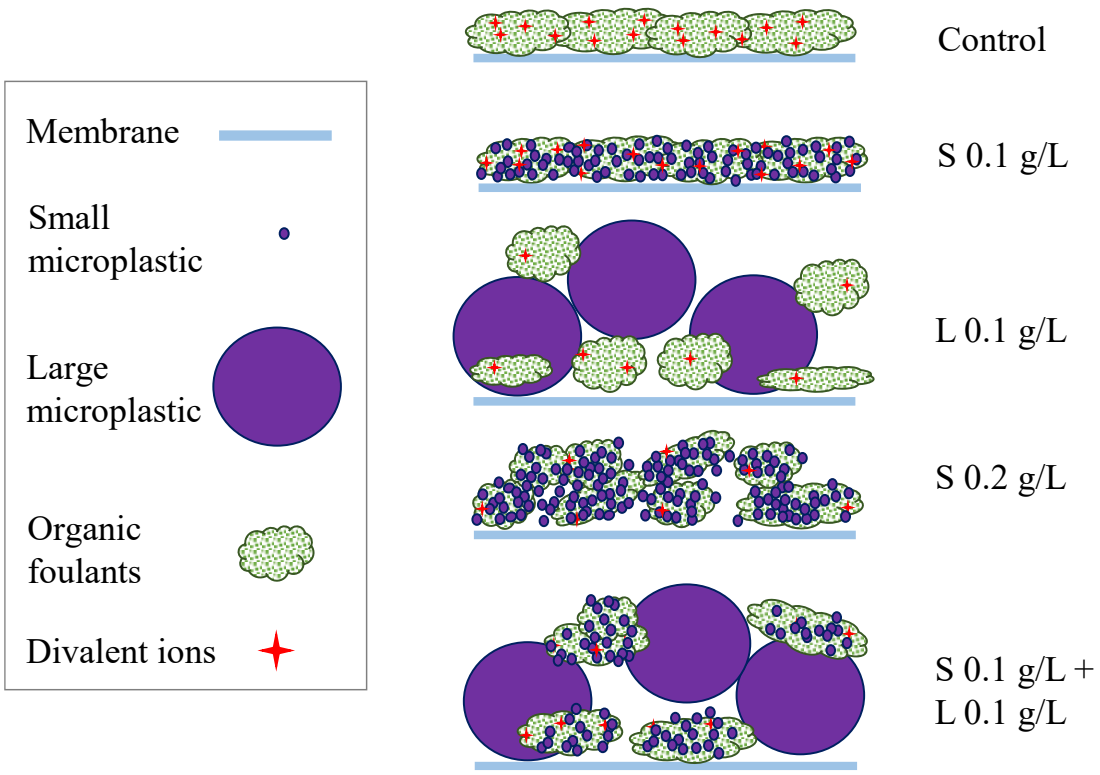

Figure 4.5. A diagram showing the proposed cake morphology in the GDM systems in the absence and presence of dosed microplastics.

4.5 Conclusions

This chapter presented the influence of microplastics on the performance of GDM system in treating municipal wastewater. It was found that:

(1) The presence of microplastic in the feed did not greatly influence permeate quality of dissolved substances.

(2) Under the studied conditions, the accumulation of microplastics on the membrane surface lowered the stabilized flux of the GDM system. The presence of microplastics in the feed water led to higher cake layer filtration constant. The pore constriction constant decreased significantly with increasing microplastic accumulation, as the cake layer prevented foulants to penetrate membrane pores.

(3) Metal analysis showed their increased accumulation in cake layers with microplastics than that in the control. Especially, with increasing microplastic amount, the accumulation of metal elements in the cake layers increased.

(4) When the small-sized microplastics (0.1 g/L) in the feed water, a denser cake layer appeared on the membrane surface due to more divalent ions bridging organics to form aggregates. The large-sized microplastics facilitated decreasing the specific cake resistance by forming porous cake layers on the membrane surface due to more space between the large beads and lower divalent ion concentration, which created weaker bonds between organic foulants.

5 Life Cycle Assessment and Cost Analysis of Decentralized Wastewater Treatment in Cold Climate

This chapter contains parts of Article 3 and Article 4:

Hube, S., Hauser, F., Burkhardt, M., Brynjólfsson, S., Wu, B. 2023. Ultrasonication-assisted fouling control during ceramic membrane filtration of primary wastewater under gravity-driven and constant flux conditions. Separation and Purification Technology, 310, 123083. https://doi.org/10.1016/j.seppur.2022.123083

Hube, S., Zaqout, T., Ögmundarson, Ó., Andradóttir, H., Wu, B. Constructed wetlands with recycled concrete for wastewater treatment in cold climate: Performance and life cycle assessment. Science of the Total Environment, 904, 166778, https://doi.org/10.1016/j.scitotenv.2023.166778.

5.1 Abstract

This chapter investigated the environmental and economic feasibility of different decentralized cold climate wastewater treatment systems. In detail, a comparative LCA of septic tank standalone, septic tank + constructed wetland, and gravity-driven ceramic membrane (GDCM) system was performed under real-life scenarios. This aims to illustrate the benefits of intensifying the existing treatment process (i.e., septic tank) with the constructed wetland, with an alternative membrane-based treatment technique as benchmark. The LCA results revealed that the use of waste materials as the substrate in constructed wetlands benefitted to reduce the environmental impact of wetlands. Installation of the wetland as posttreatment of the septic tank (1) could reduce ~50% of eutrophication potential without increasing the global warming impact compared to the septic tank alone; (2) had ~90% higher global warming impact and ~40% lower eutrophication impact compared to the GDCM system. Economic analysis revealed that the total cost of septic tank + constructed wetland (0.143 EUR/m³) was comparable to the septic tank alone (merely 3.5% difference), and 49% lower than that of GDCM (with recycled ceramic membranes). Therefore, the septic tank + constructed wetland scenario could be especially favorable for sensitive areas with eutrophication challenge with regards to its technical, economical, and environmental feasibility.

5.2 Introduction

Wastewater treatment in remote areas has gained attention, especially with increasingly stricter wastewater discharge legislation globally (Kobayashi et al., 2020) and the

implementation of the SDG No. 6 “Ensure access to water and sanitation for all” (United Nations, 2015). Compared to centralized wastewater treatment systems, decentralization of wastewater treatment holds a large potential to reduce energy consumption for water transportation and allows more modularity and adaptation to the local situation and requirements (Kobayashi et al., 2020b; Longo et al., 2016). A commonly used decentralized wastewater treatment process is the septic tank, which is mostly suitable for household-scale. However, the accumulated sludge requires regular discharging, and malfunctions in sludge settling or biodegradation efficiency (especially in cold climate) can lead to seasonally lower effluent quality. In addition, the anaerobic condition in septic tanks facilitates methane production, a greenhouse gas, which has a negative environmental impact if it is not collected properly (Mac Mahon et al., 2022).

Alternatively, nature-based constructed wetlands have been widely adopted for decentralized wastewater treatment, due to their lower maintenance requirements, simple operation, low sludge production and cost (García et al., 2013; Hijosa-Valsero et al., 2010; Kobayashi et al., 2020b). In wetlands, several behaviours, such as aerobic/anoxic/anaerobic biodegradation, filtration, sorption, plant uptake, photodegradation, facilitate removing organics, nutrients, micropollutants, and pathogens from wastewater simultaneously (Varma et al., 2021a). The application of constructed wetlands for municipal wastewater treatment in cold climate has been systematically reviewed (Ji et al., 2020; Maucieri et al., 2017; Varma et al., 2021; Wang et al., 2017a; Werker et al., 2002), in which several challenges have been addressed, such as ice formation and clogging, and reduced biological and plant activity (Varma et al., 2021). It was also illustrated that the effects of cold temperature on organic and nutrient removal efficiencies were highly associated with constructed wetland configuration and operation philosophy. For example, compared to free water surface wetlands, sub-surface flow wetlands were advantageous in cold climate because bacterial communities living below the surface can be protected from frost damage, allowing them to perform biodegradation roles (Ji et al., 2020). However, the reported GHG emission levels varied considerably, which was thought to highly depend on plant species and amount, oxygen availability, wastewater loading and composition, wetland substrate and configuration, etc. (Maucieri et al., 2017).

In wetlands, substrate materials perform an important role as they provide binding sites for biofilm development and support aquatic plants (Varma et al., 2021). Generally, natural materials (such as gravels) are widely used as wetland substrate, but they are short supply and suffer from clogging problems (Cao et al., 2021; Varma et al., 2021). In recent years, recycled aggregates from construction and demolition wastes have shown their great potential as wetlands substrates due to their relatively low density, great water absorption, and high porosity (Cao et al., 2021; Li et al., 2022). The use of low-cost recycled aggregates in wetlands would benefit for saving natural geological resources, reducing the adverse effects of waste disposal, minimizing carbon footprint of construction materials, and reducing overall costs (Cao et al., 2021; Li et al., 2022). However, using construction and demolition waste as biocarriers in constructed wetlands for decentralized wastewater treatment in cold climate has not been attempted yet.

In recent years, LCA has been gaining attention for environmental impact assessment of products and processes. LCA is a tool for quantitatively accounting emissions of a product or process considering different impact categories from a life cycle perspective (Hauschild, 2015; ISO 14040, 2006; ISO 14044, 2006). Assessing wastewater treatment options with LCA allows to reduce environmental impacts by shedding light on emission drivers and thus

supporting decision making as illustrated in previous reports (Daskiran et al., 2022; Kobayashi et al., 2020; Lutterbeck et al., 2017). Numerous comprehensive LCA on constructed wetlands as a municipal wastewater treatment process or post-treatment process have been documented (Casas Ledón et al., 2017; Corbella et al., 2017; Fang et al., 2023; Fuchs et al., 2011; Garfí et al., 2017; Lutterbeck et al., 2017; Resende et al., 2019; Vassalle et al., 2023). Previous literature has identified a trade-off between a reduction of eutrophication impact and increased global warming impact in constructed wetlands with high intensity wastewater treatment (Zang et al., 2015). However, the detailed findings were not well comparable because of differing assumptions, operation conditions or system boundaries (such as including/excluding construction, infrastructure, transportation, end-of-life stage, etc.) (Kobayashi et al., 2020; Resende et al., 2019). For example, researchers found that the construction stage could make a substantial contribution to the total impacts, especially in small scale wetland systems (Corbella et al., 2017; Fuchs et al., 2011; Lutterbeck et al., 2017). Meanwhile, other studies reported the dominance of the operation phase among the examined impact categories (64 - 100%) (Fang et al., 2023; Resende et al., 2019). Reduction of environmental impacts in the operation phase requires the adoption of optimized treatment conditions and improved removal or recycling of liquid/gaseous emissions (Li et al., 2021d; Resende et al., 2019). Depending on the type of power generation, electricity consumption can also be the major contributor to GHGs (Fang et al., 2023). For example, reducing aeration and pumping (replaced by gravity flow) in wetland systems benefitted to reduce electricity consumption, leading to lower indirect greenhouse gas emissions (e.g., carbon dioxide from fossil fuels) (Fang et al., 2023; Resende et al., 2019). Nevertheless, constructed wetlands displayed lower environmental impacts and costs than conventional activated sludge systems, and lower or similar environmental impacts and costs than other decentralized systems (such as high rate algal ponds, trickling filters, polishing ponds) (Casas Ledón et al., 2017; Garfí et al., 2017; Vassalle et al., 2023). However, LCA of recycled construction waste-based wetlands for wastewater treatment in cold climate has not been well studied.

Besides technical feasibility and environmental impacts, costs of wastewater treatment are a crucial factor for the implementation of a wastewater treatment technology. In detail, similar to LCA, comparisons between cost assessments should be conducted carefully, as they are site-specific and highly dependent on underlying assumptions (Hernández-Chover et al., 2021; Nelson et al., 2021). Moreover, costs vary between treatment technology and level, as shown in comparative study by Ozgun et al. (2021) with 16 municipal wastewater treatment plants ranging from 46000 to 600000 m^3/d. For example, it was reported that both capital (42% of total costs for tertiary treatment), and operational and maintenance (58% of total costs for tertiary treatment) costs increase with additional treatment steps (Ozgun et al., 2021). A full-scale centralized activated sludge plant (municipal wastewater; 5500 m^3/d) resulted in the total cost of ~0.82 \$/m^3 (Abbasi et al., 2021), while Pryce et al. reported an integrated fixed-film activated sludge system (municipal wastewater; 69.6 m^3/d) had the total cost of ~0.31 \$/m^3 (Pryce et al., 2022). This is due to a large share (up to 50%) of total costs for aeration in activated sludge processes (Abbasi et al., 2021; Huang et al., 2022; Pryce et al., 2022). Meanwhile, maintenance costs amount to ~25% of total operation costs, leading to higher expenses for maintenance than for construction over lifetime (Hernández-Chover et al., 2021).

Recently, increasingly stricter environmental standards lead to costs increase (32.79-55.66%) due to the high energy requirement of intensified treatment (Huang et al., 2022).

Thus, good planning is crucial to minimize costs, for example oversizing can lead to an ~8% increase in costs per water productivity due to high investments, maintenance costs and inefficient operation, especially in small-scale plants (Hernández-Chover et al., 2021). Thus, the cost for the decentralized treatment techniques (especially the newly developed advanced techniques) must be assessed considering social and environmental conditions.

This chapter aims to assess the environmental and economic feasibility of septic tank, constructed wetlands and gravity-driven ceramic membrane filtration (GDCM) for domestic wastewater treatment by performing a comparative LCA and cost analysis.

5.3 Materials and Methods

5.3.1 Recycled Construction Waste-based Constructed Wetlands

Materials and methods as well as performance assessment of recycled construction waste-based constructed wetlands are presented in the Appendix.

5.3.2 LCA Methodology

The comparative LCA, follows the DIN standards (ISO 14040, 2006; ISO 14044, 2006). It is noted that septic tanks are well adopted as a conventional decentralized treatment process in cold climate, which are generally placed underground without requiring pumping and chemicals during operation but requiring sludge removal after certain operation time. Because the treated water quality in septic tanks (especially under low temperatures) do not well meet discharge standards, a constructed wetland is implemented as a second treatment process. As illustrated in chapter 3, the biocarrier-facilitated GDCM process provided a feasible solution for decentralized wastewater treatment in cold climate. Thus, in this study, the following three scenarios were adopted for an LCA comparison: (1) septic tank alone; (2) septic tank + constructed wetlands; (3) GDCM.

The software openLCA (1.10.3), the database ecoinvent 3.7 (Wernet, 2016) and Microsoft Excel were used for system modelling and emission calculations with the TRACI method (Bare, 2002). The different treatment scenarios were compared in the impact categories "Global warming" and "Eutrophication". Generally, the impact category "Ecotoxicity" was also commonly used in wastewater LCAs (Corominas et al., 2020), however micropollutants were not measured in the present study and therefore this category was not considered. As shown in Figure 5.1, the system boundaries included construction and operation phase. Transport of construction material and end-of-life phase were not included in the system boundaries as their contributions to emissions were negligible compared to the overall system emissions as illustrated in previous studies (Corominas et al., 2020; Flores et al., 2019; Garfí et al., 2017). The lifespan of septic tanks, constructed wetlands, and inorganic membrane systems was considered as 20 years (Asif & Zhang, 2021; Flores et al., 2019; Garfí et al., 2017; Hashemi & Boudaghpour, 2020; Resende et al., 2019). The systems were sized for 10 people equivalent (PE, representing household scale), and the functional unit was one cubic meter of treated wastewater.

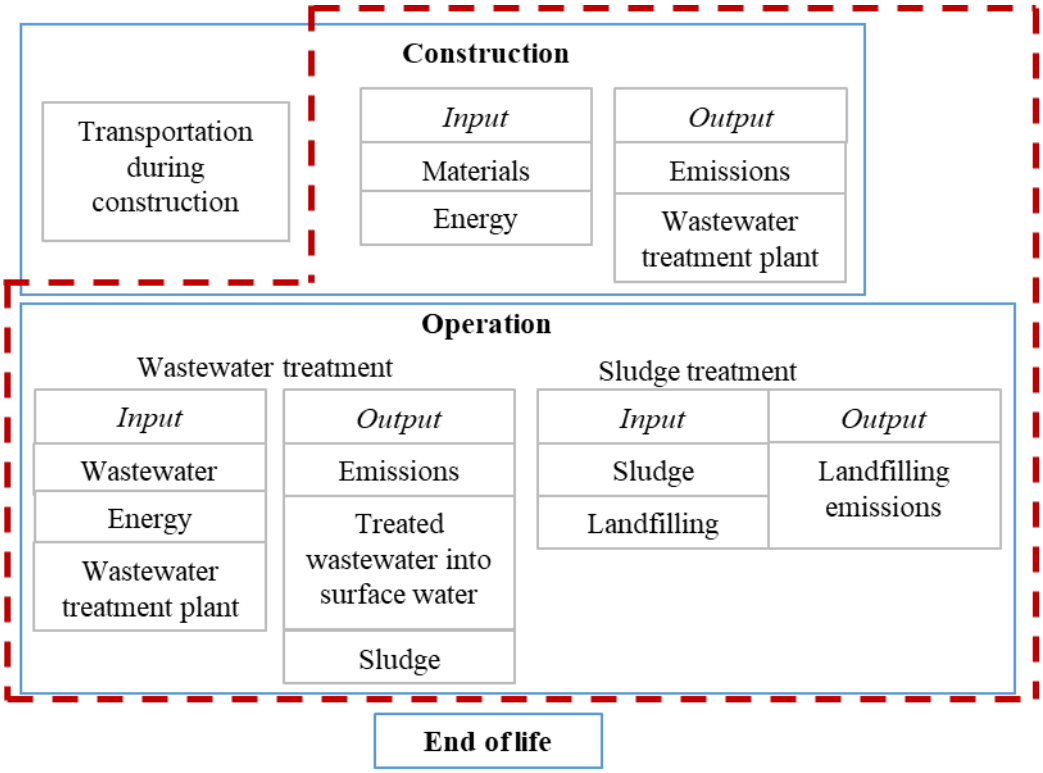

Figure 5.1. System boundaries in LCA analysis

5.3.3 Life Cycle Inventory Data

The detailed life cycle inventory data is described in Table 5.1. The experimental data from the constructed wetland experiments (see Appendix) and chapter 3 under an Icelandic scenario (representing a cold climate region) was used, including the feed water quality and pollutant removal efficiencies in constructed wetlands and GDCM. When additional data was needed, similar operation conditions as those under the Icelandic scenario were carefully selected from literature and the ecoinvent database. It is noted that the literature data was not site-specific. Depending on data availability, the priority of flow and process data that were adopted in this study followed as sequence as Icelandic scenario, EU scenario, and global scenario. Whenever openLCA processes were used, the electricity flows were changed to flows representing the average Icelandic energy mix (hydropower and geothermal) and the heat flows were replaced by tap water flows, to represent local geothermal heat production.

Table 5.1. Life cycle inventory analysis for construction & operation phase

Construction of septic tank	
Parameter and value	Details
Volume: 4 m^3	PE×200 L + 2000 L (Umhverfisstofnun, 2022) openLCA flow: “excavation, hydraulic digger”
Wastewater flow per capita: 270 L/d	Average wastewater production per capita in Iceland (Veitur, 2019)
Polyethylene: 248.89 kg	4 m^3 × 0.062 kg/L (Saeplast, 2023) openLCA flow: “polyethylene, high density, granulate”
Pipes: 203 kg	50 m×4.06 kg/m (PVC Pipe Supplies, 2023) The present scenario includes 10 PE, so ~2 households connected to the same wastewater treatment system. A conservative estimation of a

	total of 50 m of piping was taken for the septic tank scenario and another 20 m with the added constructed wetlands. openLCA process: "polyvinylchloride production" (Resende et al., 2019)
Construction of wetland	
Parameter and value	Details
Volume: 6.95 m^3	HRT×Q/0.6 = 50 h × 2 m^3/d/0.6 (considering 40% biocarrier packing ratio); Data from the experiments in this study openLCA flow: "excavation, hydraulic digger"
Biocarrier: Recycled concrete gravel: 4.61 ton	0.4×6.95m^3 ×1.66 t/m^3 Data from the experiments in this study openLCA flow: "waste concrete gravel"
Pipes: 81.2 kg	See the details on the pipes for septic tank
Plants	The plants were only relocated and thus did not produce emissions.
Liner: 1.62 kg	Wetland height: 0.4 m and Volume: 6.95 m^3, leading to length=width = 4.17 m A_{liner} = Area + 4×length×height = 17.4 m^2+4×0.4 m×4.17 m = 24.04 m^2 Liner thickness = 7 mm V = 24.04 m^2×0.007 m = 0.017 m^3 m = 0.017 m^3×95 kg/m^3 = 1.62 kg (Múrbúðin, 2023) openLCA flow: "polyethylene, low density, granulate"
Construction of GDCM	
Parameter and value	Details
Tank: 0.101 items	Effective membrane module volume/0.6 = 1.01 m^3 as explained in the previous study (Hube et al., 2023) openLCA flow: "storage, 10'000 l"
Biocarrier: 485.79 kg	40% of the tank volume: 0.404 m^3 biocarrier density: 1202.44 kg/m^3 (based on the experiments presented in the appendix) openLCA flow: "gravel, crushed" Volcanic gravel is a local resource in Iceland.
Membrane: 302.60 kg Silicon carbide	Silicon carbide membrane produced in Denmark 5.49 kg/m^2 (Cembrane) A_m: 55.14 m^2 (Hube et al., 2023) openLCA flow: "silicon carbide" The energy provider was changed to Denmark.
Pipes: 203 kg	50 m of pipes, see the details on the pipes for septic tank
Pump	A feed pump is needed to deliver the feed to the system. openLCA flow: "pump, 40W"
Operation of septic tank	
Parameter and value	Details
Septic tank effluent COD: 73.17 g/m^3 BOD_5: 30.72 g/m^3 TN: 21.92 g/m^3 PO_4: 6.10 g/m^3	The effluent data was calculated based on the typical septic tank removal ratios (EPA, 2002; Umhverfisstofnun, 2022) and the feed water quality data was taken from the experimental data in this study.
Gaseous emissions: N_2O: 0.03 g/m^3 CH_4: 55 g/m^3	Gaseous emission estimation based on the reference (Leverenz et al., 2010) CO_2 emissions from wastewater are not considered because of their biogenic origin (Eggleston et al., 2006)
Sludge production 1.91 kg/m^3	Based on the reference (Mac Mahon et al., 2022)

Sludge treatment	The sludge in Iceland is conventionally landfilled in a sanitary or unsanitary landfill. openLCA processes "treatment of municipal solid waste, sanitary landfill" and "treatment of municipal solid waste, unsanitary landfill, moist infiltration class (300mm)"
Operation of wetland	
Parameter and value	Details
Effluent COD: 35.85 g/m^3 BOD_5: 10.75 g/m^3 TN: 14.46 g/m^3 PO_4: 0.85 g/m^3	Calculated based on the septic tank effluent and removal ratios taken from the experimental data in this study.
Gaseous emissions CH_4: 0.64 g/m^3 N_2O: 0.02 g/m^3	Based on the reference (Søvik et al., 2006)
Operation of GDCM	
Parameter and value	Details
Electricity: 0.000781 kWh/m^3	Data were taken from our previous work (Hube et al., 2023) openLCA flow: "electricity, low voltage"
Permeate quality: COD: 48.71 g/m^3 BOD_5: 8.50 g/m^3 TN: 17.44 g/m^3 PO_4: 6.42 g/m^3	Calculated based on the removal ratios and feed water quality adopted from the data in the previous work (Hube et al., 2023)
N_2O and CH_4 emissions: 77 g/m^3 CO2-eq	0.22×0.35 kg/m^3 CO_2-eq ~22% of the total CO_2-eq emissions of a biological filter could be attributed to direct CH_4 and N_2O emissions (Liao et al., 2020) TRACI doesn't consider biogenic CO_2 flows in openLCA. The selected data from the literature represented both CH_4 and N_2O emissions, which would be considered in TRACI, therefore the elementary flow "Carbon dioxide, fossil" was selected.
Sludge production: 5.64 g/m^3	0.145 g TSS/g COD removed (El-Shafai & Zahid, 2013) COD removed in the biofilm + GDM process: 38.87 g/m^3

5.3.4 Cost Analysis

For simplification and comparison purposes, only primary materials were considered for the capital costs, while construction, labor, and transport costs were excluded as they highly depend on local requirements. The calculations rely on the same assumptions as those in the LCA (chapter 5.3.3). The details were summarized in Table 5.2.

Table 5.2. A summary of capital and operational cost estimation

Capital cost item	**Details**
Septic tank: 337.43 EUR	Estimated at 83 EUR/m^3*; For 4 m^3
Septic tank piping: 171.24 EUR	Estimated at 0.83 EUR/kg*; For 50 m
Constructed wetland piping: 68.50 EUR	Estimated at 0.83 EUR/kg*; For 20 m
Liner: 2.51 EUR	Estimated at 1.54 EUR/kg*; For 24.04 m^2
Biocarriers: Recycled concrete	Free of charge

GDM tank	(Effective membrane module volume / 0.6) × 160 EUR/m^3 Packing ratio of membrane module: 0.6 Tank cost is estimated at 160 EUR/m^3
Direct constant flux filtration tank	Effective membrane module volume × 160 EUR/m^3
Biocarriers	Reactor volume × packing ratio of 40% × lava stone cost Lava stone cost is estimated at 20 EUR/m^3
Pumps (feed, permeate and backwash)	Feed flow × 20 EUR/m^3 /h (Fletcher et al., 2007)
Ceramic membrane	(Feed flow/permeate flux) × 500 EUR/m^2 or 65 EUR/m^2 500 EUR/m^2 for commercial ceramic membranes; 65 EUR/m^2 for ceramic membranes made of waste material (Abdullayev et al., 2019; Dong et al., 2022)
Ultrasonication device	Effective membrane module volume × 12000 EUR/m^3 The ultrasonication device is estimated at 12000 EUR/m^3 membrane module
Control system for direct constant flux filtration	20000 EUR + 10 × feed flow (Lin et al., 2011)
Operational costs	**Details**
Septic tank sludge treatment: 75.31 EUR/year	Discharged once per 3 years (Hrunamannahreppur, 2023)
Biofilm + GDCM sludge treatment: 22.59 EUR/year	Discharged once per 10 years due to slow sludge production rate.
Pump energy	((water head × flow ×365)/(36 × 0.8)) × 0.06 EUR/kWh (Pump efficiency of 0.8; GDM feed pump at water head of 23 cm (i.e., 0.023 bar), constant flux filtration feed pump at water head of 1 bar, backwash pump at water head of 1 bar; electricity cost in Iceland of 0.06 EUR/kWh)
Ultrasonication energy	Ultrasonication duration × power input × 0.06 EUR/kWh (Power input is estimated at 1.1 kW/m^3 tank)
Geothermal water	Yearly standard rate + water volume × 0.69 EUR/m^3 (Yearly standard rate at 325 EUR/year)
Chemical cleaning	3 L/m^2/time × membrane area × 60 EUR/m^3 × 365 time/year (0.5% NaClO cost is estimated at 60 EUR/m^3 (Shami & Wu, 2021))

*The estimations are based on current prices of the materials in local hardware stores.

5.4 Results and Discussion

5.4.1 Global Warming

Figure 5.2 shows the calculated emissions in global warming and eutrophication categories from construction and operation (including both wastewater treatment and sludge treatment) as well as the contribution ratios of individual items to these impact categories.

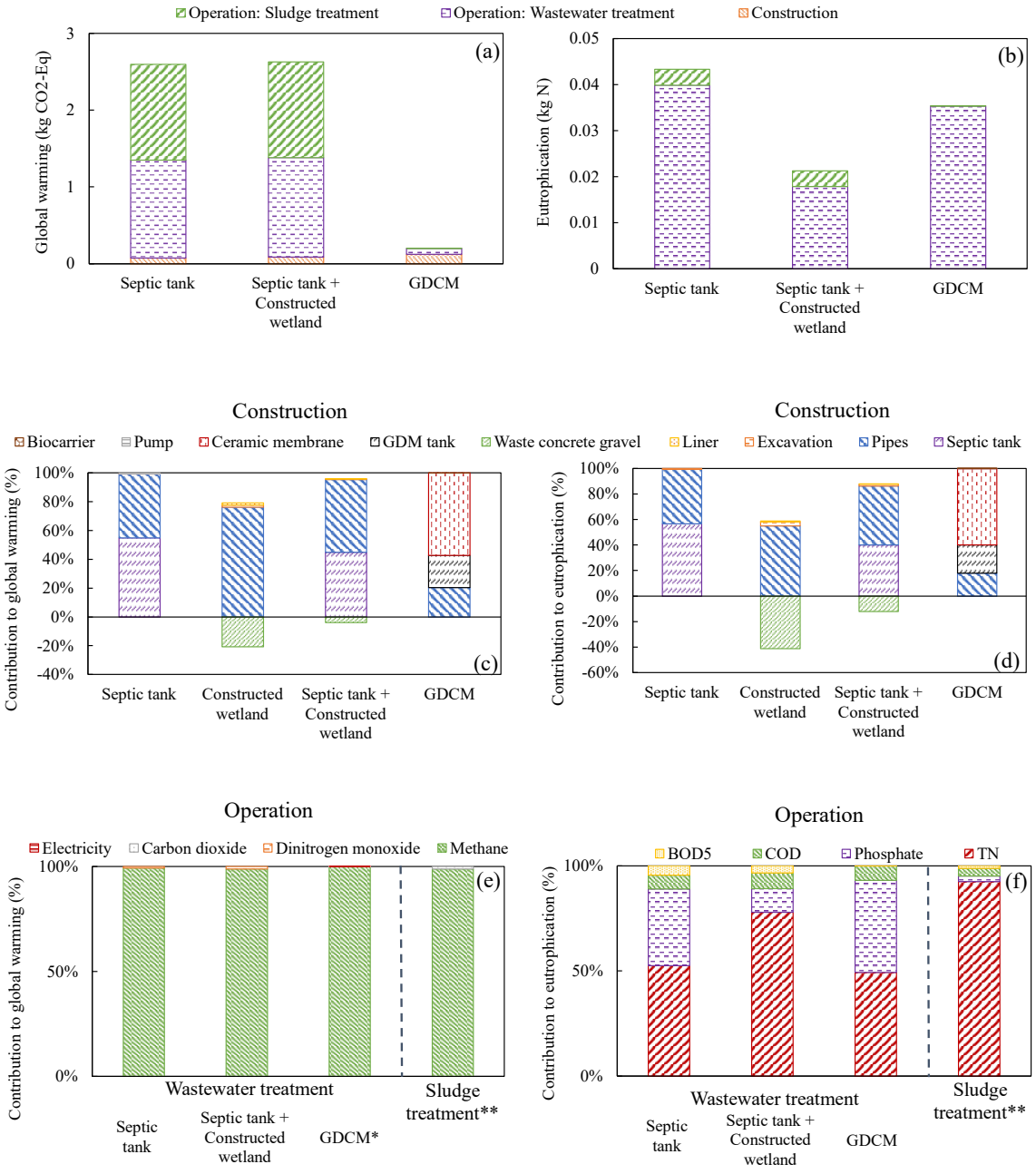

*Figure 5.2. Total impact in global warming (a) and eutrophication (b) categories. Contribution of each item to global warming (c & e) and eutrophication (d & f) during construction (c & d) and operation (e & f) phase. *GDCM methane emissions represent both methane and dinitrogen monoxide emissions; **Sludge treatment contribution was identical for all three scenarios.*

As shown in Figure 5.2a, the septic tank alone scenario resulted in 2.60 kg CO_2-Eq emissions in the global warming category, comparable to the septic tank + wetland scenario (2.63 kg CO_2-Eq), while the GDCM scenario resulted in ~90% lower emissions (0.2 kg CO_2-Eq) than these two scenarios. In detail, the construction phase for the septic tank alone and septic tank + wetland scenarios represented around 3% of the total impact in global warming category (Figure 5.2c). The low contribution of construction phase in this study was contrary to the finding in a previous study, where construction of non-intensive wastewater treatment technologies (high rate algal pond & constructed wetland) contributed majorly (~33%-50%)

(Garfí et al., 2017). This difference could be attributed to the simple setup configurations of septic tank and wetland systems, without any electrical parts such as pumps and exclusion of transportation. In addition, polyethylene tank production contributed greatly to the global warming potential of the construction phase (55% in the septic tank scenario and 57% in the septic tank + wetland scenario), similar to the contribution of pipe production (45% in the septic tank scenario and 43% in the septic tank + wetland scenario); while the remaining excavation and liner production contributed negligibly (<1%). During the construction of the wetland alone, the pipe production was largely dominant (131%), while the use of waste concrete as substrate led to a negative contribution ratio to global warming (-36%) (Figure 5.2c). It was reported that the negative contribution of recycled biocarriers could mainly be attributed to the lack of concrete disposal requirement (Cao et al., 2021). In the combined septic tank + wetland scenario, this negative contribution increased to -4%. This led to limited difference between the septic tank alone and septic tank + wetland scenarios (0.074 and 0.084 kg CO_2-eq respectively).

Meanwhile, the construction contributed 61% (0.12 kg CO_2-Eq) to the total global warming potential in the GDCM scenario (Figure 5.2c), 57% of which resulted from silicon carbide production for the inorganic membrane. It is noted that inorganic membranes were chosen for this scenario because of their high stability and longer lifetime, which is advantageous for decentralized application, especially at low temperatures (Arias et al., 2020; Hube et al., 2023; Niwa et al., 2016; Zhao et al., 2019b). This LCA was conducted with a conservative estimation of 20 years as a lifespan, however it is expected that in real application, the lifespan of inorganic membranes could be much longer (Asif & Zhang, 2021). Currently, commercially available inorganic membranes are fabricated from primary resources (such as silicon carbide, alumina, titania, zirconia), leading to higher capital cost and emission potential (Asif & Zhang, 2021). Recent studies have shown the feasibility of using low-cost materials (such as kaolin, pyrophyllite, dolomite, clays, zeolite and apatite) (Abdullayev et al., 2019; Asif & Zhang, 2021) or waste products (ash and cement) (Abdullayev et al., 2019; Samadi et al., 2022) for inorganic membrane production, which could benefit to significantly reduce their global warming emissions (Abdullayev et al., 2019; Dong et al., 2022; Samadi et al., 2022).

In the operation category (including both wastewater treatment and sludge treatment), the sludge treatment contributed significantly to the global warming impact (~50%) for the septic tank alone and the septic tank + wetland scenarios, while it was only 3.6% for the GDCM scenario. It is well known that the attached-growth biofilm processes produce less sludge than conventional activated sludge process, as microorganisms present a higher retention time and thus enhance degradation (El-Shafai & Zahid, 2013; Loupasaki & Diamadopoulos, 2013). Thus, lower sludge production in the biocarrier-facilitated GDCM system would lead to lower emissions derived from the sludge post-treatment. The global warming impact during sludge treatment could largely be attributed to methane emissions (> 99%) (Figure 5.2e), which was based on a sanitary landfill process, with well-functioning methane collection (Wernet, 2016). Note that in Iceland, only the landfill site at Álfsnes (in the capital area) has methane collection facilities, but the collection is only operated at 30% capacity (Scheutz et al., 2022). For practical reasons, the sludge from rural areas is not always transported to this landfill site, therefore the presented data was an underestimation of current methane emissions but could be closer to a future scenario with improved landfill facilities in the country. Realistically, the current emissions for the septic tank sludge post-treatment in an unsanitary landfill site (no methane collection) could reach 1.8 kg CO_2-eq

for the septic tank alone and 0.005 kg CO_2-eq for the GDCM system, as presented in Figure 5.3 (1.25 kg CO_2-eq and 0.003 kg CO_2-eq in a sanitary landfill respectively). However, these emissions could potentially be significantly reduced by implementing thermal or energetic methane reuse, which could contribute as negative emissions, balancing out the other emissions (Delre et al., 2019). Another improvement of sludge treatment could be its reuse in agriculture, where it could replace conventional fertilizer and therefore avoid emissions from fertilizer production (Polruang et al., 2018; World Health Organization, 2006). Previous studies indicated that the constructed wetlands had a higher global warming impact mostly due to pumping and aeration (Resende et al., 2019). In this study, the wetland system was designed as a completely gravity-driven process and without implementing additional aeration, which was favorable for decentralized application because of the system simplicity (Garcia et al., 2020; Hijosa-Valsero et al., 2010).

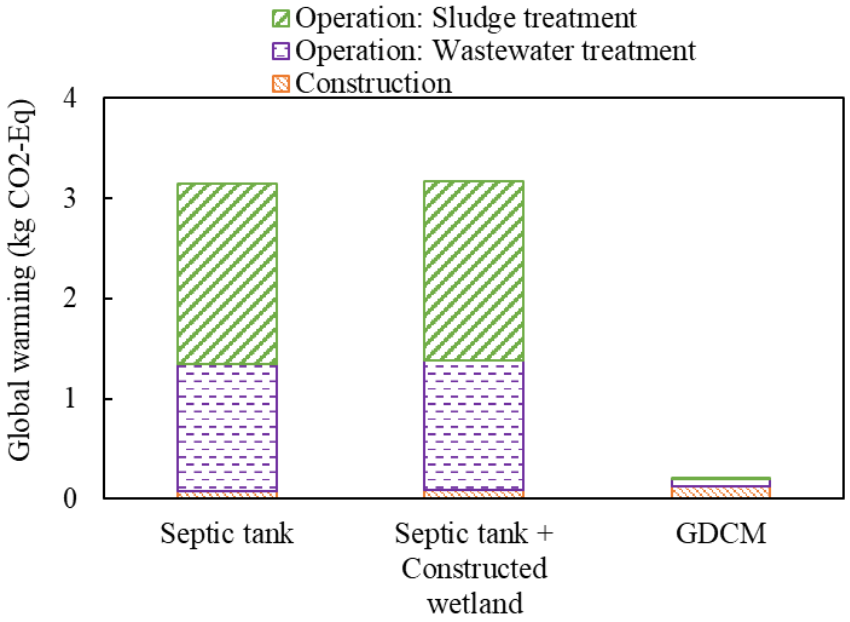

Figure 5.3. Global warming potential under different scenarios when the sludge is landfilled in an unsanitary landfill site.

In the operation category (wastewater treatment), the emissions in the GDCM system were significantly lower than those in the septic tank alone and septic tank + wetland systems. Such difference could largely be attributed to the dissimilar direct methane emissions (Figure 5.2a & e), which was in accordance with previous studies (Fuchs et al., 2011; Resende et al., 2019). The strongly anaerobic environment in septic tanks could lead to high methane emission, while the shallow wetlands and lower hydraulic retention time in the GDCM system ensured higher oxygen availability (i.e., limited methane emission). In addition, previous work revealed a lower contribution of direct greenhouse gas emissions (biogenic emissions from the wastewater operation) to the operational global warming impact, but a higher impact from electricity and transportation of feed flow in constructed wetlands for municipal wastewater treatment (Casas Ledón et al., 2017; Garfí et al., 2017). However, in the present study, the feed flow was completely gravity-driven in the septic tank and constructed wetlands, while GDCM only required pumping feed water to generate water head, which explains the high share of greenhouse gas emissions and the lack of electricity contribution. It shall be noted that the gaseous emission data for the different treatment scenarios were adopted from different references as explained in Table 5.1 (Eggleston et al., 2006; Liao et al., 2020; Søvik et al., 2006), which may add uncertainty to the results.

5.4.2 Eutrophication

In the eutrophication category, the septic tank alone scenario displayed the highest impact potential (0.043 kg N), followed by the GDCM (0.035 kg N) and septic tank + constructed wetland (0.021 kg N) scenarios (Figure 5.2b). The construction contributed less than 1% in all three scenarios. In septic tank alone, septic tank + constructed wetlands, and GDCM scenarios, wastewater treatment contributed to 92%, 94% and >99%, respectively; and sludge treatment contributed to 7.9%, 5.6% and <1%, respectively.

As shown in Figure 5.2d, the contribution ratio of each construction item showed a similar distribution pattern as that in the global warming category (Figure 5.2c). Similarly, using recycled concrete as substrate in the wetland led to a greater reduction for eutrophication potential, while the construction of septic tank contributed slightly less to eutrophication potential than that to the global warming potential.

During operation, the remaining TN in the treated water accounted for ≥50% of eutrophication potential in all three scenarios (Figure 5.2f), which was in accordance with the findings in the previous studies (Resende et al., 2019; Roux et al., 2010). In detail, the main differences between the septic tank alone and septic tank + constructed wetland scenarios were due to more effective nutrient removal in the wetland system (TN: 5% *vs.* 34%; phosphate: 5% *vs.* 86%). The eutrophication potential of the septic tank alone was slightly higher than that of the GDCM, which was mostly attributed to the higher emissions derived from sludge treatment in the septic tank alone scenario. The GDCM showed lower nutrient removals than septic tank + constructed wetland, because (1) the GDCM system had limited nitrification-denitrification for nitrogen removal and the MF/UF membrane did not reject ammonia/nitrate/phosphate; (2) the plants in the constructed wetlands would take up nutrients from the wastewater for maintaining their growth, leading to nutrient removal (Varma et al., 2021).

To further reduce eutrophication potential, nutrient mitigation in decentralized wastewater treatment systems should be improved by optimizing design and operation parameters. Moreover, in this study, the contribution ratio of sludge treatment to eutrophication potential (Figure 5.2f) was calculated based on a municipal waste landfill process with only 22% compostable material (Wernet, 2016) and the landfill construction (treating a combination of municipal wastes and sludge) was included in the operation category. This may be different from the impact of sludge treatment on eutrophication in real situations, as both liquid and gaseous emissions highly depend on landfill technology such as leachate treatment or heat recycling (Sauve & Van Acker, 2020).

Overall, the LCA results showed an advantage of implementing a constructed wetland system as a post-treatment process of the septic tank due to its significantly lower impacts in the eutrophication category, while the GDCM excelled in the global warming category. This indicated that the septic tank + wetland system is favorable for sensitive areas with eutrophication risk. In addition, the main impact item for the septic tanks in the global warming category was the sludge treatment, specifically without methane reuse at the landfill site. This could be improved by updating sludge and methane collection/reuse systems to limit its emissions, such as for agricultural reuse, electricity production, thermal reuse, conversion to biodiesel or methanol, etc. (Polruang et al., 2018; Sauve & Van Acker, 2020).

5.4.3 Cost Analysis

Septic Tank and Constructed Wetlands

Table 5.3 shows the individual item costs and total costs for septic tank alone and septic tank + wetland scenarios. The total costs for these two scenarios were almost comparable (~4% difference), which could be attributed to the extremely low capital and operation costs of the constructed wetlands. In detail, the main component was the sludge treatment in the septic tank at ~0.1 EUR/m^3, which was based on the price charged by municipalities for houseowners (Hrunamannahreppur, 2023). As sludge treatment cost was independent of wastewater flowrate, such cost would decrease with increasing wastewater treatment capacity. In addition, the material cost of the septic tank or constructed wetland was relatively low, because their operation heavily relies on natural degradation instead of active mechanical operation (i.e., simple installation). Overall, a great potential to minimize the cost of septic tank + wetland for wastewater treatment lies in reducing the sludge treatment cost, similar to the findings in LCA study relating to environmental impacts (chapter 5.4.1).

Table 5.3. Comparison of costs for septic tank and septic tank + wetland scenarios

Septic Tank		Septic tank + Constructed wetland	
Septic tank	**Cost (EUR/m^3)**	**Septic tank**	**Cost (EUR/m^3)**
Polyethylene	0.0231	Polyethylene	0.0231
Piping	0.0117	Piping	0.0117
Sludge treatment	0.1032	Sludge treatment	0.1032
		Constructed wetland	
		Biocarriers	0
		Liner Polyethylene	0.0002
		Piping	0.0047
Total	**0.1380**	**Total**	**0.1429**

Ceramic Membrane-based GDM

The economic analysis was performed for the experiments presented in Chapter 3 for both constant flux and GDM operation with different cleaning approaches (no cleaning *vs.* backwash *vs.* ultrasonication) and inorganic membrane materials (commercial ceramic membrane *vs.* recycled materials-based inorganic membrane).

When the commercial ceramic membrane was considered (Figure 5.4a), the GDM system displayed lower water production cost than the constant flux filtration system at a lower treatment capacity (< ~5 m^3/day), due to the higher capital cost of the control system required in the constant flux filtration operation. While the GDM system had a higher water production cost with a water treatment capacity at > ~5 m^3/day. In the GDM systems, employing periodic ultrasonication cleaning led to lower production cost than those with geothermal water backwash or without any cleaning at a lower treatment capacity. With increasing treatment capacity, the water production cost in the GDM systems was almost independent of treatment capacity; the cost is comparable for both with periodic geothermal water backwash and ultrasonication, which is lower than that without any cleaning. While, in the constant flux filtration system, the water production cost dramatically decreases with

increasing treatment capacity and tends to be constant when the treatment capacity is >100 m^3/day. Clearly, employing periodic ultrasonication in the constant flux filtration system requires less cost than employing chemical-enhanced backwash (~0.5 *vs.* ~0.64 EUR/m^3 water). Overall, ultrasonication-facilitated GDM systems may be economic feasible in treating wastewater at a household scale, while ultrasonication-facilitated constant flux filtration systems may be favorable at a small-community scale.

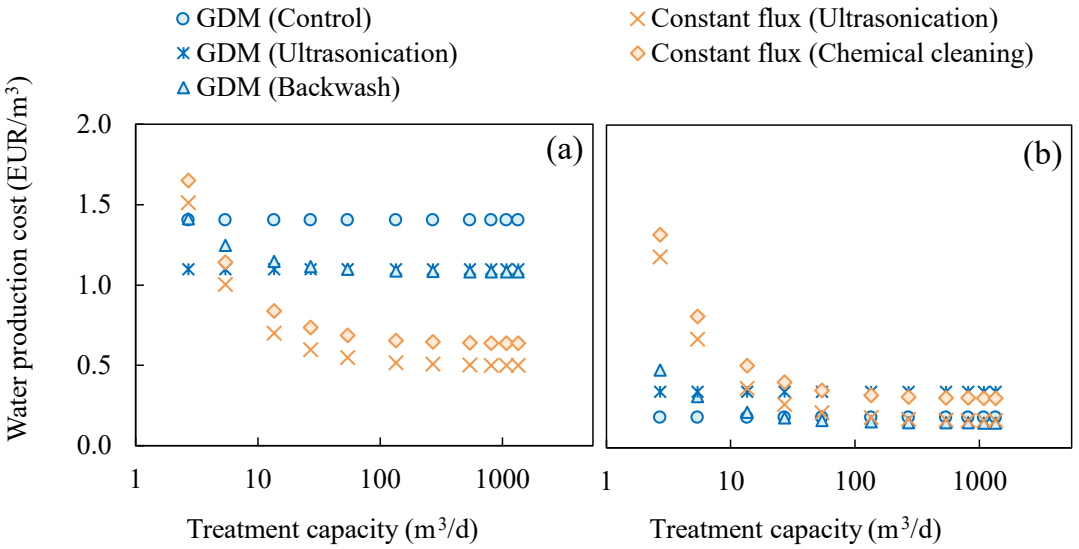

Figure 5.4. Economic analysis for GDM and constant flux filtration systems under different cleaning protocols. (a) Commercial ceramic membrane; (b) Recycled materials-based inorganic membrane. The cleaning duration was proposed as follows: GDM backwash: 30-min per week; GDM ultrasonication: 120 sec per 2-h filtration; constant flux backwash: 15-min (0.5% NaClO solution) per day; constant flux ultrasonication: 15-min per day.

Furthermore, at a household scale (Figure 5.5a and b), the major cost of GDM systems is the membrane cost (69.8-99.4%); while in the constant flux operation system, the control system contributes greatly (68.3-73.4%), followed by the membrane cost (18.9-20.3%). This could be attributed to the lower water production in the GDM systems, which requires a large membrane area (Pronk et al., 2019). With geothermal water backwash or ultrasonication, the membrane cost is reduced compared to that without cleaning due to flux recovery after cleaning (leading to more water production). At a community scale (Figure 5.5b and d), the membrane cost in the GDM system is comparable to that at a household scale (78.6-99.4%), while in constant flux operation, the membrane cost contributes majorly (59.4-75.7%). The effect of treatment capability on the major cost contributor in the constant flux filtration system is related to the control system cost, which is largely independent of the treatment capacity.

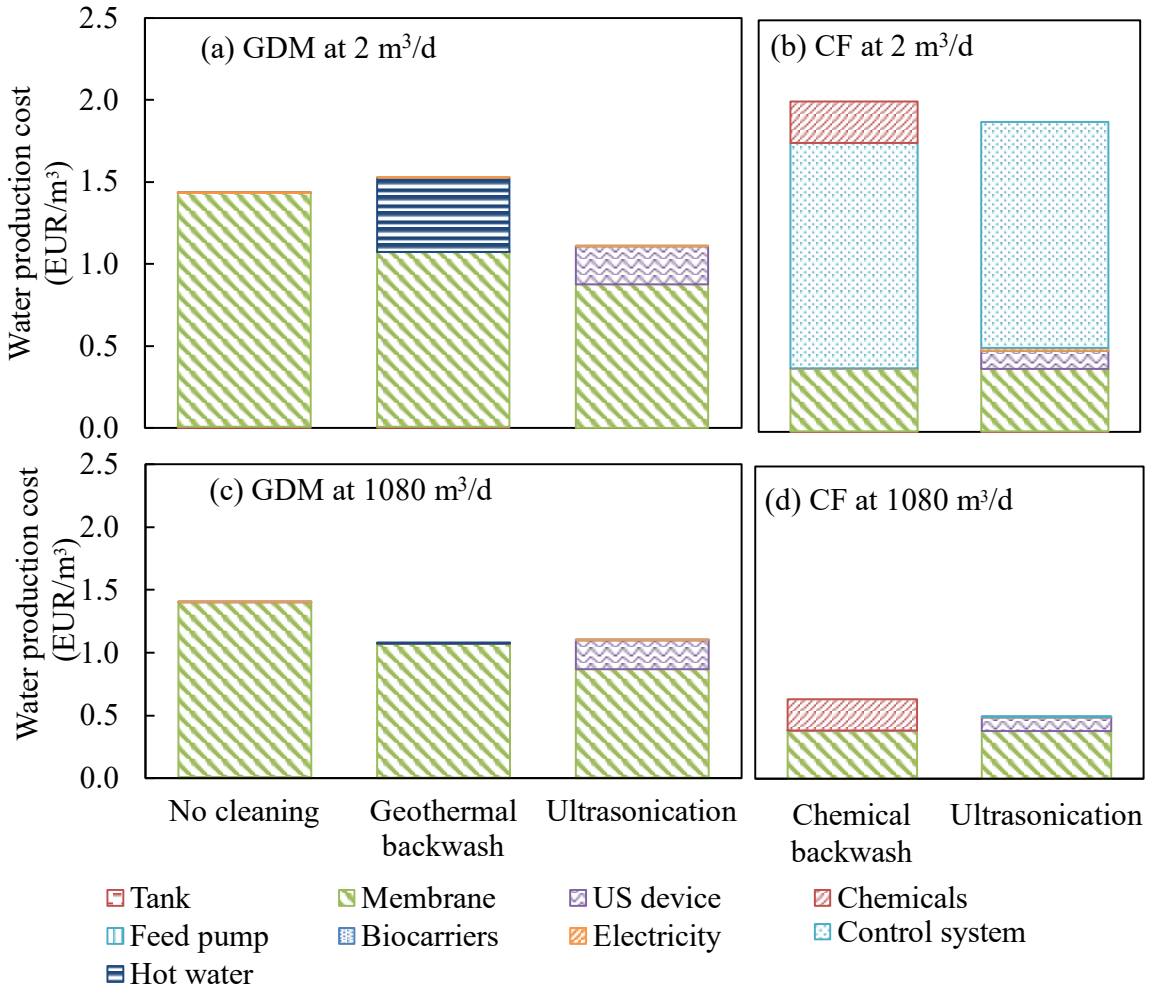

Figure 5.5. (a) and (c) Cost items in the GDM systems; (b) and (d) Cost items in the constant flux filtration systems with commercial ceramic membranes at different scales. "CF" refer to constant flux filtration.

Notably, the water production cost with commercial ceramic membranes (1.1-1.4 EUR/m^3 water) is greatly higher than that with polymeric membranes (0.31-0.37 EUR/m^3 water) in GDM systems (Shami & Wu, 2021). In this study, the lifespan of ceramic membranes is estimated at 20 years, which is adopted from the lifespan range for organic membranes (Asif & Zhang, 2021; Zhao et al., 2019a). Generally, ceramic membranes are expected to have longer lifespan than organic membranes, which would further reduce yearly membrane cost (Asif & Zhang, 2021). On the other hand, several research studies have reported that the ceramic membranes fabricated from waste materials are expected to have similar membrane cost (2-130 EUR/m^2) as that of organic membranes (Abdullayev et al., 2019; Dong et al., 2022; Samadi et al., 2022). Thus, cost estimation with recycled membranes (costs were estimated as 65 EUR/m^2) was performed and presented in Figure 5.4b. Interestingly, at a lower treatment capacity, the GDM system without any cleaning requires the lowest cost (0.19 EUR/m^3 water), showing its great potential for household application. At a higher treatment capacity (at a community level), the water production cost for the GDM system without cleaning or with backwash, and the constant flux filtration with ultrasonication was comparable. As decentralized wastewater treatment favors simple operation and maintenance (Arias et al., 2020; Hube & Wu, 2021), the GDM system without any cleaning could be the feasible option under both household and community scenarios when recycle

materials-based inorganic membranes are available in the market or low-cost ceramic membranes are successfully fabricated with advanced techniques in the near future (Dong et al., 2022; Hubadillah et al., 2022).

Finally, when comparing the same operation conditions as presented in the LCA above, sludge treatment costs were added to the GCDM scenarios (~0.023 EUR/m^3; assuming sludge disposal per 10 years) and presented in Figure 5.6. This resulted in cost of ~1.423 EUR/m^3 (commercial membrane) and ~0.213 EUR/m^3 (recycled membrane), the latter of which was in a similar range as that of the septic tank + constructed wetland scenario.

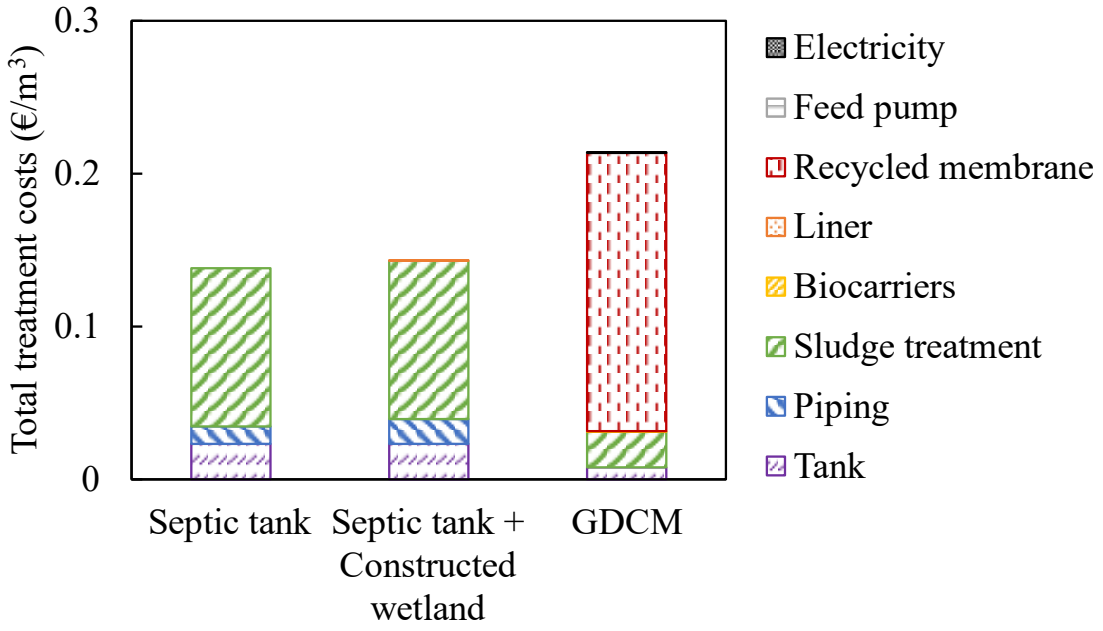

Figure 5.6 Total costs of wastewater treatment scenarios

Overall, the experimental and LCA results suggested that constructed wetlands for decentralized wastewater treatment in cold climate are technically feasible and environmentally sustainable. However, main drawbacks of constructed wetlands are their high area requirements (~10 times higher than that of a conventional activated sludge process) (Garfí et al., 2017) and potential freezing and clogging challenges in cold temperature (Varma et al., 2021). On the other hand, the GDCM system is highly compact, especially implementing with hollow fibre membrane modules, or packing biocarriers in the membrane tank (Lee et al., 2021; Pronk et al., 2019). Towards achieving low environmental impact and high treatment efficiency (especially in cold climate), a combination of GDCM system with constructed wetland is proposed, i.e., the GDCM system contributes for solids and organic removals, followed by a constructed wetland system in which the plants/natural microbial community performs roles in nutrient uptake, which will be investigated in the future.

5.5 Conclusions

This chapter assessed the environmental and economic performance of different cold climate decentralized wastewater treatment scenarios. The main findings were:

(1) Integrating septic tank + constructed wetland for decentralized wastewater treatment benefitted to alleviate eutrophication potential (~50%) with a limited trade-off in global warming potential (~2% increase) compared to the septic tank alone. Meanwhile, compared to the combined septic tank + constructed wetland, the GDCM system had ~92% less global warming potential and ~66% higher impact in the eutrophication category.

(2) Economic analysis revealed that the additional costs of implementing constructed wetland treatment were negligible. The total cost of the septic tank + constructed wetland was slightly lower than that of the GDCM system with inorganic membranes made from recycled materials.

6 Conclusions and Outlook

Conventional wastewater treatment technologies face challenges in decentralized application and cold climate conditions. With regards to increasingly stricter discharge standards, there is a need to develop low-cost decentralized wastewater treatment techniques with stable performance and simple maintenance. This work investigated the technical feasibility of applying GDM systems for decentralized wastewater treatment in cold climate, by investigating the GDM performances under different temperatures, various cleaning approaches, and the presence of microplastics. In addition, comparative LCA and cost analysis were performed by comparing GDM systems with conventional decentralized wastewater treatment techniques in terms of an environmental and economic perspective. It was found that:

(1) The GDM system with organic membrane followed cake filtration and pore constriction fouling model, regardless of operation temperature. However, the cake layer mass was higher at 22°C, presenting greater-sized foulants and a lower porosity than that at 8°C. In the presence of periodic cleaning, the operation temperature did not impact flux recovery, water productivity, and foulant deposition mass, but significantly higher cake resistances were observed at 22°C than those at 8°C. Possibly, the shear force could remove the loosely attached cake layers and subsequently cause more compression of the residual dense-nature cake layers at 22°C. The lower operation temperature only negatively influenced BOD_5 removal in the biocarrier reactor, while both GDM systems produced superior permeate quality that could meet EU discharge standards, regardless of temperature.

(2) When inorganic membrane was used in the GDM system, the dominant fouling mechanisms shifted from initial intermediate pore blocking to cake filtration after flux stabilization. The cleaning efficiency of periodic geothermal backwash in GDM system was limited, while periodic ultrasonication demonstrated effective cake fouling reduction, independent with cleaning cycle.

(3) In the GDM systems, the accumulation of microplastics on the membrane surface led to lower flux stabilization and their rapid accumulation on the membrane resulted in higher cake filtration constant than that without microplastics. The presence of large-sized microplastics in the feed water resulted in a porous cake layer formed on the membrane, while small-sized microplastics at a low concentration tended to form a dense cake layer due to bridging effect of greater concentration of divalent ions in the cake layer. The presence of microplastics led to a significant accumulation of metal elements in the cake layers.

(4) LCA revealed the environmental benefit of GDCM, as it presented a ~92% lower impact in global warming potential compared to other conventional treatment methods. However, the limited nutrient removal led to increased eutrophication impact (~66%) compared to septic tank + constructed wetland treatment. The GDCM costs with commercial ceramic membranes are significantly higher than the septic tank + constructed wetland system, however, when the recycled materials-based membranes were considered, the cost could dramatically decrease to the similar level as the septic tank + constructed wetland system.

The findings of this study showed the potential of applying GDM systems for decentralized wastewater treatment under cold climate. However, more research must be conducted on pilot- and full scale to ensure long-term stable performance in real-life conditions. Moreover, emerging pollutants are commonly found in domestic wastewaters, which requires special attention on their fates in wastewater treatment facilities. For example, the removal of accumulated microplastics from GDM systems during periodical cleaning should be investigated. Pathogens and micropollutants, such as pharmaceuticals, are found in increasing concentrations and their removals in GDM systems shall be investigated in detail to ensure safe discharge of the treated water. Finally, despite the advantages of GDCM systems, it currently cannot compete economically with the conventional decentralized wastewater treatment options. Research showed the feasibility of recycled ceramic membranes, while their real applications still need to be further investigated to reduce the capital costs of decentralized GDCM systems.

References

Abbasi, N., Ahmadi, M., Naseri, M. 2021. Quality and cost analysis of a wastewater treatment plant using GPS-X and CapdetWorks simulation programs. *Journal of Environmental Management*, **284**, 111993.

Abdullayev, A., Bekheet, M.F., Hanaor, D.A.H., Gurlo, A. 2019. Materials and Applications for Low-Cost Ceramic Membranes. *Membranes*, **9**(9).

Aghapour Aktij, S., Taghipour, A., Rahimpour, A., Mollahosseini, A., Tiraferri, A. 2020. A critical review on ultrasonic-assisted fouling control and cleaning of fouled membranes. *Ultrasonics*, **108**, 106228.

Akhondi, E., Wu, B., Sun, S., Marxer, B., Lim, W., Gu, J., Liu, L., Burkhardt, M., McDougald, D., Pronk, W., Fane, A.G. 2015. Gravity-driven membrane filtration as pretreatment for seawater reverse osmosis: linking biofouling layer morphology with flux stabilization. *Water Research*, **70**, 158-73.

Aoustin, E., Schäfer, A.I., Fane, A.G., Waite, T.D. 2001. Ultrafiltration of natural organic matter. *Separation and Purification Technology*, **22-23**, 63-78.

APHA. 1998. *Standard Methods for the examination of water and wastewater, 20th ed.*, Washington DC.

Arias, A., Feijoo, G., Moreira, M.T. 2020. Environmental profile of decentralized wastewater treatment strategies based on membrane technologies. in: *Current Developments in Biotechnology and Bioengineering*, pp. 259-287.

Arnórsson, S., Oskarsson, N. 2007. Molybdenum and tungsten in volcanic rocks and in surface and <100°C ground waters in Iceland. *Geochimica et Cosmochimica Acta*, **71**, 284-304.

Asif, M.B., Zhang, Z. 2021. Ceramic membrane technology for water and wastewater treatment: A critical review of performance, full-scale applications, membrane fouling and prospects. *Chemical Engineering Journal*, **418**, 129481.

Ayache, C., Pidou, M., Croue, J.P., Labanowski, J., Poussade, Y., Tazi-Pain, A., Keller, J., Gernjak, W. 2013. Impact of effluent organic matter on low-pressure membrane fouling in tertiary treatment. *Water Research*, **47**(8), 2633-42.

Bai, X., McKnight, M.M., Neufeld, J.D., J. Parker, W. 2023. Simultaneous nitrification, denitrification, and phosphorus removal from municipal wastewater at low temperature. *Bioresource Technology*, **368**, 128261.

Bakaraki Turan, N., Sari Erkan, H., Onkal Engin, G. 2021. Microplastics in wastewater treatment plants: Occurrence, fate and identification. *Process Safety and Environmental Protection*, **146**, 77-84.

Bare, J.C. 2002. Traci. *Journal of Industrial Ecology*, **6**(3-4), 49-78.

Bayo, J., Lopez-Castellanos, J., Olmos, S. 2020a. Membrane bioreactor and rapid sand filtration for the removal of microplastics in an urban wastewater treatment plant. *Marine Pollution Bulletin*, **156**, 111211.

Bayo, J., Olmos, S., Lopez-Castellanos, J. 2020b. Microplastics in an urban wastewater treatment plant: The influence of physicochemical parameters and environmental factors. *Chemosphere*, **238**, 124593.

Bazan, M.A., Carpintero-Tepole, V., Brito-de la Fuente, E., Drioli, E., Ascanio, G. 2020. On the use of ultrasonic dental scaler tips as cleaning technique of microfiltration ceramic membranes. *Ultrasonics*, **101**, 106035.

Broeckmann, A., Busch, J., Wintgens, T., Marquardt, W. 2006. Modeling of pore blocking and cake layer formation in membrane filtration for wastewater treatment. *Desalination*, **189**(1-3), 97-109.

Bui, X.-T., Vo, T.-D.-H., Nguyen, P.-T., Nguyen, V.-T., Dao, T.-S., Nguyen, P.-D. 2020a. Microplastics pollution in wastewater: Characteristics, occurrence and removal technologies. *Environmental Technology & Innovation*, **19**, 101013.

Bydalek, F., Ifayemi, D., Reynolds, L., Barden, R., Kasprzyk-Hordern, B., Wenk, J. 2023a. Microplastic dynamics in a free water surface constructed wetland. *Science of The Total Environment*, **858**, 160113.

Bydalek, F., Webster, G., Barden, R., Weightman, A.J., Kasprzyk-Hordern, B., Wenk, J. 2023b. Microplastic biofilm, associated pathogen and antimicrobial resistance dynamics through a wastewater treatment process incorporating a constructed wetland. *Water Research*, **235**, 119936.

Cao, Z., Zhou, L., Gao, Z., Huang, Z., Jiao, X., Zhang, Z., Ma, K., Di, Z., Bai, Y. 2021. Comprehensive benefits assessment of using recycled concrete aggregates as the substrate in constructed wetland polishing effluent from wastewater treatment plant. *Journal of Cleaner Production*, **288**, 125551.

Casas Ledón, Y., Rivas, A., López, D., Vidal, G. 2017. Life-cycle greenhouse gas emissions assessment and extended exergy accounting of a horizontal-flow constructed wetland for municipal wastewater treatment: A case study in Chile. *Ecological Indicators*, **74**, 130-139.

Cembrane. Technical Brochure – SiCBloxTM FX Cembrane a/s, Vol. Version 1.9.

Chawla, C., Zwijnenburg, A., Kemperman, A.J.B., Nijmeijer, K. 2017. Fouling in gravity driven Point-of-Use drinking water treatment systems. *Chemical Engineering Journal*, **319**, 89-97.

Chen, M., Nan, J., Xu, Y., Yao, J., Wang, H., Zu, X. 2022. Effect of microplastics on the physical structure of cake layer for pre-coagulated gravity-driven membrane filtration. *Separation and Purification Technology*, **288**.

Corbella, C., Puigagut, J., Garfi, M. 2017. Life cycle assessment of constructed wetland systems for wastewater treatment coupled with microbial fuel cells. *Science of The Total Environment*, **584-585**, 355-362.

Corominas, L., Byrne, D.M., Guest, J.S., Hospido, A., Roux, P., Shaw, A., Short, M.D. 2020. The application of life cycle assessment (LCA) to wastewater treatment: A best practice guide and critical review. *Water Research*, **184**.

Cui, L., Goodwin, C., Gao, W., Liao, B. 2017. Effect of cold water temperature on membrane structure and properties. *Journal of Membrane Science*, **540**, 19-26.

Daskiran, F., Gulhan, H., Guven, H., Ozgun, H., Ersahin, M.E. 2022. Comparative evaluation of different operation scenarios for a full-scale wastewater treatment plant: Modeling coupled with life cycle assessment. *Journal of Cleaner Production*, **341**.

De Silva, Y.S.K., Rajagopalan, U.M., Kadono, H. 2021. Microplastics on the growth of plants and seed germination in aquatic and terrestrial ecosystems. *Global Journal of Environmental Science and Management*, **7**(3), 347-368.

Delre, A., ten Hoeve, M., Scheutz, C. 2019. Site-specific carbon footprints of Scandinavian wastewater treatment plants, using the life cycle assessment approach. *Journal of Cleaner Production*, **211**, 1001-1014.

Derlon, N., Desmond, P., Rühs, P.A., Morgenroth, E. 2022. Cross flow frequency determines the physical structure and cohesion of membrane biofilms developed during gravity-

driven membrane ultrafiltration of river water: Implication for hydraulic resistance. *Journal of Membrane Science*, **643**, 120079.

Derlon, N., Peter-Varbanets, M., Scheidegger, A., Pronk, W., Morgenroth, E. 2012. Predation influences the structure of biofilm developed on ultrafiltration membranes. *Water Research*, **46**(10), 3323-33.

Dey, T.K., Jamal, M., Uddin, M.E. 2023. Fabrication and performance analysis of graphene oxide-based composite membrane to separate microplastics from synthetic wastewater. *Journal of Water Process Engineering*, **52**.

Dhineka, K., Sambandam, M., Sivadas, S.K., Kaviarasan, T., Pradhan, U., Begum, M., Mishra, P., Murthy, M.V.R. 2021. Characterization and seasonal distribution of microplastics in the nearshore sediments of the south-east coast of India, Bay of Bengal. *Frontiers of Environmental Science & Engineering*, **16**(1).

Di Trapani, D., Christensson, M., Torregrossa, M., Viviani, G., Ødegaard, H. 2013. Performance of a hybrid activated sludge/biofilm process for wastewater treatment in a cold climate region: Influence of operating conditions. *Biochemical Engineering Journal*, **77**, 214-219.

Ding, A., Liang, H., Li, G., Derlon, N., Szivak, I., Morgenroth, E., Pronk, W. 2016. Impact of aeration shear stress on permeate flux and fouling layer properties in a low pressure membrane bioreactor for the treatment of grey water. *Journal of Membrane Science*, **510**, 382-390.

Ding, A., Wang, J., Lin, D., Cheng, X., Wang, H., Bai, L., Ren, N., Li, G., Liang, H. 2018a. Effect of PAC particle layer on the performance of gravity-driven membrane filtration (GDM) system during rainwater treatment. *Environmental Science: Water Research and Technology*, **4**(1), 48-57.

Ding, A., Wang, J., Lin, D., Tang, X., Cheng, X., Li, G., Ren, N., Liang, H. 2017. In situ coagulation versus pre-coagulation for gravity-driven membrane bioreactor during decentralized sewage treatment: Permeability stabilization, fouling layer formation and biological activity. *Water Research*, **126**, 197-207.

Ding, A., Wang, J., Lin, D., Zeng, R., Yu, S., Gan, Z., Ren, N., Li, G., Liang, H. 2018b. Effects of GAC layer on the performance of gravity-driven membrane filtration (GDM) system for rainwater recycling. *Chemosphere*, **191**, 253-261.

Dong, Y., Wu, H., Yang, F., Gray, S. 2022. Cost and efficiency perspectives of ceramic membranes for water treatment. *Water Research*, **220**, 118629.

Du, P., Li, X., Yang, Y., Zhou, Z., Fan, X., Chang, H., Liang, H. 2022. Regulated-biofilms enhance the permeate flux and quality of gravity-driven membrane (GDM) by in situ coagulation combined with activated alumina filtration. *Water Research*, **209**, 117947.

Eggleston, H.S., Buendia, L., Miwa, K., Ngara, T., Tanabe, K. 2006. IPCC Guidelines for National Greenhouse Gas Inventories. *IPCC National Greenhouse Gas Inventories Programme, Intergovernmental Panel on Climate Change IPCC, c/o Institute for Global Environmental Strategies IGES, 2108 - 11, Kamiyamaguchi, Hayama, Kanagawa (Japan)*.

El-Shafai, S.A., Zahid, W.M. 2013. Performance of aerated submerged biofilm reactor packed with local scoria for carbon and nitrogen removal from municipal wastewater. *Bioresource Technology*, **143**, 476-482.

Enfrin, M., Dumée, L.F., Lee, J. 2019. Nano/microplastics in water and wastewater treatment processes – Origin, impact and potential solutions. *Water Research*, **161**, 621-638.

EPA. 2002. Onsite Wastewater Treatment Systems Manual, (Eds.) O.o. Water, O.o.R.a. Development, U.S.E.P. Agency, Vol. 625/R-00/008.

European Union. 1991. Council directive of 21 May 1991 concerning urban waste water treatment. *Official Journal of the European Communities*, **91/271/EEC**(L 135), 40-51.

Fang, Y.-K., Wang, H.-C., Fang, P.-H., Liang, B., Zheng, K., Sun, Q., Li, X.-Q., Zeng, R., Wang, A.-J. 2023. Life cycle assessment of integrated bioelectrochemical-constructed wetland system: environmental sustainability and economic feasibility evaluation. *Resources, Conservation and Recycling*, **189**.

Feng, J., Li, X., Li, H., Yang, Y. 2022a. Enhanced filtration performance of biocarriers facilitated gravity-driven membrane (GDM) by vacuum ultraviolet (VUV) pretreatment: Membrane biofouling characteristics and bacterial investigation. *Journal of Membrane Science*, **660**.

Feng, J., Li, X., Yang, Y., Fan, X., Zhou, Z., Ren, J., Tan, X., Li, H. 2022b. Insight into biofouling mechanism in biofiltration-facilitated gravity-driven membrane (GDM) system: Beneficial effects of pre-deposited adsorbents. *Journal of Membrane Science*, **662**, 121017.

Fernandes, H., Kiuchi, S., Kakuda, T., Hafuka, A., Tsuchiya, T., Matsui, Y., Kimura, K. 2023. Fouling mitigation in membrane bioreactors by nanobubble-assisted backwashing. *Journal of Water Process Engineering*, **53**, 103860.

Fletcher, H., Mackley, T., Judd, S. 2007. The cost of a package plant membrane bioreactor. *Water Research*, **41**(12), 2627-2635.

Flores, L., García, J., Pena, R., Garfí, M. 2019. Constructed wetlands for winery wastewater treatment: A comparative Life Cycle Assessment. *Science of The Total Environment*, **659**, 1567-1576.

Fortunato, L., Ranieri, L., Naddeo, V., Leiknes, T. 2020. Fouling control in a gravity-driven membrane (GDM) bioreactor treating primary wastewater by using relaxation and/or air scouring. *Journal of Membrane Science*, **610**, 118261.

Fu, S.F., Ding, J.N., Zhang, Y., Li, Y.F., Zhu, R., Yuan, X.Z., Zou, H. 2018. Exposure to polystyrene nanoplastic leads to inhibition of anaerobic digestion system. *Science of The Total Environment*, **625**, 64-70.

Fuchs, V.J., Mihelcic, J.R., Gierke, J.S. 2011. Life cycle assessment of vertical and horizontal flow constructed wetlands for wastewater treatment considering nitrogen and carbon greenhouse gas emissions. *Water Research*, **45**(5), 2073-81.

Gallego-Schmid, A., Tarpani, R.R.Z. 2019. Life cycle assessment of wastewater treatment in developing countries: A review. *Water Research*, **153**, 63-79.

Galvín, A.P., Sabrina, S., Auxi, B., Peña, A., López-Uceda, A. 2023. Leaching performance of concrete eco-blocks: Towards zero-waste in precast concrete plants. *Journal of Environmental Management*, **344**, 118409.

Garcia, J., Garcia-Galan, M.J., Day, J.W., Boopathy, R., White, J.R., Wallace, S., Hunter, R.G. 2020. A review of emerging organic contaminants (EOCs), antibiotic resistant bacteria (ARB), and antibiotic resistance genes (ARGs) in the environment: Increasing removal with wetlands and reducing environmental impacts. *Bioresource Technology*, **307**, 123228.

García, J.A., Paredes, D., Cubillos, J.A. 2013. Effect of plants and the combination of wetland treatment type systems on pathogen removal in tropical climate conditions. *Ecological Engineering*, **58**, 57-62.

Garfí, M., Flores, L., Ferrer, I. 2017. Life Cycle Assessment of wastewater treatment systems for small communities: Activated sludge, constructed wetlands and high rate algal ponds. *Journal of Cleaner Production*, **161**, 211-219.

Ghaffour, N., Qamar, A. 2020. Membrane fouling quantification by specific cake resistance and flux enhancement using helical cleaners. *Separation and Purification Technology*, **239**, 116587.

Guðjónsdóttir, S., Ge, L., Zhao, K., Lisak, G., Wu, B. 2022. Gravity-driven membrane filtration of primary wastewater effluent for edible plant cultivations: Membrane performance and health risk assessment. *Journal of Environmental Chemical Engineering*, **10**(1), 107046.

Gunnarsdottir, M.J., Gardarsson, S.M., Jonsson, G.S., Armannsson, H., Bartram, J. 2014. Natural background levels for chemicals in Icelandic aquifers. *Hydrology Research*, **46**(4), 647-660.

Guo, X., Jiang, S., Wang, Y., Wang, Y., Wang, J., Huang, T., Liang, H., Tang, X. 2022a. Effects of pre-treatments on the filtration performance of ultra-low pressure gravity-driven membrane in treating the secondary effluent: Flux stabilization and removal improvement. *Separation and Purification Technology*, **303**, 122122.

Guo, X., Wang, Y., Jiang, S., Wang, Y., Wang, J., Liang, H., Tang, X. 2022b. Influence of operation modes on gravity-driven membrane process in treating the secondary effluent: Flux improvement and biocake layer property. *Chemosphere*, **310**, 136692.

Hashemi, S., Boudaghpour, S. 2020. Economic analysis and probability of benefit of implementing onsite septic tank and resource-oriented sanitation systems in Seoul, South Korea. *Environmental Technology & Innovation*, **18**, 100762.

Hauschild, M.Z. 2015. *Life Cycle Impact Assessment*. Springer Netherlands, Dordrecht.

Hermia, J. 1982. Constant Pressure Blocking Filtration Laws - Application to Power-Law Non-Newtonian Fluids. *Transactions of the Institution of Chemical Engineers*, **60**(3), 183-187.

Hernández-Chover, V., Bellver-Domingo, Á., Hernández-Sancho, F. 2021. The influence of oversizing on maintenance cost in wastewater treatment plants. *Process Safety and Environmental Protection*, **147**, 734-741.

Hijosa-Valsero, M., Matamoros, V., Martin-Villacorta, J., Becares, E., Bayona, J.M. 2010. Assessment of full-scale natural systems for the removal of PPCPs from wastewater in small communities. *Water Research*, **44**(5), 1429-39.

Ho, C.C., Zydney, A.L. 2000. A combined pore blockage and cake filtration model for protein fouling during microfiltration. *Journal of Colloid and Interface Science*, **232**(2), 389-399.

Ho, C.C., Zydney, A.L. 2002. Transmembrane pressure profiles during constant flux microfiltration of bovine serum albumin. *Journal of Membrane Science*, **209**, 363-377.

Hou, L., Kumar, D., Yoo, C.G., Gitsov, I., Majumder, E.L.W. 2021. Conversion and removal strategies for microplastics in wastewater treatment plants and landfills. *Chemical Engineering Journal*, **406**, 126715.

How, S.W., Sin, J.H., Wong, S.Y.Y., Lim, P.B., Aris, A.M., Ngoh, G.C., Shoji, T., Curtis, T.P., Chua, A.S.M. 2020. Characterization of slowly-biodegradable organic compounds and hydrolysis kinetics in tropical wastewater for biological nitrogen removal. *Water Science and Technology*, **81**(1), 71-80.

Hrunamannahreppur. 2023.

Huang, Y., Cheng, P., Tan, F.J., Huang, Y., Li, P., Xia, S. 2021. Effect of coagulation pretreatment on the performance of gravity-driven membrane filtration with Yangtze River water. *Journal of Cleaner Production*, **297**, 126736.
Huang, Y., Wu, L., Li, P., Li, N., He, Y. 2022. What's the cost-effective pattern for rural wastewater treatment? *Journal of Environmental Management*, **303**, 114226.
Hubadillah, S.K., Jamalludin, M.R., Dzarfan Othman, M.H., Iwamoto, Y. 2022. Recent progress on low-cost ceramic membrane for water and wastewater treatment. *Ceramics International*, **48**(17), 24157-24191.
Hube, S., Eskafi, M., Hrafnkelsdottir, K.F., Bjarnadottir, B., Bjarnadottir, M.A., Axelsdottir, S., Wu, B. 2020. Direct membrane filtration for wastewater treatment and resource recovery: A review. *Science of the Total Environment*, **710**, 136375.
Hube, S., Hauser, F., Burkhardt, M., Brynjólfsson, S., Wu, B. 2023. Ultrasonication-assisted fouling control during ceramic membrane filtration of primary wastewater under gravity-driven and constant flux conditions. *Separation and Purification Technology*, **310**, 123083.
Hube, S., Lee, S., Chong, T.H., Brynjolfsson, S., Wu, B. 2022. Biocarriers facilitated gravity-driven membrane filtration of domestic wastewater in cold climate: Combined effect of temperature and periodic cleaning. *Science of The Total Environment*, **833**, 155248.
Hube, S., Wang, J., Sim, L.N., Chong, T.H., Wu, B. 2021a. Direct membrane filtration of municipal wastewater: Linking periodical physical cleaning with fouling mechanisms. *Separation and Purification Technology*, **259**, 118125.
Hube, S., Wang, J., Sim, L.N., Ólafsdóttir, D., Chong, T.H., Wu, B. 2021b. Fouling and mitigation mechanisms during direct microfiltration and ultrafiltration of primary wastewater. *Journal of Water Process Engineering*, **44**, 102331.
Hube, S., Wu, B. 2021. Mitigation of emerging pollutants and pathogens in decentralized wastewater treatment processes: A review. *Science of the Total Environment*, **779**, 146545.
Huber, S.A., Balz, A., Abert, M., Pronk, W. 2011. Characterisation of aquatic humic and non-humic matter with size-exclusion chromatography--organic carbon detection--organic nitrogen detection (LC-OCD-OND). *Water Research*, **45**(2), 879-85.
Hyeon, Y., Kim, S., Ok, E., Park, C. 2023. A fluid imaging flow cytometry for rapid characterization and realistic evaluation of microplastic fiber transport in ceramic membranes for laundry wastewater treatment. *Chemical Engineering Journal*, **454**.
Im, D., Nakada, N., Fukuma, Y., Tanaka, H. 2019. Effects of the inclusion of biological activated carbon on membrane fouling in combined process of ozonation, coagulation and ceramic membrane filtration for water reclamation. *Chemosphere*, **220**, 20-27.
IMO, I.M.O. 2023. Climatological Data, Vol. 2023.
ISO 14040. 2006. Environmental management - Life cycle assessment - Principles and framework.
ISO 14044. 2006. Environmental management - Life cycle assessment - Requirements and guidelines.
Ji, B., Zhao, Y., Vymazal, J., Qiao, S., Wei, T., Li, J., Mander, Ü. 2020. Can subsurface flow constructed wetlands be applied in cold climate regions? A review of the current knowledge. *Ecological Engineering*, **157**.
Jiang, L., Chen, M., Huang, Y., Peng, J., Zhao, J., Chan, F., Yu, X. 2022. Effects of different treatment processes in four municipal wastewater treatment plants on the transport and fate of microplastics. *Science of The Total Environment*, **831**, 154946.

Jin, X., Wang, W., Wang, S., Jin, P.K., Wang, X.C.C., Zhang, W.S., An, W.J., Wang, Y. 2019. Application of a hybrid gravity-driven membrane filtration and dissolved ozone flotation (MDOF) process for wastewater reclamation and membrane fouling mitigation. *Journal of Environmental Sciences*, **81**, 17-27.

Kan, C.-C., Genuino, D.A.D., Rivera, K.K.P., de Luna, M.D.G. 2016. Ultrasonic cleaning of polytetrafluoroethylene membrane fouled by natural organic matter. *Journal of Membrane Science*, **497**, 450-457.

Kim, L.H., Lee, D., Oh, J., Kim, S., Chae, S.-H., Youn, D., Kim, Y. 2022. Performance of a novel granular activated carbon and gravity-driven membrane hybrid process: Process development and removal of emerging contaminants. *Process Safety and Environmental Protection*, **168**, 810-819.

Kinnunen, J., Rossi, P.M., Herrmann, I., Ronkanen, A.-K., Heiderscheidt, E. 2023. Factors affecting effluent quality in on-site wastewater treatment systems in the cold climates of Finland and Sweden. *Journal of Cleaner Production*, **404**, 136756.

Kobayashi, Y., Ashbolt, N.J., Davies, E.G.R., Liu, Y. 2020. Life cycle assessment of decentralized greywater treatment systems with reuse at different scales in cold regions. *Environment International*, **134**, 105215.

Kosek, K., Luczkiewicz, A., Fudala-Książek, S., Jankowska, K., Szopińska, M., Svahn, O., Tränckner, J., Kaiser, A., Langas, V., Björklund, E. 2020. Implementation of advanced micropollutants removal technologies in wastewater treatment plants (WWTPs) - Examples and challenges based on selected EU countries. *Environmental Science & Policy*, **112**, 213-226.

Kramer, F.C., Shang, R., Rietveld, L.C., Heijman, S.J.G. 2020. Fouling control in ceramic nanofiltration membranes during municipal sewage treatment. *Separation and Purification Technology*, **237**, 116373.

Krishnan, R.Y., Manikandan, S., Subbaiya, R., Karmegam, N., Kim, W., Govarthanan, M. 2023. Recent approaches and advanced wastewater treatment technologies for mitigating emerging microplastics contamination - A critical review. *Science of The Total Environment*, **858**(Pt 1), 159681.

Kristmannsdóttir, H., Arnórsson, S., Sveinbjörnsdóttir, Á.E., Ármannsson, H. 2010. Geochemistry and classification of cold groundwater in Iceland. in: *Water-Rock Interaction*, pp. 207-210.

Krzeminski, P., Iglesias-Obelleiro, A., Madebo, G., Garrido, J.M., van der Graaf, J.H.J.M., van Lier, J.B. 2012. Impact of temperature on raw wastewater composition and activated sludge filterability in full-scale MBR systems for municipal sewage treatment. *Journal of Membrane Science*, **423-424**, 348-361.

Lares, M., Ncibi, M.C., Sillanpää, M., Sillanpää, M. 2018. Occurrence, identification and removal of microplastic particles and fibers in conventional activated sludge process and advanced MBR technology. *Water Research*, **133**, 236-246.

Lee, S., Badoux, G.O., Wu, B., Chong, T.H. 2021. Enhancing performance of biocarriers facilitated gravity-driven membrane (GDM) reactor for decentralized wastewater treatment: Effect of internal recirculation and membrane packing density. *Science of the Total Environment*, **762**, 144104.

Lee, S., Sutter, M., Burkhardt, M., Wu, B., Chong, T.H. 2019. Biocarriers facilitated gravity-driven membrane (GDM) reactor for wastewater reclamation: Effect of intermittent aeration cycle. *Science of The Total Environment*, **694**, 133719.

Leverenz, H., Tchobanoglous, G., Darby, J. 2010. *Evaluation of Greenhouse Gas Emissions from Septic Systems*. Water Environment Research Foundation & IWA Publishing.

Li, H., Zhang, Y., Wu, L., Jin, Y., Gong, Y., Li, A., Li, J., Li, F. 2021a. Recycled aggregates from construction and demolition waste as wetland substrates for pollutant removal. *Journal of Cleaner Production*, **311**.

Li, J., Wang, B., Chen, Z., Ma, B., Chen, J.P. 2021b. Ultrafiltration membrane fouling by microplastics with raw water: Behaviors and alleviation methods. *Chemical Engineering Journal*, **410**, 128174.

Li, L., Liu, D., Song, K., Zhou, Y. 2020. Performance evaluation of MBR in treating microplastics polyvinylchloride contaminated polluted surface water. *Marine Pollution Bulletin*, **150**, 110724.

Li, P., Yang, C., Sun, F., Li, X.Y. 2021c. Fabrication of conductive ceramic membranes for electrically assisted fouling control during membrane filtration for wastewater treatment. *Chemosphere*, **280**, 130794.

Li, Y., Wang, J., Lin, X., Wang, H., Li, H., Li, J. 2022. Purification effects of recycled aggregates from construction waste as constructed wetland filler. *Journal of Water Process Engineering*, **50**, 103335.

Li, Y., Xu, Y., Fu, Z., Li, W., Zheng, L., Li, M. 2021d. Assessment of energy use and environmental impacts of wastewater treatment plants in the entire life cycle: A system meta-analysis. *Environmental Research*, **198**, 110458.

Liao, X., Tian, Y., Gan, Y., Ji, J. 2020. Quantifying urban wastewater treatment sector's greenhouse gas emissions using a hybrid life cycle analysis method – An application on Shenzhen city in China. *Science of The Total Environment*, **745**, 141176.

Lin, H., Chen, J., Wang, F., Ding, L., Hong, H. 2011. Feasibility evaluation of submerged anaerobic membrane bioreactor for municipal secondary wastewater treatment. *Desalination*, **280**(1), 120-126.

Lin, L., Zhang, Y., Fu, B., Yan, W., Fu, Q., Li, S. 2022. Pre-depositing versus mixing powdered activated carbons for gravity-driven membrane systems during treated domestic wastewater filtration: Permeability stabilization and removal performance. *Separation and Purification Technology*, **288**, 120659.

Lin, X.H., Xu, J.C., Keller, A.A., He, L., Gu, Y.H., Zheng, W.W., Sun, D.Y., Lu, Z.B., Huang, J.W., Huang, X.F., Li, G.M. 2020. Occurrence and risk assessment of emerging contaminants in a water reclamation and ecological reuse project. *Science of the Total Environment*, **744**, 140977.

Long, Y., Zhou, Z., Yin, L., Wen, X., Xiao, R., Du, L., Zhu, L., Liu, R., Xu, Q., Li, H., Nan, R., Yan, S. 2022. Microplastics removal and characteristics of constructed wetlands WWTPs in rural area of Changsha, China: A different situation from urban WWTPs. *Science of The Total Environment*, **811**, 152352.

Longo, S., d'Antoni, B.M., Bongards, M., Chaparro, A., Cronrath, A., Fatone, F., Lema, J.M., Mauricio-Iglesias, M., Soares, A., Hospido, A. 2016. Monitoring and diagnosis of energy consumption in wastewater treatment plants. A state of the art and proposals for improvement. *Applied Energy*, **179**, 1251-1268.

Loupasaki, E., Diamadopoulos, E. 2013. Attached growth systems for wastewater treatment in small and rural communities: a review. *Journal of Chemical Technology & Biotechnology*, **88**(2), 190-204.

Lu, H.-C., Ziajahromi, S., Locke, A., Neale, P.A., Leusch, F.D.L. 2022. Microplastics profile in constructed wetlands: Distribution, retention and implications. *Environmental Pollution*, **313**, 120079.

Luo, H., Wang, Z. 2022. A new ultrasonic cleaning model for predicting the flux recovery of the UF membrane fouled with humic acid. *Journal of Environmental Chemical Engineering*, **10**(2), 107156.

Luo, Y., Guo, W., Ngo, H.H., Nghiem, L.D., Hai, F.I., Zhang, J., Liang, S., Wang, X.C. 2014. A review on the occurrence of micropollutants in the aquatic environment and their fate and removal during wastewater treatment. *Science of The Total Environment*, **473-474**, 619-41.

Lutterbeck, C.A., Kist, L.T., Lopez, D.R., Zerwes, F.V., Machado, Ê.L. 2017. Life cycle assessment of integrated wastewater treatment systems with constructed wetlands in rural areas. *Journal of Cleaner Production*, **148**, 527-536.

Ma, X.Y.Y., Li, Q.Y., Wang, X.C., Wang, Y.K., Wang, D.H., Ngo, H.H. 2018. Micropollutants removal and health risk reduction in a water reclamation and ecological reuse system. *Water Research*, **138**, 272-281.

Ma, Z., Wen, X.H., Zhao, F., Xia, Y., Huang, X., Waite, D., Guan, J. 2013. Effect of temperature variation on membrane fouling and microbial community structure in membrane bioreactor. *Bioresource Technology*, **133**, 462-468.

Mac Mahon, J., Knappe, J., Gill, L.W. 2022. Sludge accumulation rates in septic tanks used as part of the on-site treatment of domestic wastewater in a northern maritime temperate climate. *Journal of Environmental Management*, **304**, 114199.

Mårtensson, L.M., Fransson, A.M., Emilsson, T. 2016. Exploring the use of edible and evergreen perennials in living wall systems in the Scandinavian climate. *Urban Forestry & Urban Greening*, **15**, 84-88.

Maucieri, C., Barbera, A.C., Vymazal, J., Borin, M. 2017. A review on the main affecting factors of greenhouse gases emission in constructed wetlands. *Agricultural and Forest Meteorology*, **236**, 175-193.

Mohamad Annuar, A., Mat Nawi, N.I., Bilad, M.R., Jaafar, J., Marbelia, L., Nandianto, A.B.D. 2020. Improved bubbling for membrane fouling control in filtration of palm oil mill effluent anaerobic digester sludge. *Journal of Water Process Engineering*, **36**, 101350.

Mohana, A.A., Rahman, M., Sarker, S.K., Haque, N., Gao, L., Pramanik, B.K. 2022. Nano/microplastics: Fragmentation, interaction with co-existing pollutants and their removal from wastewater using membrane processes. *Chemosphere*, **309**(Pt 1), 136682.

Múrbúðin. 2023. Rakasperruplast.

Nascimento, T.A., Miranda, M.P. 2021. Control strategies for the long-term operation of direct membrane filtration of municipal wastewater. *Journal of Environmental Chemical Engineering*, **9**(4), 105335.

Nelson, M.J., Nakhla, G., Zhu, J. 2021. The circulating fluidized bed bioreactor as a biological nutrient removal process for municipal wastewater treatment: Process modelling and costing analysis. *Journal of Environmental Management*, **299**, 113604.

Ninomiya, Y., Kimura, K., Sato, T., Kakuda, T., Kaneda, M., Hafuka, A., Tsuchiya, T. 2020. High-flux operation of MBRs with ceramic flat-sheet membranes made possible by intensive membrane cleaning: Tests with real domestic wastewater under low-temperature conditions. *Water Research*, **181**, 115881.

Niwa, T., Hatamoto, M., Yamashita, T., Noguchi, H., Takase, O., Kekre, K.A., Ang, W.S., Tao, G., Seah, H., Yamaguchi, T. 2016. Demonstration of a full-scale plant using an UASB followed by a ceramic MBR for the reclamation of industrial wastewater. *Bioresource Technology*, **218**, 1-8.

Oka, P.A., Khadem, N., Berube, P.R. 2017. Operation of passive membrane systems for drinking water treatment. *Water Research*, **115**, 287-296.

Okeke, E.S., Okoye, C.O., Atakpa, E.O., Ita, R.E., Nyaruaba, R., Mgbechidinma, C.L., Akan, O.D. 2022. Microplastics in agroecosystems-impacts on ecosystem functions and food chain. *Resources, Conservation and Recycling*, **177**.

Ozgun, H., Cicekalan, B., Akdag, Y., Koyuncu, I., Ozturk, I. 2021. Comparative evaluation of cost for preliminary and tertiary municipal wastewater treatment plants in Istanbul. *Science of The Total Environment*, **778**, 146258.

Ozgun, H., Tao, Y., Ersahin, M.E., Zhou, Z., Gimenez, J.B., Spanjers, H., van Lier, J.B. 2015. Impact of temperature on feed-flow characteristics and filtration performance of an upflow anaerobic sludge blanket coupled ultrafiltration membrane treating municipal wastewater. *Water Research*, **83**, 71-83.

Peter-Varbanets, M., Gujer, W., Pronk, W. 2012. Intermittent operation of ultra-low pressure ultrafiltration for decentralized drinking water treatment. *Water Research*, **46**(10), 3272-82.

Peter-Varbanets, M., Hammes, F., Vital, M., Pronk, W. 2010. Stabilization of flux during dead-end ultra-low pressure ultrafiltration. *Water Research*, **44**(12), 3607-16.

Peter-Varbanets, M., Margot, J., Traber, J., Pronk, W. 2011. Mechanisms of membrane fouling during ultra-low pressure ultrafiltration. *Journal of Membrane Science*, **377**(1-2), 42-53.

Polruang, S., Sirivithayapakorn, S., Prateep Na Talang, R. 2018. A comparative life cycle assessment of municipal wastewater treatment plants in Thailand under variable power schemes and effluent management programs. *Journal of Cleaner Production*, **172**, 635-648.

Pramanik, B.K., Pramanik, S.K., Monira, S. 2021. Understanding the fragmentation of microplastics into nano-plastics and removal of nano/microplastics from wastewater using membrane, air flotation and nano-ferrofluid processes. *Chemosphere*, **282**, 131053.

Pronk, W., Ding, A., Morgenroth, E., Derlon, N., Desmond, P., Burkhardt, M., Wu, B., Fane, A.G. 2019. Gravity-driven membrane filtration for water and wastewater treatment: A review. *Water Research*, **149**, 553-565.

Pryce, D., Kapelan, Z., Memon, F.A. 2022. Economic evaluation of a small wastewater treatment plant under different design and operation scenarios by life cycle costing. *Development Engineering*, **7**.

PVC Pipe Supplies. 2023. PVC AND CPVC PIPE SIZES AND WEIGHTS, Vol. 2023.

Qiao, R., Lu, K., Deng, Y., Ren, H., Zhang, Y. 2019. Combined effects of polystyrene microplastics and natural organic matter on the accumulation and toxicity of copper in zebrafish. *Science of The Total Environment*, **682**, 128-137.

Resende, J.D., Nolasco, M.A., Pacca, S.A. 2019. Life cycle assessment and costing of wastewater treatment systems coupled to constructed wetlands. *Resources, Conservation and Recycling*, **148**, 170-177.

Reuter, F., Lauterborn, S., Mettin, R., Lauterborn, W. 2017. Membrane cleaning with ultrasonically driven bubbles. *Ultrasonics Sonochemistry*, **37**, 542-560.

Roux, P., Boutin, C., Risch, E., Heduit, A. 2010. Life Cycle environmental Assessment (LCA) of sanitation systems including sewerage: Case of Vertical Flow Constructed Wetlands versus activated sludge. *International Water Association - 12th IWA International Conference on Wetland Systems for Water Pollution Control*, **2**.

Rozman, U., Klun, B., Kalčíková, G. 2023. Distribution and removal of microplastics in a horizontal sub-surface flow laboratory constructed wetland and their effects on the treatment efficiency. *Chemical Engineering Journal*, **461**, 142076.

Saeplast. 2023. Rotþró 4500 L.

Samadi, A., Gao, L., Kong, L., Orooji, Y., Zhao, S. 2022. Waste-derived low-cost ceramic membranes for water treatment: Opportunities, challenges and future directions. *Resources, Conservation and Recycling*, **185**, 106497.

Sauve, G., Van Acker, K. 2020. The environmental impacts of municipal solid waste landfills in Europe: A life cycle assessment of proper reference cases to support decision making. *Journal of Environmental Management*, **261**, 110216.

Sauve, S., Desrosiers, M. 2014. A review of what is an emerging contaminant. *Chemistry Central Journal*, **8**, 15.

Scheutz, C., Kjeld, A., Fredenslund, A.M. 2022. Methane emissions from Icelandic landfills - A comparison between measured and modelled emissions. *Waste Management*, **139**, 136-145.

Shami, I.U.H., Wu, B. 2021. Gravity-Driven Membrane Reactor for Decentralized Wastewater Treatment: Effect of Reactor Configuration and Cleaning Protocol. *Membranes (Basel)*, **11**(6), 388.

Shi, D., Liu, Y., Fu, W., Li, J., Fang, Z., Shao, S. 2020. A combination of membrane relaxation and shear stress significantly improve the flux of gravity-driven membrane system. *Water Research*, **175**, 115694.

Song, Z., Li, Y., Wang, Z., Wang, M., Wang, Z., Zhang, Y., Sun, J., Liu, C., Liu, Y., Xu, B., Qi, F. 2020. Effect of the coupling modes on EfOM degradation and fouling mitigation in ozonation-ceramic membrane filtration. *Chemical Engineering Journal*, **394**, 124935.

Song, Z., Zheng, Z., Li, J., Sun, X., Han, X., Wang, W., Xu, M. 2006. Seasonal and annual performance of a full-scale constructed wetland system for sewage treatment in China. *Ecological Engineering*, **26**(3), 272-282.

Søvik, A.K., Augustin, J., Heikkinen, K., Huttunen, J.T., Necki, J.M., Karjalainen, S.M., Kløve, B., Liikanen, A., Mander, U., Puustinen, M., Teiter, S., Wachniew, P. 2006. Emission of the greenhouse gases nitrous oxide and methane from constructed wetlands in europe. *Journal of Environmental Quality*, **35**(6), 2360-73.

Stoffel, D., Rigo, E., Derlon, N., Staaks, C., Heijnen, M., Morgenroth, E., Jacquin, C. 2021. Low maintenance gravity-driven membrane filtration using hollow fibers: Effect of reducing space for biofilm growth and control strategies on permeate flux. *Science of The Total Environment*, **811**, 152307.

Sun, X., Chen, B., Li, Q., Liu, N., Xia, B., Zhu, L., Qu, K. 2018. Toxicities of polystyrene nano- and microplastics toward marine bacterium Halomonas alkaliphila. *Science of The Total Environment*, **642**, 1378-1385.

Talvitie, J., Mikola, A., Koistinen, A., Setälä, O. 2017. Solutions to microplastic pollution – Removal of microplastics from wastewater effluent with advanced wastewater treatment technologies. *Water Research*, **123**, 401-407.

Tang, X., Ding, A., Qu, F., Jia, R., Chang, H., Cheng, X., Liu, B., Li, G., Liang, H. 2016. Effect of operation parameters on the flux stabilization of gravity-driven membrane (GDM) filtration system for decentralized water supply. *Environmental Science and Pollution Research International*, **23**(16), 16771-80.

Tang, Y., Zhang, S., Su, Y., Wu, D., Zhao, Y., Xie, B. 2021. Removal of microplastics from aqueous solutions by magnetic carbon nanotubes. *Chemical Engineering Journal*, **406**, 126804.

Tao, C., Parker, W., Bérubé, P. 2021a. Assessing the role of cold temperatures on irreversible membrane permeability of tertiary ultrafiltration treating municipal wastewater. *Separation and Purification Technology*, **278**, 119556.

Tao, C., Parker, W., Bérubé, P. 2021b. Characterization and modelling of soluble microbial products in activated sludge systems treating municipal wastewater with special emphasis on temperature effect. *Science of the Total Environment*, **779**, 146471.
Umhverfisstofnun. 2022. Minni fráveitur leiðbeiningar.
United Nations, G.A. 2015. Transforming our World: Agenda 2030 for Sustainable Development A/RES/70/1, Vol. 2019.
van den Brink, P., Satpradit, O.A., van Bentem, A., Zwijnenburg, A., Temmink, H., van Loosdrecht, M. 2011. Effect of temperature shocks on membrane fouling in membrane bioreactors. *Water Research*, **45**(15), 4491-500.
Varma, M., Gupta, A.K., Ghosal, P.S., Majumder, A. 2021. A review on performance of constructed wetlands in tropical and cold climate: Insights of mechanism, role of influencing factors, and system modification in low temperature. *Science of The Total Environment*, **755**(Pt 2), 142540.
Vassalle, L., Ferrer, I., Passos, F., Filho, C.R.M., Garfí, M. 2023. Nature-based solutions for wastewater treatment and bioenergy recovery: A comparative Life Cycle Assessment. *Science of The Total Environment*, 163291.
Veitur. 2019. Wastewater, Vol. 2020.
Vitali, C., Peters, R., Janssen, H.-G., W.F.Nielen, M. 2022. Microplastics and nanoplastics in food, water, and beverages; part I. Occurrence. *TrAC Trends in Analytical Chemistry*, 116670.
Wan, H., Shi, K., Yi, Z., Ding, P., Zhuang, L., Mills, R., Bhattacharyya, D., Xu, Z. 2022. Removal of polystyrene nanoplastic beads using gravity-driven membrane filtration: Mechanisms and effects of water matrices. *Chemical Engineering Journal*, **450**.
Wang, J., Gao, X., Xu, Y., Wang, Q., Zhang, Y., Wang, X., Gao, C. 2016. Ultrasonic-assisted acid cleaning of nanofiltration membranes fouled by inorganic scales in arsenic-rich brackish water. *Desalination*, **377**, 172-177.
Wang, M., Zhang, D.Q., Dong, J.W., Tan, S.K. 2017a. Constructed wetlands for wastewater treatment in cold climate - A review. *Journal of Environmental Science (China)*, **57**, 293-311.
Wang, Q., Hernández-Crespo, C., Santoni, M., Van Hulle, S., Rousseau, D.P.L. 2020. Horizontal subsurface flow constructed wetlands as tertiary treatment: Can they be an efficient barrier for microplastics pollution? *Science of The Total Environment*, **721**, 137785.
Wang, Q., Li, Y., Liu, Y., Zhou, Z., Hu, W., Lin, L., Wu, Z. 2022. Effects of microplastics accumulation on performance of membrane bioreactor for wastewater treatment. *Chemosphere*, **287**(Pt 1), 131968.
Wang, S. 2014. Values of decentralized systems that avoid investments in idle capacity within the wastewater sector: A theoretical justification. *Journal of Environmental Management*, **136**, 68-75.
Wang, Y., Fortunato, L., Jeong, S., Leiknes, T. 2017b. Gravity-driven membrane system for secondary wastewater effluent treatment: Filtration performance and fouling characterization. *Separation and Purification Technology*, **184**, 26-33.
Wei, S., Luo, H., Zou, J., Chen, J., Pan, X., Rousseau, D.P.L., Li, J. 2020. Characteristics and removal of microplastics in rural domestic wastewater treatment facilities of China. *Science of The Total Environment*, **739**, 139935.
Wei, W., Huang, Q.S., Sun, J., Wang, J.Y., Wu, S.L., Ni, B.J. 2019. Polyvinyl Chloride Microplastics Affect Methane Production from the Anaerobic Digestion of Waste Activated Sludge through Leaching Toxic Bisphenol-A. *Environmental Science & Technology*, **53**(5), 2509-2517.

Werker, A.G., Dougherty, J.M., McHenry, J.L., Loon, W.A.V. 2002. Treatment variability for wetland wastewater treatment design in cold climates. *Ecological Engineering*, **19**(1-11).

Wernet, G., Bauer, C., Steubing, B., Reinhard, J., Moreno-Ruiz, E., and Weidema, B. 2016. The ecoinvent database version 3 (part I): overview and methodology. *The International Journal of Life Cycle Assessment* pp. 1218–1230.

World Health Organization. 2006. *Guidelines for the safe use of wastewater, excreta and greywater - Volume ii (wastewater use in agriculture)*.

Wu, B., Hochstrasser, F., Akhondi, E., Ambauen, N., Tschirren, L., Burkhardt, M., Fane, A.G., Pronk, W. 2016. Optimization of gravity-driven membrane (GDM) filtration process for seawater pretreatment. *Water Research*, **93**, 133-140.

Xu, D., Yin, X., Zhou, S., Jiang, Y., Xi, X., Sun, H., Wang, J. 2022. A review on the remediation of microplastics using constructed wetlands: Bibliometric, co-occurrence, current trends, and future directions. *Chemosphere*, **303**, 134990.

Yang, F.L., Zhang, H.R., Zhang, X.Z., Zhang, Y., Li, J.H., Jin, F.M., Zhou, B.X. 2021. Performance analysis and evaluation of the 146 rural decentralized wastewater treatment facilities surrounding the Erhai Lake. *Journal of Cleaner Production*, **315**, 128159.

Yang, X., Man, Y.B., Wong, M.H., Owen, R.B., Chow, K.L. 2022. Environmental health impacts of microplastics exposure on structural organization levels in the human body. *Science of The Total Environment*, **825**, 154025.

Ye, Y., Le Clech, P., Chen, V., Fane, A.G., Jefferson, B. 2005. Fouling mechanisms of alginate solutions as model extracellular polymeric substances. *Desalination*, **175**(1), 7-20.

Yuan, W., Zydney, A.L. 1999. Humic acid fouling during microfiltration. *Journal of Membrane Science*, **157**(1), 1-12.

Zang, Y., Li, Y., Wang, C., Zhang, W., Xiong, W. 2015. Towards more accurate life cycle assessment of biological wastewater treatment plants: a review. *Journal of Cleaner Production*, **107**, 676-692.

Zhang, K., Zhang, Z.H., Wang, H., Wang, X.M., Zhang, X.H., Xie, Y.F. 2020. Synergistic effects of combining ozonation, ceramic membrane filtration and biologically active carbon filtration for wastewater reclamation. *Journal of Hazardous Materials*, **382**, 121091.

Zhang, Z., Chen, Y. 2020. Effects of microplastics on wastewater and sewage sludge treatment and their removal: A review. *Chemical Engineering Journal*, **382**, 122955.

Zhao, Y.X., Li, P., Li, R.H., Li, X.Y. 2019a. Characterization and mitigation of the fouling of flat-sheet ceramic membranes for direct filtration of the coagulated domestic wastewater. *Journal of Hazardous Materials*, 121557.

Zhao, Y.X., Li, P., Li, R.H., Li, X.Y. 2019b. Direct filtration for the treatment of the coagulated domestic sewage using flat-sheet ceramic membranes. *Chemosphere*, **223**, 383-390.

Zhou, G., Wang, Q., Li, J., Li, Q., Xu, H., Ye, Q., Wang, Y., Shu, S., Zhang, J. 2021. Removal of polystyrene and polyethylene microplastics using PAC and FeCl3 coagulation: Performance and mechanism. *Science of The Total Environment*, **752**, 141837.

Zhou, H., Li, X., Xu, G., Yu, H. 2018. Overview of strategies for enhanced treatment of municipal/domestic wastewater at low temperature. *Science of The Total Environment*, **643**, 225-237.

Zhou, H., Zhou, L., Ma, K. 2020. Microfiber from textile dyeing and printing wastewater of a typical industrial park in China: Occurrence, removal and release. *Science of The Total Environment*, **739**, 140329.

Zhu, H., Wen, X., Huang, X. 2012. Characterization of membrane fouling in a microfiltration ceramic membrane system treating secondary effluent. *Desalination*, **284**, 324-331.

Appendix

Constructed Wetlands Experiments

Materials and Methods

Experimental setup and operation conditions

The lab-scale two-stage horizontal flow constructed wetland was set up, as illustrated in Figure A. 1. In detail, each tank had a volume of 7 L, 40% of which was packed with the substrate. The primary wastewater was periodically collected from Veitur wastewater treatment plant at Klettagarður, Reykjavík, which serves ~150000 people. The water was delivered to the first wetland tank (i.e., Stage 1) by a peristaltic pump (Longer, China), and the treated effluent from the first wetland tank freely flowed to the second wetland tank (i.e., Stage 2) via an overflow line. The hydraulic retention time of the two-stage wetland system was ~50 h. A LED lamp (42 W, 6500 K) was located above the wetland and provided light at a cycle of 12 h on/12 h off.

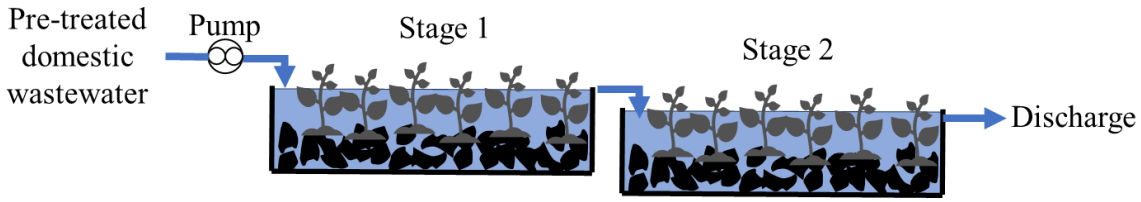

Figure A. 1. A two-stage constructed wetland setup

As shown in Table A. 1, the constructed wetland systems were operated at 22°C and 5°C, which represented an average Summer temperature in the Nordic countries of EU and the yearly average on the South coast of Iceland (IMO, 2023) respectively. In detail, this is a potential location for adopting constructed wetlands and served as representative for other subpolar oceanic climate areas. During Day 0-59, two wetland systems packed with lava stone and concrete blocks respectively, were operated in parallel at a temperature of 22°C. The lava stones represented conventionally used biocarriers and concrete blocks were recycled construction waste. In the first stage of the wetland system, *Menyanthes trifoliata, Carex lyngbyei, Rhytidiadelphus squarrosus, and Calliergon sp.*, (collected from the local nature conservation pond Vatnsmýri), were used as the testing plants. Because these plants were well established in the local pond, they were expected to easily adapt to the wetland systems under the subpolar oceanic conditions. In the second stage of the wetland system, *Vesicularia dubyana*, *Ceratophyllum demersum*, and *Microsorum pteropus* purchased from a local shop (Skrautfiskar) were used as the testing plants. Specifically, these aquatic plants were suitable to be cultivated at 15-30°C. Meanwhile, basil (*Ocimum basilicum*, Johnsons, UK) and lettuce (*Lactuca sativa*, Sluis Garden, Netherlands) were chosen as the testing vegetables and cultivated in the second wetland tank for investigating heavy metal uptake. In detail, several seeds were planted in sponge cubes (2.5 cm × 2.5 cm × 2.5 cm). The sponges containing basil and lettuce seeds were placed in a tray with tap water and a lid (under dark condition). After the seeds germinated (~3 weeks), the sponges with the plants

were transferred to pots (packed with 10-15 clay granules, Jongkind, Netherlands), which were then placed in the second wetland tank. During Day 61-120, the wetland system packed with concrete blocks was placed in a refrigerating unit (at ~5°C), which was installed with a ventilation system. In both wetland tanks, *Menyanthes trifoliata Carex lyngbyei, Rhytidiadelphus squarrosus, and Calliergon sp.* were used as the testing plants.

Table A. 1. Constructed wetland operation conditions

Wetland abbreviation and operation duration	Substrate	Temp/Light	Plants
Wetland system 1 (Day 0-60)	Lava stone	22°C (12 h on - 12 h off)	Stage I: *Menyanthes trifoliata, Carex lyngbyei, Rhytidiadelphus squarrosus,* and *Calliergon sp*. Stage II: Java Moss (*Vesicularia dubyana), Ceratophyllum demersum*, Java Fern *(Ceratophyllum demersum*), basil (*Ocimum basilicum*), lettuce (*Lactuca sativa*)
Wetland system 2 (Day 0-60)	Concrete blocks		
Wetland system 3 (Day 61-120)	Concrete blocks	5°C (12 h on - 12 h off)	Stage I and II: *Menyanthes trifoliata; Carex lyngbyei, Rhytidiadelphus squarrosus*, and *Calliergon sp*.

Water quality analysis

The water quality of feed, effluent from the first tank and second tank was analysed weekly, as explained in chapter 2.3.6. Phosphate (PO_4^{3-}) was also measured using the respective analytical kit (Hach, US) and a spectrophotometer (DR3900, Hach, US), according to the manufacturer's manual. After dismantling of the wetlands, the plant samples were collected and air-dried before heavy metal analysis. Heavy metal contents in the water samples and plant samples were analysed by an inductively coupled plasma-optical emission spectroscopy (ICP-OES, OPTIMA 8300, PerkinElmer, US) and an inductively coupled plasma-mass spectrometry (ICP-MS, iCAP-Q, Thermo Scientific, US), as described in our previous work (Guðjónsdóttir et al., 2022).

Results and discussion

Effect of substrate and temperature on constructed wetlands performance

In this study, the constructed wetlands with different substrates (lava stone *vs.* concrete blocks) under different temperatures (5°C *vs.* 22°C) were operated for ~60 days. The water quality profiles with operation time were shown in Figure A. 2a-e and the summarized data were described in Table A. 2 and Figure A. 2f. As shown in Table A. 2, the pH level remained relatively stable at 7.3-8.3 in the three wetlands. However, the conductivity showed high fluctuations in feed and effluents. This could be attributed to weather and seasonal changes

(such as stormwater collection and salt usage on the roads), which affected the wastewater composition. Clearly, the final effluents from the constructed wetlands met EU discharge standards for non-sensitive areas (BOD_5 < 25 mg/L; COD < 125 mg/L; TSS < 35 mg/L) (European Union, 1991), and sensitive areas (TP < 2 mg/L; TN < 15 mg/L), except the TN level in the effluent of the wetland at 5°C.

Table A. 2. Water quality and pollutant removal ratios in the wetlands

	Feed	Lava stones (22°C)		Concrete (22°C)		Concrete (5°C)	
		Stage 1	Stage 2	Stage 1	Stage 2	Stage 1	Stage 2
pH	7.4±0.4	7.8±0.2	8.3±0.4	8.0±0.2	8.4±0.7	7.3±0.2	7.5±0.6
Conductivity (µS/cm)	1637± 624	1765± 364	1752± 332	1942± 416	1967± 411	1405± 590	1510± 553
Removal ratios (%)							
COD	-	63±28	88±6	71±20	85±7	44±29	51±31
BOD_5	-	71±16	90±9	80±11	80±24	75±15	65±26
TN	-	56±19	70±16	50±19	67±13	32±31	34±32
PO_4	-	32±18	63±15	32±16	48±12	16±14	18±19
TSS	-	65±30	98±4	64±32	94±3	73±28	86±12

As summarized in Figure A. 2f, at 22°C, the effluent water quality was comparable in the wetlands with lava stones and concrete blocks ($p > 0.05$), leading to their similar pollutant removal effectiveness, i.e., 85-88% of COD removal; 80-90% of BOD_5 removal; 67-70% of TN removal; 58-63% of PO_4 removal; 94-98% of TSS removal (Table A. 2). The COD and TN removal ratios in this study were higher than those in a previously reported vertical flow constructed wetland with recycled concrete waste as substrate (66.3% of COD removal and 16.2% of TN removal) (Li et al., 2021a). This may be attributed to the lower organic content in the feed wastewater, limited nitrification at a relatively lower temperature (~17.1°C), and vertical flow wetland configuration in the previously reported study. Specifically, the first stage of the wetland system contributed majorly to pollutant removals (Table A. 2). In the second stage, COD, TN, PO_4 and TSS were further removed in all wetland systems, while BOD_5 displayed dissimilar removal behaviors under different conditions. It is noted that the composition of municipal wastewater fluctuated significantly depending on local freshwater consumption and weather conditions (Figure A. 2). It is therefore necessary to employ a second stage in the constructed wetlands, which can act as a buffer tank to achieve constant pollutant removal efficiencies.

Clearly, the wetland with concrete operated at 5°C produced the effluent with significantly higher BOD_5 and TN concentrations than that at 22°C. As shown in Figure A. 3, the testing plants well grew with extending operation time in the wetlands at 22°C; while at 5°C, the testing plants appeared to stop growing and their leaves dried out. Thus, such low organic and nutrient removals may be attributed to limited plant sorption, biodegradation of rhizobacterial communities, and reduced nitrification and denitrification at a lower temperature (Bai et al., 2023; Varma et al., 2021). To implement nutrient recycling at cold temperatures, plant species, which are more suitable for colder temperatures, such as *Vaccinium vitis-idea*, *Allium schoenoprasum*, *Calamintha nepeta*, and *Fragaria vesca (Mårtensson et al., 2016)* could be tested in constructed wetlands in future research. Nevertheless, the organic removal ratios at 5°C were comparable to those in the previous studies employing free surface flow constructed wetland (substrate: soil) for domestic

wastewater treatment under cold climate (~51% *vs.* 59.4% of COD removal; ~65% *vs.* 67.8% of BOD_5 removal) (Ji et al., 2020; Song et al., 2006).

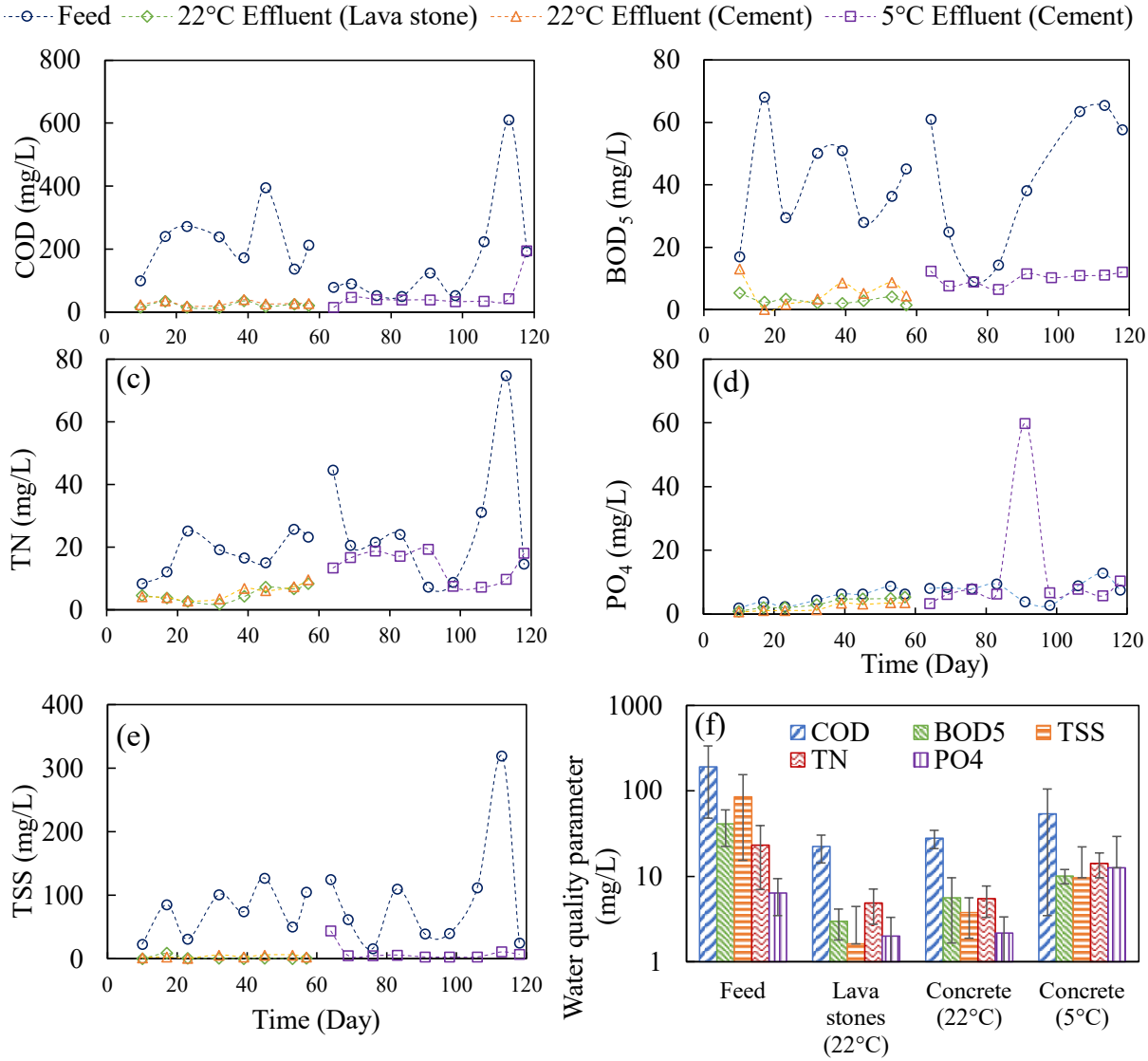

Figure A. 2. COD (a), BOD5 (b), TN (c), PO4 (d), TSS (e), and a summary of water quality parameters (f) in the feed and final effluents of the wetland systems.

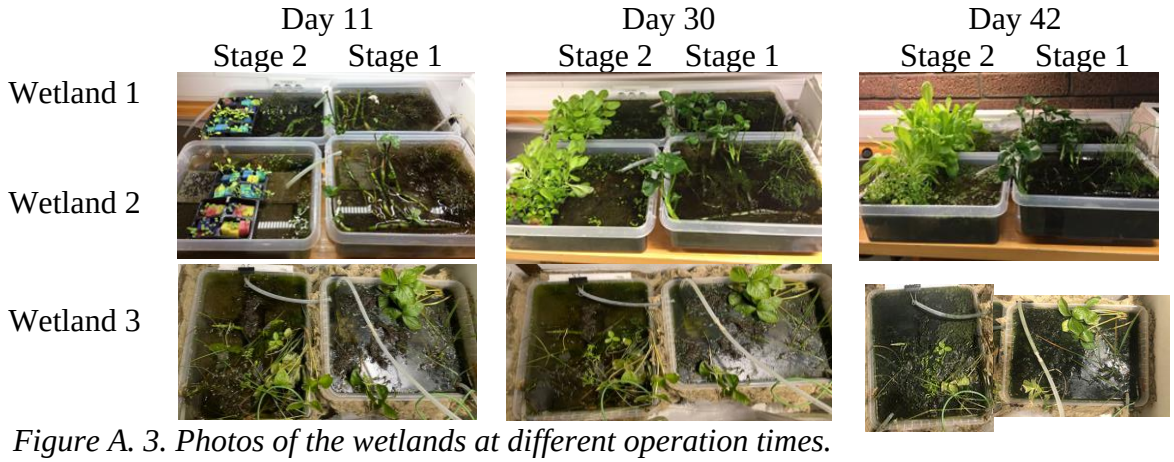

Figure A. 3. Photos of the wetlands at different operation times.

The metal contents in the feed and effluent of the wetland system operated at 22°C were described in Table A. 3. It was observed that higher levels of Ca, Si, Sr, and Ti occurred in the effluent of the wetland with concrete, while the effluent in the wetland with lava stones presented higher Cu, Mn, Mo, and Zn levels. As illustrated in a previous study (Li et al., 2022), leaching of Cu, Zn and Pb from concrete substrates led to higher concentrations of these heavy metals in the wetlands; while when red bricks were used as the substrate, higher levels of Cu, Zn, Pb and Cr were present, revealing that the types and amounts of leaching heavy metals were associated with the substrate materials. Thus, dissimilar heavy metal contents in the wetland with concrete and lava stones may be associated with different leaching behaviors from concrete and lava stones (Arnórsson & Oskarsson, 2007). Furthermore, at 5°C, the final effluent had lower or comparable heavy metal contents compared to the feed, which may be associated with limited leaching from the concrete at a low temperature and potential biosorption and plant uptake (although low temperature was not favorable for biodegradation and plant growth) (Li et al., 2022). (Li et al., 2022). It is noted that the metal leaching amount could decrease with extending operation time, followed by reaching the equilibrium (Galvín et al., 2023). As the leaching dynamics depends on multiple factors, the detailed leaching behaviors in the wetland with recycled concrete needs to be further investigated.

To illustrate the feasibility of nutrient recovery through hydroponic agriculture, the lettuce and basil were cultivated in the second stage of the wetland systems with lava stone and concrete (22°C). At the end of operation of the wetlands, their growth parameters (leaf number, leaf length, and maximum plant (without root) length) were measured and shown in Table A. 4. The lettuce plants in the lava stone and concrete wetlands grew to a similar height of ~18 cm, however, significant differences were found in the leaf number and max leaf length (p<0.05). The lettuce plants from the lava stone wetlands developed better with ~2 more leaves per plant and longer leaves. The basil plants showed an opposite pattern, where only the significant difference of the plant height between lava stone and concrete wetlands was noticed, i.e., the plants in the wetland with concrete being ~1.6 cm higher. The levels of organics and nutrient in the two wetlands were relatively similar, so these differences might result from the dissimilar availabilities of micronutrients (such as Zn, Mo, Cu, Mo, Table A. 3; due to different leaching behaviors of the lava stone and concrete) for the plants.

Table A. 3. Heavy metal and metalloid concentrations (mg/L) in the feed and final effluents of the wetland systems (n=3)

	Feed (22°C)	Final effluent		Feed (5°C)	Final effluent
		Lava stone (22°C)	Concrete (22°C)		Concrete (5°C)
Al	0.039±0.036	0.035±0.026	0.021±0.019	10.20±7.91	2.88±0.66
As	<0.001	<0.001	<0.001	0.002±0.001	0.001±0.001
Ba	0.005±0.002	0.009±0.002	0.010±0.001	0.060±0.033	0.028±0.018
Ca	21.21±1.37	20.05±0.97	**30.02±1.17**	31.62±10.12	28.22±9.11
Cd	<0.001	<0.001	<0.001	0.001±0.000	<0.001
Co	<0.001	<0.001	<0.001	0.008±0.006	0.002±0.000
Cr	<0.001	<0.001	<0.001	0.019±0.052	0.002±0.001
Cu	<0.001	**0.006±0.000**	<0.001	0.060±0.064	0.015±0.003
Fe	<0.001	<0.001	<0.001	11.91±12.24	3.36±1.23
K	11.07±2.46	8.62±1.52	10.06±2.11	18.00±3.66	16.17±10.13
Mg	19.97±4.53	18.46±2.58	19.88±4.68	36.83±17.41	37.67±20.45
Mn	0.016±0.018	**0.019±0.012**	0.008±0.009	0.278±0.191	0.144±0.612
Mo	0.001±0.001	**0.005±0.002**	0.002±0.000	0.359±0.500	0.009±0.007
Na	>500	>500	>500	227.42±154.20	236.47±144.69
Ni	0.011±0.009	0.005±0.002	0.004±0.006	0.025±0.020	0.006±0.001
Pb	<0.001	<0.001	<0.001	0.021±0.014	0.004±0.001
Sb	<0.001	<0.001	<0.001	0.003±0.003	0.001±0.000
Se	<0.001	<0.001	<0.001	-	-
Si	19.87±3.42	6.85±5.57	**9.98±2.65**	17.80±6.22	10.02±3.40
Sn	<0.001	<0.001	<0.001	0.001±0.000	0.001±0.000
Sr	0.114±0.021	0.111±0.011	**0.202±0.021**	0.263±0.114	0.261±0.139
Ti	0.042±0.003	0.041±0.002	**0.060±0.002**	0.076±0.082	0.037±0.034
V	0.004±0.001	0.003±0.000	0.002±0.000	0.112±0.104	0.007±0.001
Zn	0.022±0.006	**0.046±0.043**	0.017±0.012	1.36±1.15	0.137±0.037
Hg	<0.001	<0.001	<0.001	<0.001	<0.001

Table A. 4. The growth parameters of plants in the wetland (22°C)

		Lava stone	Concrete	*p*-value
Lettuce (collected on Day 42)	Leaf number	9.3±1.7	7.3±1.3	0.02
	Max. leaf length (cm)	12.9±2.4	10.1±0.8	0.01
	Total height (cm)	17.9±3.3	17.6±3.2	0.87
Basil (collected on Day 58)	Leaf number	9.8±2.8	9.7±2.9	0.84
	Max. leaf length (cm)	2.4±0.6	2.6±0.6	0.14
	Total height (cm)	3.6±1.6	5.3±2.3	0.00

Meanwhile, the *Menyanthes trifoliata*, basil, and lettuce plants collected from the wetlands at 22°C were dried and the heavy metal contents in the dried plants were analyzed, as shown in Table A. 5. The metal contents in the three types of plants met the WHO standards for human consumption (World Health Organization, 2006), which showed a potential for nutrient recycling. Specifically, the basil plants contained higher levels of Al, Co, Ni, Se and Zn elements, while the lettuce plants contained more Mn in the lava rock-based wetland compared to those in the concrete -based wetland. Meanwhile, *Menyanthes trifoliata* in the lava rock-based wetland contained more As, while that in the concrete-based wetland contained more Ba, Co and Se. This was possibly related to the different contents of these elements in the wetlands with concrete and lava stones (Table A. 3) and dissimilar nutrient uptake behaviors of different plants.

Table A. 5. Heavy metal and metalloid contents (mg/g dry weight) in dried plant samples.

mg/g	WHO guide-line	Concrete			Lava stone		
		Menyanthes trifoliata	Basil	Lettuce	*Menyanthes trifoliata*	Basil	Lettuce
Al	-	0.1581±0.0154	0.0395±0.0013	0.0332±0.0007	0.0865±0.0490	0.0898±0.0000	0.0298±0.0032
As	0.008	0.0003	<0.0003	<0.0003	0.0027±0.0000	<0.0004	<0.0002
Ba	0.302	0.0066±0.0008	0.0049±0.0005	0.0050±0.0007	0.0033±0.0002	0.0050±0.0004	0.0049±0.0009
Ca	-	4.9790±0.0279	9.6630±0.3897	14.4414±0.3558	4.6689±0.1718	10.3228±0.0192	13.1959±0.8500
Cd	0.004	<0.0003	<0.0003	<0.0003	<0.0003	<0.0004	0.0003±0.0000
Co	-	0.0031±0.0010	0.0014±0.0001	0.0003	0.0018±0.0004	0.0047±0.0001	0.0005±0.0002
Cr	-	0.0007±0.0001	0.0004±0.0000	0.0005	0.0005±0.0000	0.0009±0.0003	0.0008±0.0001
Cu	-	0.0209±0.0023	0.0148±0.0013	0.0115±0.0011	0.0194±0.0006	0.0212±0.0025	0.0140±0.0017
Fe	-	1.3307±0.1328	0.0760±0.0009	0.0818±0.0057	0.8739±0.1799	0.0626±0.0073	0.0784±0.0081
K	-	26.1725±3.0755	41.8221±2.3736	45.0533±1.4805	25.9388±3.0051	40.6733±0.5670	55.0729±4.8438
Mg	-	3.9166±0.3054	7.1420±0.4602	4.0176±0.3371	5.3547±1.0082	9.5481±0.2207	4.8554±0.3183
Mn	-	0.3887±0.1044	0.0803±0.0089	0.0567±0.0022	0.2247±0.0022	0.1685±0.0021	0.1023±0.0258
Mo	0.0006	0.0006±0.0000	0.0004±0.0001	0.0003	0.0004±0.0000	0.0005	0.0004±0.0001
Na	-	7.9827±1.9583	1.9518±0.2525	10.5041±1.2934	9.3918±2.0592	1.5547±0.2086	11.9966±3.4579
Ni	0.107	0.0072±0.0033	0.0037±0.0003	0.0011±0.0004	0.0026±0.0001	0.0094±0.0003	0.0012±0.0002
Pb	0.084	0.0004	0.0003	0.0003	0.0003	<0.0004	<0.0002
Sb	-	<0.0003	<0.0003	<0.0003	<0.0003	<0.0004	<0.0002
Se	0.006	0.0022±0.0005	0.0016±0.0002	0.0026±0.0005	0.0010±0.0001	0.0037±0.0002	0.0026±0.0003
Si	-	0.6180±0.0470	0.1861±0.1861	0.3753±0.0292	0.6779±0.0093	0.0000±0.0000	0.2895±0.0097
Sn	-	0.0005±0.0000	0.0004	0.0003	0.0004	0.0005	0.0004
Sr	-	0.0411±0.0008	0.0661±0.0048	0.0873±0.0026	0.0374±0.0023	0.0558±0.0019	0.0652±0.0134
Ti	-	0.0197±0.0021	0.0193±0.0005	0.0261±0.0009	0.0172±0.0068	0.0188±0.0003	0.0249±0.0026
V	0.047	0.0016±0.0002	<0.0003	0.0003±0.0000	0.0008	0.0004	0.0003
Zn	-	0.0855±0.0022	0.0510±0.0067	0.0600±0.0007	0.0847±0.0042	0.1064±0.0060	0.0960±0.0075
Hg	0.007	<0.0003	<0.0003	<0.0003	<0.0003	<0.0004	<0.0002

Conclusions

This chapter examined the feasibility of using construction wastes as substrate in constructed wetlands for wastewater treatment in cold climate. The main findings are as follows:

(1) The wetland with concrete waste material as the substrate achieved similar organic and nutrient removal effectiveness as that with lava stones. The wetland operated at the cold temperature (5°C) achieved significantly lower BOD_5 and TN removals than that at the warm temperature (22°C), possibly due to limited plant sorption and biodegradation.

(2) The treated water in the tested wetland systems met European discharge standards (for sensitive areas) in terms of BOD_5, COD, TSS, and TN, except the TN level in the treated water from the wetland operated at the cold temperature.

(3) Heavy metal analysis revealed dissimilar leaching behaviours from lava stones and concrete. However, all plants met WHO guidelines for human consumption, which showed the potential for nutrient recycling in constructed wetlands.